BIOMECHANICS AND ELECTROPHYSIOLOGY OF SENSORY REGULATION DURING LOCOMOTION IN A NOVEL IN VITRO SPINAL CORD-HINDLIMB PREPARATION

A Dissertation
Presented to
The Academic Faculty

By

Heather Brant Hayes

In Partial Fulfillment
of the Requirements for the Degree
Doctor of Philosophy in the
School of Biomedical Engineering

Georgia Institute of Technology
December 2010

BIOMECHANICS AND ELECTROPHYSIOLOGY OF SENSORY REGULATION DURING LOCOMOTION IN A NOVEL IN VITRO SPINAL CORD-HINDLIMB PREPARATION

Approved by:

Dr. Shawn Hochman, Advisor
Department of Physiology
Emory University School of Medicine

Dr. Young-Hui Chang, Advisor
School of Applied Physiology
Georgia Institute of Technology

Dr. T. Richard Nichols
School of Applied Physiology
Georgia Institute of Technology

Dr. Boris I. Prilutsky
School of Applied Physiology
Georgia Institute of Technology

Dr. Lena H. Ting
Department of Biomedical Engineering
Emory University School of Medicine &
Georgia Institute of Technology

Dr. Matthew C. Tresch
Department of Biomedical Engineering
Northwestern University

Date Approved: September 02, 2010

The more I study nature, the more I stand amazed at the work of the Creator.
Louis Pasteur, The Literary Digest, 1902

My motto is to research in terror, write with confidence, and publish with humility: terror, lest something escape me; confidence, lest the narrative seem weak and uncertain; and humility because some sources and interpretations, not to mention perfect literary grace, always lie beyond the grasp of any writer.
T.J. Stiles, The First Tycoon: The Epic Life of Cornelius Vanderbilt, 2009

ACKNOWLEDGEMENTS

Some say there's no I in team, but I say there's no I in graduate school. My journey would not have been possible without the support of many.

First, I would like to thank my advisors, Shawn Hochman and Young-Hui Chang. I could not have asked for better advisors, who cared about me personally as well as scientifically. Your encouragement helped me through the tough times when I thought the hindlimbs would never walk dorsal-up or the data would never make sense. Thank for fostering my passions and helping me achieve my goals. Without either of you, my project and my experience would be half full.

Shawn, thank you for imparting your endless knowledge of the spinal cord. Thank you for teaching me the ways of an electrophysiologist and how to be a discerning experimentalist. Thank you for the hours spent discussing data in your office. Thank you for sharing in the highs and the lows, but especially for sharing my joy and excitement as we discovered new ideas. Most importantly, thank you for providing invaluable insights, while also challenging me to be an independent researcher.

Young-Hui, thank you for guiding me from the very beginning of graduate school. Thank you for teaching me the ways of research, how to form pointed hypotheses, and reminding me by example to remain passionate about "learning how we get from here to there." Your insights into motor control and neuromechanics have been invaluable, so thank you for the hours spent discussing joint angle trajectories and how my data fits into the big picture.

I am also grateful to my committee members, for sharing their intellectual resources and challenging me to become a better scientist. Lena Ting, thank you for

sharing your expertise in data analysis and keen insights into motor control theory. Thank you for knowing the power of the contralateral limb. You always challenged me to form more pointed hypotheses and to look at my data in a new light. Richard Nichols, I value your rich insight into sensory systems and spinal cord literature. Each time we met, I left with new knowledge that made my ideas better and clearer. Boris Prilutsky, thank you for sharing your expertise on the intersection between the nervous system and limb mechanics and for helping me quantify the relationships between neural activity and behavior. Matt Tresch, thank you for bringing invaluable insights from the world of *in vitro* spinal cord electrophysiology and helping me shape my experimental design and data analysis techniques. Thank you especially for taking time out of your Argentina trip to attend my defense.

To my labmates, thank you for creating a wonderful work environment and for walking this road with me. I don't think anyone could do this alone, without someone saying, "You can do it" or "It'll be okay" or "Just add some aluminum foil." Thank you for your encouragement, equipment troubleshooting, and conference adventures. Thank you sharing ideas, editing text, and offering an extra pair of hands during experiments. Arick Auyang and Jasper Yen, your Matlab expertise is unrivaled. Where would my data be without you? Jay Bauman, thank you sharing ideas on rat locomotion, kinematics, and motor control and empathizing with the tedium of digitizing. To my undergraduate assistants, Natalia Estrada and Joon Kim, thank you for the hours spent digitizing long videos. Joon, even as an undergraduate, you brought curiosity and insight to the data. Thank you for your work ethic and always being timely with each task. JoAnna Anderson and Amanda Zimmerman, you made lab, classes, and conferences so much fun. Thank

for you for your help along the way, from picking out figures to troubleshooting Matlab code to tracking down equations. Thank you for being my fellow biomedical engineers. Lisa Gozal, I'm so glad we've shared this journey, especially in these final months. Thank you for teaching me how to make "Lisa quality" electrodes and humoring my enthusiasm during experiments. Jacob Shreckengost, thank you for sharing your wealth of presynaptic inhibition knowledge and your tall stack of Jankowska, Eccles, Rudomin, and Wall papers. Thank you for helping me find "real DRPs." Katie Wilkinson, having just finished, you brought great wisdom. Thank you for constantly telling me I could do it and reminding me, "That's plenty of time." Mike Sawchuk, without you the lab might just come to a screeching halt. Thank for the many trips to the hobby store to find a new RC car motor or gear and the many hours spent troubleshooting the treadmill system. Most importantly, thank you for keeping the first aid kit stocked. I wouldn't have all my fingers without it. Quite a list....but each one added a piece to my project and my journey.

Many outside the lab supported me as well. I cannot mention them all, but I want to specifically thank Isaac Clements, Kyla Ross, Jenn Wilhelm, Claire Honeycutt, and Victoria Stahl for their support, advice, and companionship. Also, Brock Wester graciously spent several hours teaching me ProEngineer and Object Printing when I first designed my force platforms and perfusion tank. Bill Goolsby provided his time and expertise in constructing the Wheatstone bridge and amplifier circuitry for my force platform system.

Then, to my family: Mom, Dad, and Hunter, without your endless support, patience, and love, I would not have achieved any of my goals. Thank you being my biggest fans and for always believing in me. Mom and Dad, thank you most of all for

leading me to my faith in God. He is my rock and my salvation, and I found that rock because of you. His creation amazes me, imparting the deep curiosity and love of discovery that inspires my pursuits. Mom, your example taught me to pursue my passions wholeheartedly and to never give less than my best to God's calling on my life. You are a constant source of love and encouragement that has empowered me to cross every hurdle thus far. I love you. Dad, your example taught me to have a tenacious work ethic and to strive for excellence in all I do. Thank you for your wise advice over the years. Thank you for generously giving me a wonderful education and allowing me to pursue my dreams with your support every step of the way. I love you. In 2007 when I married Nathan, I also welcomed a new family into my life. Thank you Cris and Jerry Hayes, Natalie and Eric Schmook for your added support and for allowing me to share my passion with you. The very next year, Hunter brought Kristina Brant into my life as well. Kristina and Hunter, thank you both for your support, your prayers, and your sincere interest in my research.

To my wonderful, amazing, incredible husband, Nathan: I could not imagine a more understanding, loving, and selfless person. Your faithful love and support have carried me through this journey called graduate school. You never let me quit when times got hard, but gave me limitless hugs and encouragement. You regularly reminded me to pursue my passion for helping patients with motor disabilities and never let me lose sight of that goal. Most importantly though, you helped me keep life in perspective. Especially during this last year, thank you for the many home-cooked meals and grocery store trips when I had a long day of experimenting or writing. Thank you for the hours spent reading with me at coffee shops, you with your tome and I with my journal articles. Thank you

for your patience and company during the many long nights of data crunching and writing. Thank you for listening to my worries and frustrations, while sharing in my joys. My burdens have been halved and my joys multiplied. I could go on for pages, but we must get to the data! You are simply the best! I love you more than words can express and can never repay you for all you bring to my life.

To my Lord and Savior, Jesus Christ, may you be glorified in my life and in my work. "Whatever you do, work at it with all your heart, as working for the Lord, not for men." Colossians 3:23

TABLE OF CONTENTS

LIST OF TABLES

Page

LIST OF FIGURES

Page

LIST OF ABBREVIATIONS

SCHP	spinal cord-hindlimb preparation
CPG	central pattern generator
PAD	primary afferent depolarization
DRP	dorsal root potential
Ia	group Ia muscle spindle afferents
Ib	group Ib Golgi tendon organ afferents
EPSP	excitatory postsynaptic potential
aCSF	artificial cerebral spinal fluid
5HT	serotonin or 5-hydroxytryptamine
NMDA	N-methyl-D-aspartate
DA	dopamine
TA	tibialis anterior muscle
LG	lateral gastrocnemius muscle
RF	rectus femoris muscle
VL	vastus lateralis muscle
FDL	flexor digitorum longus
FHL	flexor hallucis longus
EDL	extensor digitorum longus
EHL	extensor hallucis longus
iL2 VR	ipsilateral lumbar ventral root 2
iL5 VR	ipsilateral lumbar ventral root 5
iL2 DRP	dorsal root potential from ipsilateral lumbar dorsal root 2

cL2 DRP	dorsal root potential from contralateral lumbar dorsal root 2
iL5 DRP	dorsal root potential from ipsilateral lumbar dorsal root 5
cL5 DRP	dorsal root potential from contralateral lumbar dorsal root 5

SUMMARY

During locomotion, the spinal cord integrates sensory feedback with central commands to generate appropriate motor behavior. The spinal cord must determine which sensory inputs are important and which to ignore and then use these inputs to regulate motor output. Exactly how the spinal cord achieves this daunting task remains a major question in motor control and sensorimotor rehabilitation.

The broad purpose of this dissertation was to gain new insight into spinal sensory regulation during locomotion. To this end, I developed a novel *in vitro* spinal cord-hindlimb preparation (SCHP) composed of the isolated *in vitro* neonatal rat spinal cord oriented dorsal-up with intact hindlimbs allowed to locomote on a custom-built treadmill or instrumented force platforms. The SCHP combines the neural and pharmacological accessibility of classic *in vitro* spinal cord preparations with intact sensory feedback from physiological hindlimb movements. In this way, the SCHP expands our ability to study spinal sensory function and regulation. Following development, I validated the efficacy of the SCHP for studying behaviorally-relevant, sensory-modulated locomotion by showing the impact of sensory feedback on *in vitro* locomotion. When locomotion was activated by serotonin (5HT) and N-methyl D-aspartate (NMDA), the SCHP was capable of producing kinematics and muscle activation patterns similar to the intact adult rat. Even when activated by the same neurochemicals, the mechanosensory environment could significantly alter SCHP kinematics and muscle activitation patterns, showing that sensory feedback regulates *in vitro* spinal function. I further demonstrated that sensory feedback could reinforce or even initiate SCHP locomotion. In addition to validating the SCHP, these findings also provided the first biomechanical characterization of *in vitro*

locomotion.

Using the SCHP and a custom-designed force platform system, I then investigated how presynaptic inhibition dynamically regulates sensory feedback during locomotion and how hindlimb mechanics influences this regulation. I hypothesized that contralateral limb mechanics would modulate presynaptic inhibition, and thus sensory regulation, on the ipsilateral limb. My results indicate that the contralateral limb, specifically stance-phase limb loading, plays a pivotal role in regulating ipsilateral swing-phase sensory inflow. As contralateral stance-phase force increases, contralateral afferents act via a GABAergic pathway to increase ipsilateral presynaptic inhibition, thereby inhibiting sensory feedback entering the spinal cord during ipsilateral swing. Such force-sensitive contralateral presynaptic inhibition likely serves to preserve swing by reducing or redirecting counterproductive sensory feedback. It may also help coordinate the limbs during locomotion, reduce sensory feedback at higher speeds, and adjust the sensorimotor strategy for task-specific demands.

This work has important implications for sensorimotor rehabilitation. After spinal cord injury, sensory feedback is one of the few remaining inputs available for accessing spinal locomotor circuitry. Thus, understanding how sensory feedback regulates and reinforces spinally-generated locomotion is vital for designing effective rehabilitation strategies. Further, sensory regulation is degraded by many neural injuries and diseases, including spinal cord injury, Parkinson's disease, and stroke, resulting in spasticity and impaired locomotor function. This work suggests that contralateral limb loading may be an important and readily manipulated variable for restoring appropriate sensory regulation during locomotion.

CHAPTER 1

INTRODUCTION

Locomotion is a complex task that requires the coordination of multiple limbs, joints, and muscles, as well as the integration of sensory feedback with central signals. With each step, numerous sensory receptors send information to the spinal cord. The spinal cord must determine which inputs are important and which to ignore and then use these inputs to adapt its motor output to respond to environmental demands and unexpected perturbations. Exactly how the cord achieves this daunting task remains a major question in motor control research.

The broad purpose of this work is to gain insight into sensory regulation in the spinal cord during locomotion through the development of a novel *in vitro* spinal cord-hindlimb preparation (SCHP). Here I present background work on the importance of sensory feedback during locomotion and the power of presynaptic inhibition for regulating that feedback. I show that there is a need for a new model that combines *in vitro* neural accessibility and manipulability with intact sensory feedback to investigate spinal sensorimotor function. Without such models, our knowledge of sensorimotor mechanisms, such as presynaptic inhibition, and their function during behavior remains limited. In the subsequent chapters, I present the development of an *in vitro* spinal cord-hindlimb preparation. This preparation offers exquisite neural accessibility in the presence of physiological, sensory-influenced behavior, enabling us to study spinal sensorimotor circuitry in ways not previously possible. Using this preparation, I then investigated how sensory feedback reinforces and regulates spinal motor output, how sensory access to spinal circuitry is dynamically and selectively regulated at the entry

way to the spinal cord, and how the mechanical state of the hindlimbs influences this regulation.

1.1 Source and organization of sensory feedback from the hindlimbs

Numerous receptors in the hindlimb contribute to movement-related sensory feedback. Input from proprioceptors, such as muscle spindles and Golgi tendon organs, provide muscle length and force feedback. Muscle spindles (Ia and II) lie in parallel with muscle fibers and thus respond to changes in muscle length. Within the spinal cord, Ia projections provide primarily monosynaptic excitatory feedback to the muscle of origin and close synergists, as well as reciprocal inhibition to antagonists (Eccles et al. 1957; Eccles and Lundberg 1958; Nichols et al. 1999). While several pathways project across joints and many muscles are multifunctional, Ia feedback is most powerfully distributed to muscles of similar action and limited to the ipsilateral limb (Harrison and Zytnicki 1984; Nichols et al. 1999). Group II projections are more wide spread, similar to the patterns discussed below for Ib afferents, and the related interneurons project ipsilaterally and contralaterally (Bannatyne et al. 2006). Functionally, length feedback regulates muscle and joint stiffness, helps sculpt locomotion, and contributes to perturbation responses (Nichols and Houk 1973)

Golgi tendon organs (Ib), located within the tendon, lie in series with the muscle to report muscle-tendon force. Because they respond to muscle force, they fire most vigorously during homonymous muscle contraction. In contrast to the Ia system, force feedback is strongest between joints and between groups of similarly acting muscles, especially extensors, while autogenic inhibitory force feedback is rather weak (Jankowska 1992; Nichols et al. 1999). In most cases, this force feedback is primarily

inhibitory, but some muscles about the ankle joint can exhibit antigravity positive force feedback during locomotion (Pearson and Collins 1993; Ross and Nichols 2009). Within the spinal cord, interneurons in Ib pathways receive a broad spectrum of convergent inputs from multiple modalities, from flexors and extensors, and from Ia and Ib afferents. Their outputs are also highly divergent, acting on motoneurons of multiple motor nuclei, interneurons, afferents, and the contralateral circuitry (Jankowska 1992). To manage this extensive complexity, different pathways can be selectively opened or inhibited by descending systems (e.g. monoamines), presynaptic and postsynaptic inhibition, and even limb mechanics to create different coordination strategies (Grillner and Rossignol 1978a). Depending on the task, this diversely projecting force feedback system provides varying degrees of interjoint coordination to regulate whole limb stiffness and plays a prominent role in muscle activation during the stance-phase of locomotion.

Other receptors also provide information regarding limb state. While typically insensitive to midrange movement, joint receptors are sensitive to joint angle at the extremes of joint range (Grigg and Greenspan 1977). Cutaneous receptors can signal paw pad pressure, skin motion during limb movements, and vertical and shear forces (Birznieks et al. 2001; Johansson et al. 1992; Ting and Macpherson 2004). This allows cutaneous input to contribute to the magnitude of postural responses (Honeycutt and Nichols 2010) and to precise paw placement during locomotion (Bouyer and Rossignol 2003a; b).

1.2 Role of sensory feedback in locomotion

Sensory feedback plays an important role in refining the spatiotemporal features of motor output. First, sensory signals, particularly limb extension and loading, are

primary determinants of phase transition timing (Duysens and Pearson 1980b; Grillner and Rossignol 1978b; c; Hiebert et al. 1996; Pearson et al. 1998; Whelan et al. 1995b). Stretching or vibrating hip or ankle flexors can alter the timing of swing onset (Hiebert et al. 1996), while preventing hip extension thwarts swing initiation (Grillner and Rossignol 1978c). Stretch-sensitive muscle spindle receptors in hindlimb flexors, which respond to stretch and vibration, are likely responsible for sensing hip extension and subsequently initiating flexion via autogenic and synergistic excitatory inputs. Even passive oscillatory hip extensions can entrain locomotor speed by altering the duration of stance and the timing of the stance-to-swing transition (Andersson and Grillner 1983; Kriellaars et al. 1994). Finally, stimulation of peripheral nerves during fictive locomotion can reset or entrain centrally-generated rhythms in a task- and phase-dependent manner (Conway et al. 1987; Iizuka et al. 1997; Kiehn et al. 1992; Perreault et al. 1995; Quevedo et al. 2000; Quevedo et al. 2005; Stecina et al. 2005).

Loading contributes to swing initiation as well. Preventing limb unloading can stall swing initiation (Duysens and Pearson 1980a; Pang and Yang 2000), suggesting that force-sensitive Golgi tendon organs (Ibs) in loaded extensors can inhibit flexion generation at the stance-to-swing transition. The contralateral limb also contributes load-related signals. Even once the ipsilateral limb reaches critical hip extension with low load, swing will only initiate if the contralateral limb is prepared to accept the load (Grillner and Rossignol 1978c; Pang and Yang 2000). This effect is consistent in both spinal cats and human infants. Overall, a balance between the excitatory stretch and inhibitory load sensory signals determines the exact timing of the stance-to-swing transition.

In addition to timing, sensory feedback regulates the magnitude and duration of extensor activity during stance, particularly at the ankle (Hiebert and Pearson 1999; Juvin et al. 2007; Pearson and Collins 1993; Pearson et al. 1998). For example, if the cat hindlimb steps in a hole reducing the loading on ankle extensors, ankle extensor magnitude is significantly reduced (Gorassini et al. 1994; Hiebert and Pearson 1999). In contrast, if ankle extensors are artificially stretched, ankle extensor activity and force production increase (Donelan and Pearson 2004). According to studies in both cats and human, length changes in ankle extensors may provide up to 30% of extensor force production and 50% of soleus muscle activation (Sinkjaer et al. 2000; Stein et al. 2000). Responses to length changes are often attributed to Ia muscle spindles, but Ib afferents actually contribute substantially to the generation of ankle extensor activity and their response to extensor muscle lengthening. While Ib feedback is typically inhibitory (Ross and Nichols 2009), Ib feedback onto ankle extensors during locomotion can actually be excitatory. Thus, as force increases, Ibs in ankle extensors can further increase stance-phase extensor activity and force production (Donelan and Pearson 2004; Pearson and Collins 1993).

While less is known about modulation of flexor activity, sensory feedback can influence several facets of swing-phase flexor activity. Stimulation of group I and II flexor nerves during swing or resisting hip flexion both enhance flexor activity (Lam and Pearson 2001; Perreault et al. 1995; Quevedo et al. 2000). Stimulation of toe flexors during swing can prolong and enhance swing (Stecina et al. 2005). In human cycling, changes to contralateral movement and loading also influence the timing and magnitude of recovery-phase flexion in a compensatory manner (Alibiglou et al. 2009; Ting et al.

1998). Chapter 3 offers an additional mechanism that may contribute to swing-phase flexor activity.

In sum, sensory feedback allows the nervous system to dynamically alter its strategy for biomechanical constraints, environmental demands, and injury. Sensory signals can sculpt the timing and the magnitude of both flexors and extensors, and their effects vary across the gait cycle. *Despite this overwhelming importance of sensory feedback, many studies on spinal sensorimotor circuitry are undertaken in the absence of intact feedback. In fact, no current in vitro preparations allow for study of spinal sensorimotor circuitry with adequate and behaviorally-relevant sensory feedback.*

1.3 *In vitro* spinal cord models

In the absence of sensory feedback, the spinal cord contains sufficient circuitry for producing the basic rhythmic patterns that underlie locomotion. This circuitry is termed the central pattern generator (CPG). Because of this property, many of the known mechanistic details of spinal locomotor circuitry have been elucidated using the isolated rodent spinal cord maintained *in vitro*, in which the CPG can be robustly recruited through neurochemical application or electrical stimulation. The circuitry can then be dissected anatomically, physiologically, pharmacologically, and, more recently, molecularly with the advent of transgenic approaches (Kiehn 2006). The ability to apply drugs in known concentrations without interference from the blood-brain barrier and to control the ionic composition of the extracellular environment imparts a great advantage over *in vivo* approaches (Bagust and Kerkut 1981; Smith and Feldman 1987; Smith et al. 1988). Moreover, the mechanical stability of the isolated cord allows for stable intracellular recordings from small neurons (Smith and Feldman 1987; Smith et al. 1988),

a challenging technical feat *in vivo* (Eccles et al. 1961a) and unprecedented during non-fictive hindlimb locomotion. While these advantages make the *in vitro* spinal cord a powerful model system for investigating neural mechanisms of locomotion, the isolated cord alone fails to incorporate sensory feedback from ongoing limb movements (Bagust and Kerkut 1981; Pearson 1995; Pearson et al. 1998; Wheatley and Stein 1992). Thus, many spatiotemporal features of motor output, including phase transition timing and extensor amplitude, as well as the ability to study spinal sensory processing, are lost.

In Chapter 2, I describe the development of a novel mammalian preparation that combines the neural accessibility of *in vitro* preparations with the modulatory influence of sensory feedback from ongoing, physiological hindlimb movements. Previous work in the amphibian (mudpuppy) forelimb has progressed toward this goal (Wheatley and Stein 1992), but no such mammalian nor hindlimb locomotor preparation exists. This model greatly expands our ability to study the spinal sensorimotor circuitry and to relate the neural substrates of movement to their functional outcomes. This model allows for recordings from sensory neurons not possible in the moving intact animal, while monitoring behavior and perturbing the mechanical state of the hindlimbs.

1.4 Regulation of sensory inflow by presynaptic inhibition

Precisely because sensory feedback wields such powerful influence over motor output, it must be tightly regulated. During a task like locomotion, the spinal cord receives vast amounts of sensory information from an array of peripheral receptors. Ideally, the nervous system would establish a mechanism to focus on relevant sensory inputs while reducing or ignoring the effects of inputs that are irrelevant to the task or that might interfere with the intended movement. The nervous system may also need to

open interneuronal pathways to specific postsynaptic targets while closing others. During locomotion, many sensory inputs help modify muscle timing and magnitude to meet environmental demands, but powerful short-latency reflexes could work against locomotion if activated in inappropriate phases. For example, the Ia monosynaptic reflex may contribute to stance-phase muscle activity but could impede swing progression by inappropriately activating extensors. Thus, regulation is important for proper motor task execution.

Both presynaptic and postsynaptic inhibition regulate the effectiveness of sensory transmission onto central circuits (Rudomin et al. 1987; Solodkin et al. 1984), but their actions are quite different. However, presynaptic inhibition of afferents is "more powerful than postsynaptic inhibition in depressing the central excitatory actions of almost all primary afferent fibers (Eccles 1964)." Presynaptic inhibition occurs at the intraspinal terminals of afferents before even the first synapse, so it is the first site for regulating sensory inflow and can prevent any and all effects on spinal neurons. Additionally, presynaptic inhibition exerts longer lasting effects, reducing synaptic efficacy for hundreds of milliseconds (300-400msec), while postsynaptic inhibition lasts only tens of milliseconds (~10-30msec) (Eccles et al. 1962c; Gossard and Rossignol 1990). Presynaptic inhibition can also be highly selective by inhibiting specific intraspinal collaterals of an afferent without affecting transmission in other collaterals of the same afferent (Eguibar et al. 1994; Eguibar et al. 1997b). In this way, presynaptic inhibition converts intraspinal afferent arborizations from hard-wired pathways for afferent transmission into "dynamic substrates in which information arising from the periphery can be addressed to specific neuronal targets (Rudomin 2009)." In contrast, postsynaptic

inhibition alters responses to *all* inputs to a postsynaptic cell by changing the postsynaptic cell's excitability. For a cell with multiple inputs, all inputs are affected equally by postsynaptic inhibition, while presynaptic inhibition can selectively regulate some inputs and not others. Although postsynaptic changes are certainly important (e.g. (Kiehn et al. 2000)) and co-exist with presynaptic effects (Solodkin et al. 1984), presynaptic inhibition is a highly selective and effective way to gate and/or redirect afferent actions.

1.4.1 History and mechanism of presynaptic inhibition

In the 1950s, Hagbarth, Kerr, Wall and colleagues first suggested that afferent transmission might be blocked at the first synapse before any contact with spinal neurons (Hagbarth and Kerr 1954; Howland et al. 1955). Frank and Fourtes (Frank and Fourtes 1957) later confirmed that Ia-evoked motoneuron excitatory post-synaptic potentials (EPSPs) could be reduced without changing motoneuron excitability, confirming a presynaptic source of regulation. Eccles and colleagues later showed that the presynaptic inhibition of the Ia monosynaptic reflex involved the depolarization of Ia terminals that then reduced Ia impulses (Eccles et al. 1961b; Eccles et al. 1962c). They suggested that GABAergic interneurons acting at axo-axonic synapses were responsible for this depolarization.

It is now well-established that presynaptic inhibition often begins with activation of $GABA_A$ receptors on the intraspinal terminals of primary afferents (Rudomin 2009; Rudomin et al. 1998) (Fig. 1.1). Due to an active sodium-potassium-chloride co-transport pump, NKCC1, found on primary afferents, the concentration of chloride is higher in the intracellular space such that the chloride gradient favors outward flow.

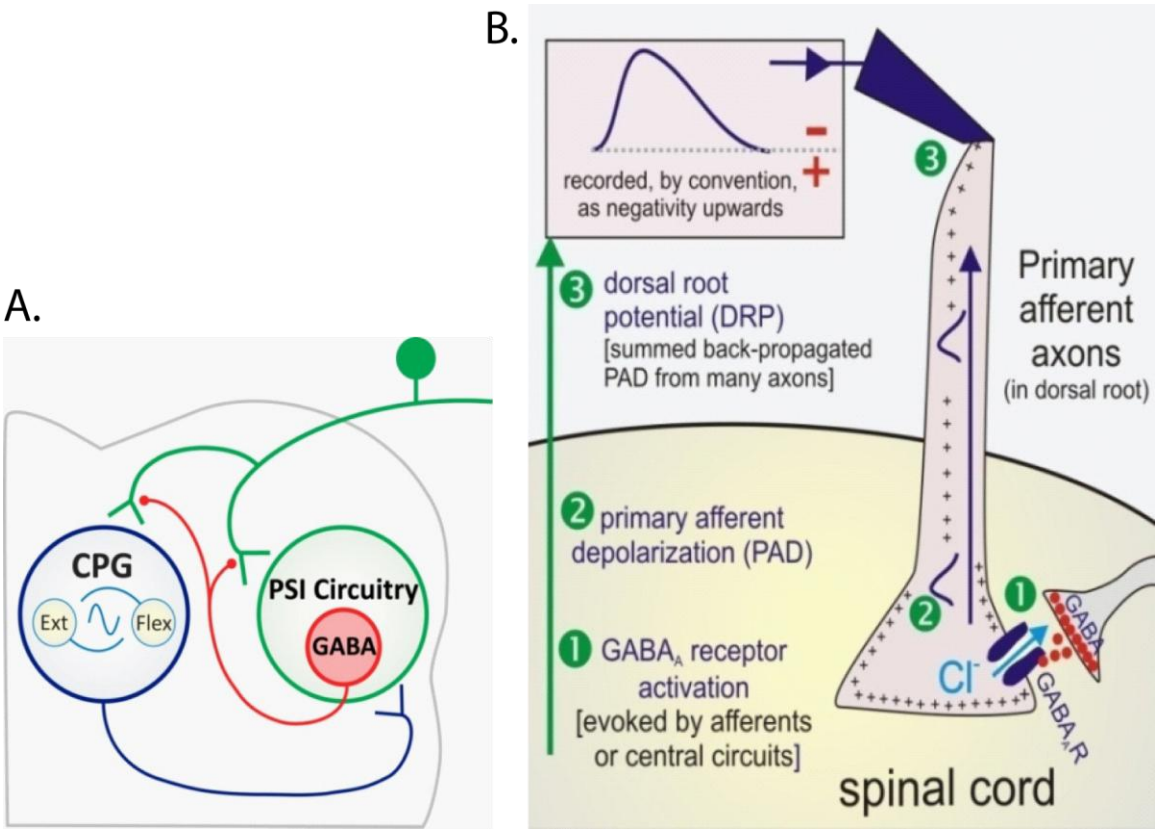

Figure 1.1 : Mechanisms of Presynaptic Inhibition

A: Presynaptic inhibition (PSI) can be evoked by homonymous afferents, heteronymous afferents, or central circuits such as the spinal locomotor circuitry. B: Measurement of and mechanism underlying $GABA_A$-mediated presynaptic inhibition by primary afferent depolarization (modified from (Hochman et al. 2010)). The order of events is numbered 1-3. Following activation by one of the events shown in A, $GABA_A$ergic neurons activate $GABA_A$ receptors are primary afferent terminals in the spinal cord. Because the chloride gradient is maintained to favor outward flow in afferents, chloride effluxes resulting a depolarization wave that travels antidromically into the dorsal root. The depolarization wave can be then be monitored as a dorsal root potential (DRP) at the dorsal root entry zone.

Thus, when $GABA_A$ receptors are activated, chloride flows out of the terminals. This chloride efflux initiates a primary afferent depolarization (PAD) that then travels electrotonically back out the dorsal root toward the periphery. This depolarization then reduces the transmitter released in response to an incoming action potential by inactivating sodium and calcium channels and/or by shunting. In this way, PAD reduces the central action of incoming sensory events (Eccles et al. 1961b; Eccles et al. 1962a; Eccles et al. 1962b; Ménard et al. 2003). Further, because PAD travels back out the dorsal root, presynaptic inhibition can be monitored as a dorsal root potential (DRP), which is the summed back propagated PAD from many axons recorded at the dorsal root entry zone. [Note: Throughout this dissertation, PAD and DRP will be used to indicate presynaptic inhibition.]

Presynaptic inhibition can be activated by homonymous afferents, heteronymous afferents, descending systems, or spinal circuits, such as the locomotor circuitry, typically via $GABA_A$ergic pathways (for review see (Rudomin 2009; Rudomin and Schmidt 1999)). However, since the 1960s, evidence has arisen for several other mechanisms that may contribute to these various forms of presynaptic inhibition. Based on synaptic delays, afferent-evoked presynaptic inhibition was conventionally thought to occur via a minimally trisynaptic pathway, in which afferents activated GABAergic interneurons that then formed axo-axonic synapses on the afferents of origin (homonymous) or on distinct afferents (heteronymous) (Rudomin 2009; Rudomin and Schmidt 1999). New evidence now suggests that afferents in the rat and turtle may also act via more direct synaptic mechanisms, such as the co-release of amino acids or acetylcholine acting on $GABA_A$ receptors or via non-spiking dendro-axonic synapses (Russo et al. 2000; Shreckengost et

al. 2010). In addition to ionotropic $GABA_A$ receptors, metabotropic $GABA_B$ receptors may play a role in longer-term depression of afferent transmission. Non-GABAergic receptors, such $5HT_3$ (Lopez-Garcia and King 1996; Peng et al. 2001), AMPA (Lee et al. 2002), or NMDA (Bardoni et al. 2004) receptors, are also implicated in presynaptic inhibition in the spinal cord dorsal horn.

1.4.2 Patterns of presynaptic inhibition on hindlimb afferents

Afferents themselves, descending systems, and spinal circuits, such as the locomotor circuitry, all contribute to the regulation of sensory transmission via presynaptic inhibition (Fig. 1.1A). The sheer number of potential sources and receiving afferents creates quite a complex system. Through the past fifty years, numerous researchers have mapped the many sources of presynaptic inhibition onto group I muscle, group II muscle, and cutaneous afferents using both intra-axonal and extracellular monitoring of PAD in response to peripheral nerve stimulation at rest or during fictive locomotion. Most investigations have focused on ipsilateral interactions. These findings are summarized in Figure 1.2.

1.4.2.1 Presynaptic inhibition of Ia afferents

Group Ia afferents have received the most attention regarding their presynaptic inhibition patterns. Due to their monosynaptic connections onto motoneurons, only two sites exist for modulation of Ia effects on motor output, making presynaptic inhibition even more important. Without modulation, the powerful inputs from Ia afferents could saturate motoneurons, thereby reducing motoneuron sensitivity to further afferent input(Capaday and Stein 1987).

In contrast to the precise organization of their reflex pathways, Ia afferents

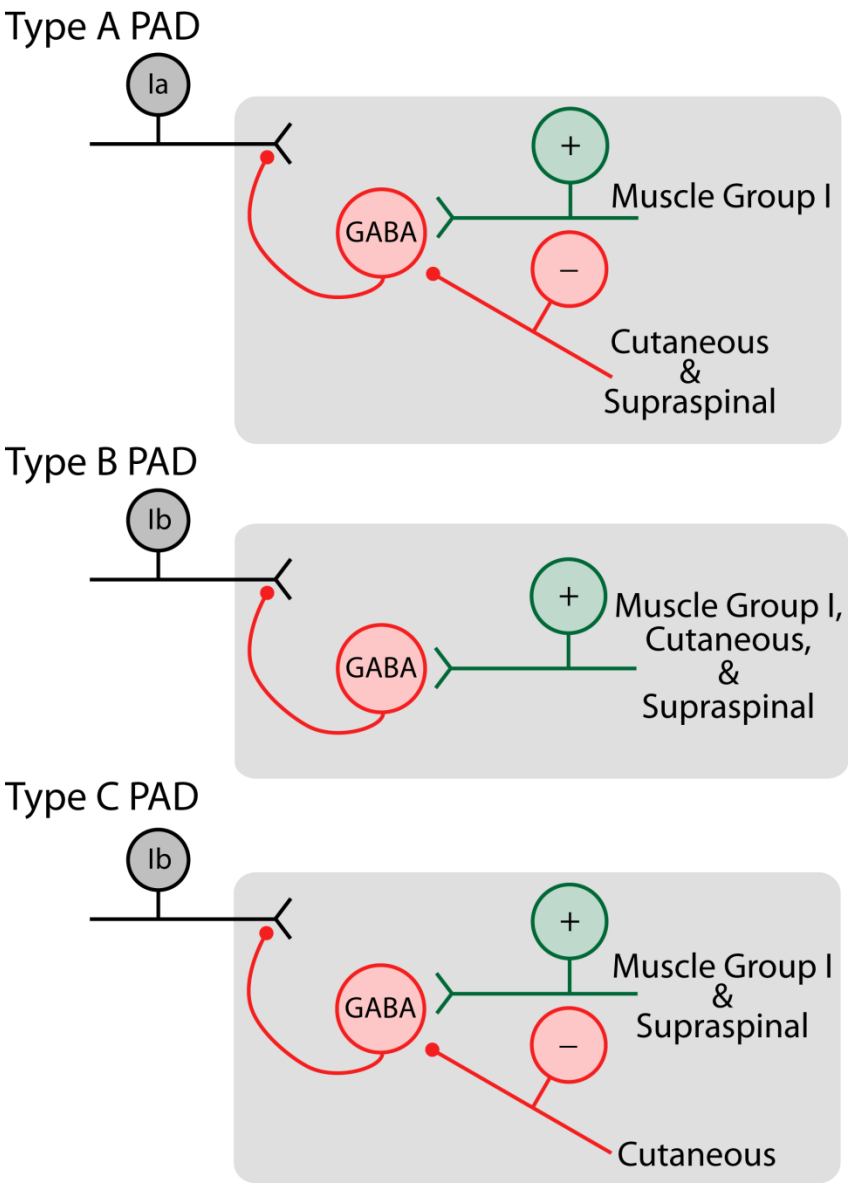

Figure 1.2 : Patterns of PAD-related Presynaptic Inhibition

Muscle afferents typically exhibit three patterns of afferent-evoked presynaptic inhibition derived from ipsilateral afferents. Type A PAD: Muscle group I afferents produce PAD in the receiving group I afferent, but conditioning with cutaneous stimulation reduces this PAD likely by inhibiting interposed interneurons in the PAD pathway. Type B PAD: Muscle group I, cutaneous, and many descending supraspinal systems all produce PAD in the receiving group I afferent. Type C PAD: Muscle group I afferents and many descending supraspinal systems produce PAD in the receiving group I afferent, but cutaneous input reduces this PAD as in Type A. Most group Ia afferents exhibit Type A and most group Ib afferents exhibit Type B or C, but all three patterns have been observed in both populations.

receive presynaptic inhibition from group I muscle afferents, both Ia and Ib, from across the ipsilateral hindlimb and across functional groups (Eccles et al. 1961b; Eccles et al. 1962c; Enríquez et al. 1996; Iles 1996; Rudomin and Schmidt 1999). In general, flexor group I afferents are more effective than extensors in evoking presynaptic inhibition of Ia afferents, but the presynaptic inhibition of extensor Ia afferents is often stronger than that seen in flexors (Eccles et al. 1962c; Rudomin 2009). Thus, flexors are stronger *sources* of Ia presynaptic inhibition while extensors *receive* stronger inhibition. The reticulospinal system can also induce presynaptic inhibition in Ia afferents, while other supraspinal systems only weakly contribute (Jankowska 1992; Rudomin et al. 1983).

In contrast, stimulation of cutaneous nerves or supraspinal centers actually reduces the PAD produced in Ia afferents by stimulation of group I muscle afferents (Eguibar et al. 1997a; Enríquez et al. 1996; Rudomin et al. 1983; Rudomin and Schmidt 1999). For example, conditioning stimuli in the superficial peroneal cutaneous nerve reduces the PAD produced in plantaris Ia afferents by stimulation of a hamstring nerve (Menard et al. 2002). Based on these results, many postulate that PAD pathway interneurons receive convergent segmental, multimodal, and supraspinal inputs that can modulate PAD transmission, thereby adjusting presynaptic inhibition of other afferent inputs.

In sum, most group Ia afferents receive PAD-related presynaptic inhibition from group I muscle afferents while supraspinal and cutaneous inputs reduce that PAD. This pattern is often termed Type A PAD (Fig. 1.2).

1.4.2.2 Presynaptic inhibition of Ib afferents

Because Ib afferents receive such widely convergent input from diverse afferents,

presynaptic inhibition may serve to modulate and filter the relative contribution of each afferent type (Jankowska 1992; Zytnicki and Jami 1998). While Ia modulation adjusts primarily excitatory input onto synergistic motoneurons, Ib modulation adjusts the gain of negative feedback onto a diversity of motoneurons.

Ib afferents receive PAD-related presynaptic inhibition from group I afferents and from many descending supraspinal systems, including the rubrospinal, reticulospinal, corticospinal, vestibulospinal, and pyramidal tracts. Stimulation of cutaneous nerves can either produce PAD or reduce the PAD produced by other inputs (Rudomin 2009; Rudomin et al. 1998). If group I, descending, and cutaneous inputs all produce PAD, the pattern is called Type B PAD; if group I and descending inputs produce PAD, but cutaneous inputs reduce that PAD, the pattern is called Type C PAD (Fig 1.2). Additionally, Ib afferents receive strong autogenic PAD from other Ib afferents (Zytnicki and Jami 1998).

1.4.2.3 Differences within modalities

As with all biology, things are not as simple as they may first appear. While Ia afferents typically exhibit A and Ibs B or C, Enriquez and colleagues showed that type A, B, and C PAD can be found in both Ia and Ib afferents (Enríquez et al. 1996). On average, approximately 52% of Ia afferents exhibit type A, 26% type B, and 13% type C. The proportions are reversed for Ib afferents, with approximately 11% exhibiting type A, 35% type B, and 54% type C. Thus, PAD-related presynaptic inhibition exhibits complex multimodal and multisystem integration such that activation of afferents, spinal circuits, and supraspinal systems interact to influence the ultimate pattern during a behavior.

1.4.2.4 Presynaptic inhibition of cutaneous and other afferents

Cutaneous afferents receive the strongest presynaptic inhibition from other modality-specific cutaneous afferents (Eccles et al. 1963). Low-threshold cutaneous afferents, which likely contribute to movement, are also inhibited by group Ib II and III muscle afferents as well as supraspinal systems (Rudomin and Schmidt 1999).

Similarly, group II muscle afferents receive the strongest inhibition from other group IIs, but may also receive weaker presynaptic inhibition from group I, cutaneous, and/or supraspinal inputs.

Unlike most other afferents, joint afferents receive little autogenic PAD and often preserve the information from the periphery, possibly serving to monitor any extreme deviations in posture (Rudomin 2009). However, joint afferents can be inhibited by cutaneous afferents, group I and II muscle afferents, and select descending systems. Cutaneous afferents may also reduce the group I-evoked PAD in joint afferents, as seen in Ia afferents (Jankowska et al. 1993).

1.4.2.5 Contralateral contributions to presynaptic inhibition

Most of the investigations on afferent-evoked presynaptic inhibition have focused on ipsilateral effects with little attention given to contralateral afferents. A small number of early studies found that stimulation of group I and flexor reflex afferents produced a contralateral DRP along with the larger ipsilateral DRP (Devanandan et al. 1965; Gossard and Rossignol 1990; Jankowska et al. 1966). Figure 1.3 summarizes these findings. As shown, most contralateral presynaptic inhibition involves Ib afferents as both the source and receiving afferents (Devanandan et al. 1965). In the pentobarbital anesthetized cat, Ib afferents evoked presynaptic inhibition of contralateral Ib afferents, but Ia afferents neither gave nor received contralateral presynaptic inhibition, mirroring the largely

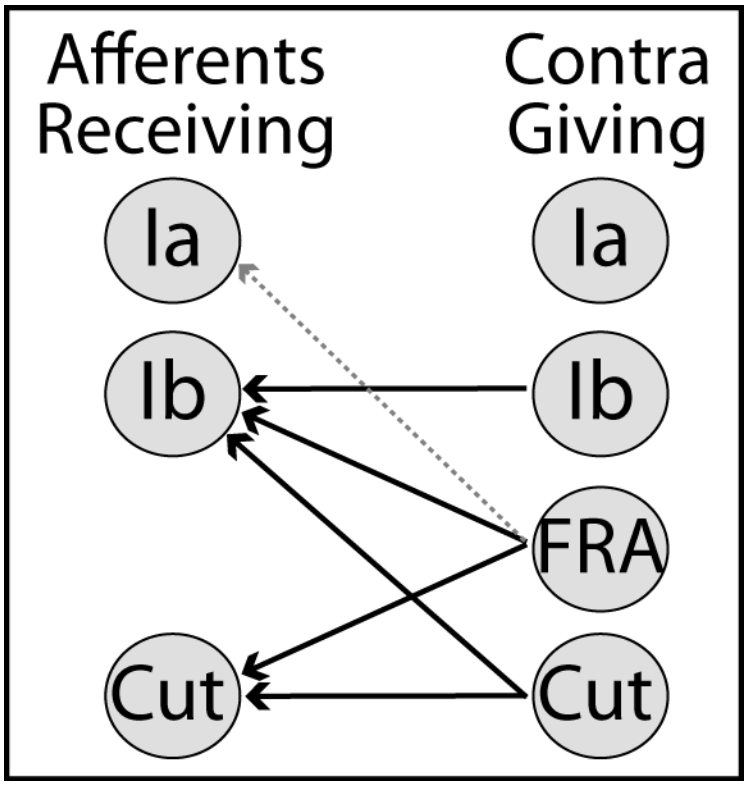

Figure 1.3 : Identified Pathways for Contralateral Presynaptic Inhibition

Previous studies have shown that contralateral afferents (contra giving) can evoke PAD-related presynaptic inhibition in ipsilateral afferents (afferents receiving). Cut = cutaneous afferents. FRA = flexor reflex afferents, such as group II, III, and high threshold cutaneous afferents. **Ias:** Muscle spindle Ia afferents do not exert contralateral presynaptic inhibition on any fibers. Under certain states, such as L-DOPA, Ias may receive inhibition from FRAs. **Ibs:** Golgi tendon Ib afferents both give and receive contralateral presynaptic inhibition, particularly Ib onto Ib. Contralateral FRAs (mostly group III) and cutaneous afferents can also evoke PAD in Ibs. **Cutaneous:** Finally, cutaneous afferents receive contralateral PAD-related presynaptic inhibition from similar cutaneous afferents as well as FRAs. Modified from (Baldissera et al. 1981; Devanandan et al. 1965). Data taken from (Baldissera et al. 1981; Devanandan et al. 1965; Eccles et al. 1964; Jankowska et al. 1966)

ipsilateral Ia afferent reflex patterns (Devanandan et al. 1965; Jankowska 1992). In the presence of L-DOPA, which is known to gate flexor reflex pathways, higher threshold flexor reflex afferents (typically group III not II) could evoke inhibition of contralateral Ia afferents (Jankowska et al. 1966). No studies have demonstrated Ia-evoked crossed inhibition under any conditions.

Studies in cycling further affirm that sensory inputs from the contralateral limb affect ipsilateral sensory transmission and motor output, particularly of flexors (Alibiglou et al. 2009; Ting et al. 1998). Although contralateral influences may be attributed to central interlimb coupling or postsynaptic effects, these finding coupled with identified crossed presynaptic inhibition pathways imply that contralateral movement-related feedback may play a role in ipsilateral sensory regulation. *Yet, no recent work has investigated crossed presynaptic pathways, and little is known about the potential role of contralateral presynaptic inhibition during movements like locomotion that require interlimb coordination.*

1.4.3 Presynaptic inhibition during behavior

While much is known about afferent-evoked presynaptic inhibition at rest, less is known about presynaptic inhibition during behavior. It has been difficult to study both centrally-evoked and afferent-evoked presynaptic inhibition during non-fictive locomotion because it is "almost technically *impossible* to record PADs during *real* walking (Menard et al. 1999)." The DC recordings required to monitor slow changes in afferent membrane potential are simply too sensitive to spinal cord movement. To the best of our knowledge, there is only one brief report in the literature of DRPs recording during non-fictive locomotion (Yakhnitsa et al. 1988). However, studies during fictive

locomotion and inferences from reflex studies in humans and primates indicate that presynaptic inhibition may be quite active during movement and exhibit both phase and task dependencies.

1.4.3.1 Fictive locomotor studies indicate phase- and task-dependent presynaptic modulation of reflex transmission

From fictive locomotion studies, we know that DRPs and intra-axonal PAD are rhythmic during locomotion (e.g. (Duenas and Rudomin 1988; Gossard et al. 1991)). Locomotor-related rhythmic DRPs persist in the low-spinal cat, confirming that the spinal locomotor circuitry induce rhythmic presynaptic inhibition in the absence of descending systems and rhythmic afferent feedback. Intra-axonal recordings from afferents, as well as extracellular DRP recordings, indicate that centrally-evoked locomotor-related inhibition is typically maximum during the flexion phase in the majority of flexor, extensor, and bifunctional group I and group II muscle afferents, as well as cutaneous afferents (Gossard et al. 1989; Gossard et al. 1991). However, based on coupled intracellular recordings from afferents and motoneurons, afferent-evoked PAD is much more effective than locomotor-related PAD at inhibiting the monosysnaptic reflex during locomotion (Gossard 1996). Importantly though, activation of the locomotor circuitry modulates the effectiveness of sensory-evoked PAD for reducing the monosynaptic reflex in a phase-dependent and muscle-dependent manner (Menard et al. 1999; Ménard et al. 2003). During fictive locomotion, stimulation of the posterior-biceps-semitendinosus nerve reduces the plantaris monosynaptic reflex most effectively between late flexion and mid stance. However, the most effective phase for PBSt-evoked presynaptic inhibition varies significantly depending on the target muscle for the monosynaptic reflex. This

change in effective phase is particularly strong between flexors and extensors. Therefore, while the centrally-evoked PAD alone may not strongly affect afferent transmission, the spinal locomotor circuitry does influence the effectiveness of sensory-evoked PAD for modulating afferent transmission, likely by regulating the excitability of interposed PAD pathways (Menard et al. 1999; Ménard et al. 2003).

Additionally, both central and afferent-evoked presynaptic inhibition patterns are task dependent. By comparing fictive behaviors, Cote and Gossard showed that rhythmic PAD during fictive locomotion was ~34% smaller and maximum during late flexion, while PAD during fictive scratching was larger and maximum during early extension (Cote and Gossard 2003). On the other hand, afferent-evoked PAD from peripheral nerve stimulation was more reduced during scratch than during locomotion, suggesting that the scratch may involve more centrally-evoked presynaptic inhibition while locomotion may involve more afferent-evoked presynaptic inhibition.

In addition to interactions between the locomotor circuitry and afferent-evoked presynaptic inhibition, there are also afferent modality interactions that vary depending on the task. For example, cutaneous stimulation typically propduces presynaptic inhibition of Ib afferents at rest (Rudomin et al. 1983), but reduces muscle-evoked presynaptic inhibition of Ib afferents during fictive locomotion (Menard et al. 2002). Again, this reveals task-dependency, particularly for Ib afferents.

Together, these findings indicate that spinal locomotor circuitry and afferent modalities interact to create dynamic patterns of presynaptic sensory regulation that are highly phase and task dependent. *Given these complex interactions, it is vital to study the patterns of locomotion in the most behaviorally relevant conditions possible and with the*

most natural patterns of afferent interactions possible. Peripheral nerve stimulation during fictive locomotion artificially activates all afferents of a given threshold simultaneously in a pattern that differs from natural afferent patterns. While stimulation of multiple modalities shows that afferents influence presynaptic inhibition by other afferents, *the resultant pattern produced during different forms of locomotor behavior remains elusive.* Finally, most of the work has focused on the most direct reflex pathway, the monosynaptic reflex. Many afferent pathways contribute to locomotor modulation and, therefore, deserve further investigation.

1.4.3.2 H-reflex studies suggest role of presynaptic inhibition in voluntary movement

Because presynaptic inhibition is technically difficult to monitor during movement, researchers often utilize the H-reflex, the electrical activation of the monosynaptic reflex, to predict presynaptic inhibition of Ia afferents during voluntary movement. Early work by Hultborn and colleagues showed that the H-reflex of the contracting muscle increases while the H-reflex of antagonist muscles decreases just prior to and during voluntary contraction in humans. This work suggests that descending presynaptic inhibition may selectively increase monosynaptic reflex sensitivity in contracting muscles and reduce sensitivity in muscles whose monosynaptic reflex could resist the intended movement (Hultborn et al. 1987). Recent work in monkeys also implicated descending contributions to presynaptic regulation of cutaneous inputs just prior to and during voluntary contractions (Seki et al. 2003).

In agreement with PAD and DRP patterns during fictive locomotion, the soleus H-reflex is phasically modulated during locomotion, with a maximum during stance and minimum during swing. As during fictive locomotion, H-reflex modulation is task-

dependent. For example, H-reflexes are significantly lower during running compared to walking, suggesting increased presynaptic inhibition during running, particularly during the swing phase. In addition to active movements, passive movement can also elicit cyclic H-reflex modulation (Brooke et al. 1995a; McIlroy et al. 1992). In agreement with peripheral nerve stimulation during fictive locomotion, these results all imply that sensory input, even during passive movements, can powerfully and presynaptically inhibit Ia monosynaptic transmission during locomotion.

H-reflexes also suggest a role for contralaterally-mediated presynaptic inhibition. Both active and passive stepping or pedaling of the contralateral limb result in H-reflex depression on the ipsilateral limb (Brooke et al. 1995a; Collins et al. 1993; McIlroy et al. 1992). Although the depression is smaller and less phasic compared to ipsilateral effects, contralateral movement appears to play a role in ipsilateral sensory regulation purportedly via presynaptic inhibition of Ia afferents. Non-reflex studies further highlight contralateral influences on ipsilateral motor output and reflex sensitivity, particularly during flexion. During cycling, changes in contralateral phasing or the absence of contralateral movement alters the spatiotemporal features of flexor muscle activation (Alibiglou et al. 2009; Ting et al. 1998). In spinal cats, altering the position of the contralateral limb reverses the effects of sensory inputs on the ipsilateral limb, again suggesting contralateral afferents may regulate ipsilateral sensory pathways (Grillner and Rossignol 1978a).

It should be noted again that no contralateral low-threshold afferents sources could evoke presynaptic inhibition of Ia afferents in the pentobarbital anesthetized cat (Devanandan et al. 1965). This finding contradicts the assertion that H-reflex modulation

(i.e. Ia afferent reflex modulation) partially results from presynaptic inhibition of Ia afferents. This apparent discrepancy may be explained by pentobarbital suppression of the polysynaptic transmission required for crossed inhibition (Eccles 1946; Mehta and Ticku 1999; Ziskind-Conhaim 1990), postsynaptic rather than presynaptic H-reflex modulation, or differences between cat and human sensory organization. However, more research is clearly needed to determine the existence of contralaterally-derived presynaptic inhibition of Ia afferents.

Like fictive locomotion studies, H-reflexes suggest that presynaptic inhibition may selectively regulate sensory input in a phase- and task-dependent manner to prevent counteractive effects during voluntary motor tasks. However, as emphasized by Stein, H-reflex studies alone cannot truly distinguish pre and postsynaptic effects (Stein 1995). Both presynaptic and postsynaptic inhibition can result in H-reflex reduction. Intracellular studies in the cat, as well as computer modeling studies, suggest that postsynaptic changes cannot account for large changes in monosynaptic reflex amplitude independent of motor pool recruitment level (Capaday and Stein 1989; Heckman and Binder 1993). Holding background muscle activity constant helps to ensure constant motor pool excitability and recruitment to isolate presynaptic inhibition, but postsynaptic threshold changes cannot be fully ruled out since different motor units may contribute at any time. In addition, the work of Sinkjaer and colleagues showed that modulation of the electrically-activated H-reflex can differ significantly from modulation of the physiologically-activated stretch reflex during human walking, highlighting the need for caution when interpreting H-reflex studies (Anderson and Sinkjaer 1999). The observed discrepancies may reflect the difference between artificial and synchronouos activation of

all low-threshold afferents used in H-reflex testing and the more specific and natural activation of Ia afferents during muscle stretch. Additionally, fusimotor drive and initial muscle length affect the stretch reflex but not the H-reflex due to the direct electrical activation of afferents. Therefore, while H-reflex studies offer insight into the potential contributions of presynaptic inhibition to voluntary motor control, their results should be validated with more direct measures of presynaptic inhibition.

1.4.4 Limitations of previous presynaptic inhibition studies

As Rudomin stated in his 2009 review, "After 50 years of continuous research it is fairly well established that the synaptic effectiveness of muscle, articular and cutaneous afferents can be modulated by a variety of peripheral and central mechanisms...There is still limited information on the functional organization of the pathways...and even less information on their role in the control of sensory information in behaving organisms (Rudomin 2009)." Eccles, Rudomin, Jankowska, Gossard, and others have spent years mapping the pathways of presynaptic inhibition. Yet, due to technical challenges, our understanding of the role of presynaptic inhibition in behavior remains limited. We know that presynaptic inhibition is highly task-dependent and influenced by strong central and multimodal afferent interactions. Therefore, it is vital to study the patterns of locomotion in the most behaviorally relevant conditions possible and with the most natural afferent interactions possible to identify the true function of presynaptic inhibition in locomotion.

Further, only a limited number of studies have investigated crossed pathways, primarily under pentobarbital anesthesia which alters polysynaptic transmission and potentiates $GABA_A$ receptor activity (Eccles 1946; Mehta and Ticku 1999; Ziskind-Conhaim 1990). Due to the interlimb nature of locomotion, the nervous system must

coordinate the limbs to avoid falling and efficiently move the body. While central circuitry and peripheral mechanical coupling may contribute to this goal, cycling and H-reflex studies suggest that contralateral sensory inputs and contralaterally-derived presynaptic inhibition are likely valuable tools for interlimb coupling and coordination. Therefore, contralateral presynaptic inhibition deserves much further investigation.

By providing for stable DC recordings, development of the *in vitro* spinal cord-hindlimb preparation (SCHP) described in Chapter 2 allows us to investigate the role of presynaptic inhibition with intact sensory inputs and central-sensory interactions. The SCHP also offers us the unique opportunity to investigate both the contralateral and ipsilateral contributions to presynaptic inhibition, while manipulating the mechanics and neural system in ways not otherwise possible.

1.5 Aims and objectives

The objective of this dissertation is to gain insight into sensory regulation in the spinal cord during locomotion using an *in vitro* spinal cord-hindlimb preparation. This objective was divided into four specific aims. **1)** First, I developed the dorsal-up *in vitro* spinal cord-hindlimb preparation (SCHP) in the neonatal rat (Chapter 2). This preparation offers exquisite neural accessibility in the presence of physiological, sensory-influenced behavior, enabling us to study spinal sensorimotor circuitry in ways not previously possible. **2)** I then validated the efficacy of the SCHP for studying behaviorally-relevant and sensory modulated spinal function by showing the impacts of sensory feedback on *in vitro* spinal function and locomotion (Chapter 2). In addition to validating the SCHP, these studies provided insight into how sensory feedback can reinforce and regulate spinal motor output. **3)** Using the SCHP, I then investigated how presynaptic inhibition

dynamically regulates sensory feedback during non-fictive locomotion. Specifically, I asked how the mechanical state of the ipsilateral and contralateral hindlimb influences presynaptic inhibition (Chapter 3). **4)** Finally, I considered the neural sources generating the most prominent characteristics of locomotor presynaptic inhibition (Chapter 3).

1.6 Clinical and scientific significance

After spinal cord injury, sensory feedback is one of the few remaining inputs for accessing spinal circuitry. Understanding how sensory feedback influences spinal cord function and how sensory feedback can reinforce locomotion in the absence of descending brain inputs is vital to designing effective rehabilitation strategies. By combining neural accessibility with sensory-influenced behavior, the novel *in vitro* preparation enhances our ability to study spinal locomotor circuitry in a behaviorally-relevant state. The SCHP allows us to investigate how mechanosensory manipulations influence behavior as well as neural circuit function.

Sensory regulation is often dysfunctional after spinal cord injury and other neural injuries or diseases, such as stroke, peripheral nerve injury, or Parkinson's disease (Calancie et al. 1993; Enríquez et al. 1996; Garcia et al. 2006; Milanov 1992; Morita et al. 2000). Due to the loss or damage of descending systems, presynaptic inhibition is typically reduced, contributing to spasticity and interfering with locomotor training (Calancie et al. 1993; Morita et al. 2000; Stein 1995). Appropriate sensory regulation is important for effective locomotor retraining and recovery. Thus, understanding how presynaptic inhibition functions during locomotion and how peripheral inputs can manipulate that function will help us restore sensory regulation after injury and disease and hopefully improve locomotor outcomes.

CHAPTER 2

AN IN VITRO SPINAL-CORD HINDLIMB PREPARATION FOR STUDYING BEHAVIORALLY RELEVANT RAT LOCOMOTOR FUNCTION

This chapter was originally published in the Journal of Neurophysiology: Hayes HB, Chang Y-H, and Hochman S. An *in vitro* spinal cord-hindlimb preparation for studying behaviorally relevant rat locomotor function. *J Neurophysiol* 101: 1114-1122, 2009 (doi:10.1152/jn.90523.2008). *Used with permission from the American Physiological Society*. Asterisks* indicate post-publication additions.

2.1 Introduction

The spinal cord contains all the circuitry required for producing the basic rhythmic motor patterns that underlie locomotion. While this spinal circuitry, often termed the central pattern generator (CPG), can produce locomotor behavior in the absence of phasic sensory input, sensory feedback is known to play an important role in refining the spatiotemporal features of these motor patterns to match environmental demands and correct for unexpected errors. Sensory signals are a major determining factor in both the timing of phase transitions (Duysens and Pearson 1980b; Grillner and Rossignol 1978b; Hiebert et al. 1996; Pearson et al. 1998; Whelan et al. 1995b) and the magnitude and duration of extensor activity during stance (Hiebert and Pearson 1999; Juvin et al. 2007; Pearson and Collins 1993; Pearson et al. 1998; Rossignol et al. 2006). They are also capable of resetting and entraining centrally-generated rhythms in a phase-dependent manner (Conway et al. 1987; Iizuka et al. 1997; Kriellaars et al. 1994; Pearson et al. 1998).

Many of the known properties of the locomotor CPG have been elucidated using the isolated rodent spinal cord, in which the CPG can be robustly recruited through neurochemical application or electrical stimulation. The circuitry can then be dissected anatomically, physiologically, pharmacologically, and, more recently, molecularly with the advent of transgenic approaches. The ability to apply drugs in known concentrations without interference from the blood-brain barrier and to control the ionic composition of the extracellular environment imparts a great advantage over *in vivo* approaches (Bagust and Kerkut 1981; Smith and Feldman 1987; Smith et al. 1988). Moreover, the mechanical stability of the isolated cord allows for stable intracellular recordings from small neurons (Cheng et al. 2002; Smith and Feldman 1987; Smith et al. 1988; Wheatley et al. 1994a), a challenging technical feat *in vivo* (Eccles et al. 1961a) and unprecedented during non-fictive hindlimb locomotion. While these advantages make the *in vitro* preparation a powerful model system for investigating neuronal mechanisms of locomotion, the isolated cord fails to incorporate sensory feedback from ongoing limb movements which is known to be vital in the patterning of locomotion (Bagust and Kerkut 1981; Pearson 1995; Pearson et al. 1998; Wheatley and Stein 1992). Many of the spatiotemporal features of motor output, such as phase transition timing and extensor amplitude modulation, are lost in the absence of sensory influences.

The goal of this work is to develop a novel mammalian preparation that combines the neural accessibility and manipulability of *in vitro* preparations with the modulatory influence of sensory feedback from ongoing, physiologically-relevant movement. This requires the retention of dorsal roots and intact hindlimbs as well as an appropriate environment for natural limb stepping, including appropriate orientation relative to

gravity and mechanical interactions. Previous work in the amphibian (mudpuppy) forelimb has progressed toward this goal (Wheatley and Stein 1992), but no such mammalian nor hindlimb locomotor preparation exists. Our new preparation is composed of a fully-exposed neonatal rat spinal cord with hindlimbs attached. The isolated cord and hindlimbs are oriented dorsal-up in a physiologically-appropriate locomotor posture with the limbs allowed to step on a treadmill.

Here I present the first biomechanical characterization of *in vitro* rat hindlimb locomotion, including kinematics from the dorsal-up preparation. I compare these kinematics to those from mechanically similar *in vivo* conditions to provide a framework for understanding their behavioral relevance. I also show electromyography from hindlimbs during both dorsal-up and ventral-up *in vitro* locomotion. While electromyography of the restrained or air-stepping limb has been reported (Atsuta et al. 1990; Kiehn and Kjaerulf 1996), electromyography from appropriately oriented (dorsal-up) and unrestrained hindlimbs during *in vitro* locomotion has not been shown. Finally, to demonstrate the importance of sensory feedback in motor patterning, I compare muscle activation patterns between dorsal- and ventral-up locomotion and demonstrate the effect of sensory perturbations on muscle activation patterns and stride timing. A portion of these results have been presented in abstract form (Brant and Chang 2006; Brant et al. 2006).

2.2 Methods

All procedures described here comply with the principles of The Care and Use of Animals outlined by the American Physiological Society and were approved by the Emory University Institutional Animal Care and Use Committee.

2.2.1 Dissection

Neonatal rats (Sprague-Dawley) postnatal days 1-4 were first decapitated and eviscerated, leaving only the vertebral column, pelvis, and hindlimbs attached to the cord. All skin was removed except that covering the feet. The preparation was then secured in a dissection chamber filled with continuously oxygenated low calcium, high magnesium artificial cerebrospinal fluid (aCSF - see *Bathing Solutions*). Ventral vertebrectomy and dorsal laminectomy exposed the ventral and dorsal sides from the upper cervical transection to mid-sacral level. Care was taken to preserve all ventral and dorsal roots to maintain complete hindlimb innervation.

The isolated cord-hindlimb preparations were then transferred to a perfusion chamber designed to allow dorsal-up, unrestrained hindlimb locomotion (Fig. 2.1 described below*)*. The cords were secured to the Sylgard with insect pins through the remaining ribs in a dorsal-up posture, with the hindlimbs and sacral cord hanging pendant in the caudal portion of the chamber. Cord position was adjusted to approximate physiological locomotor posture.

2.2.2 Perfusion chamber and treadmill

Rectangular perfusion chambers were constructed from 3mm thick, transparent lucite acrylic sheets (GE Polymer Shapes) and filled with Sylgard. A small Sylgard block was then cut from the caudal portion of each chamber to create space for a custom treadmill and unrestrained hindlimb locomotion.

The treadmill belt, composed of a 30mm wide by 130mm long polyurethane belt (McMaster-Carr), was mounted around plastic rollers (Tamiya Inc) and two metal shafts. The shafts were drilled perpendicularly through the lucite walls and the holes sealed

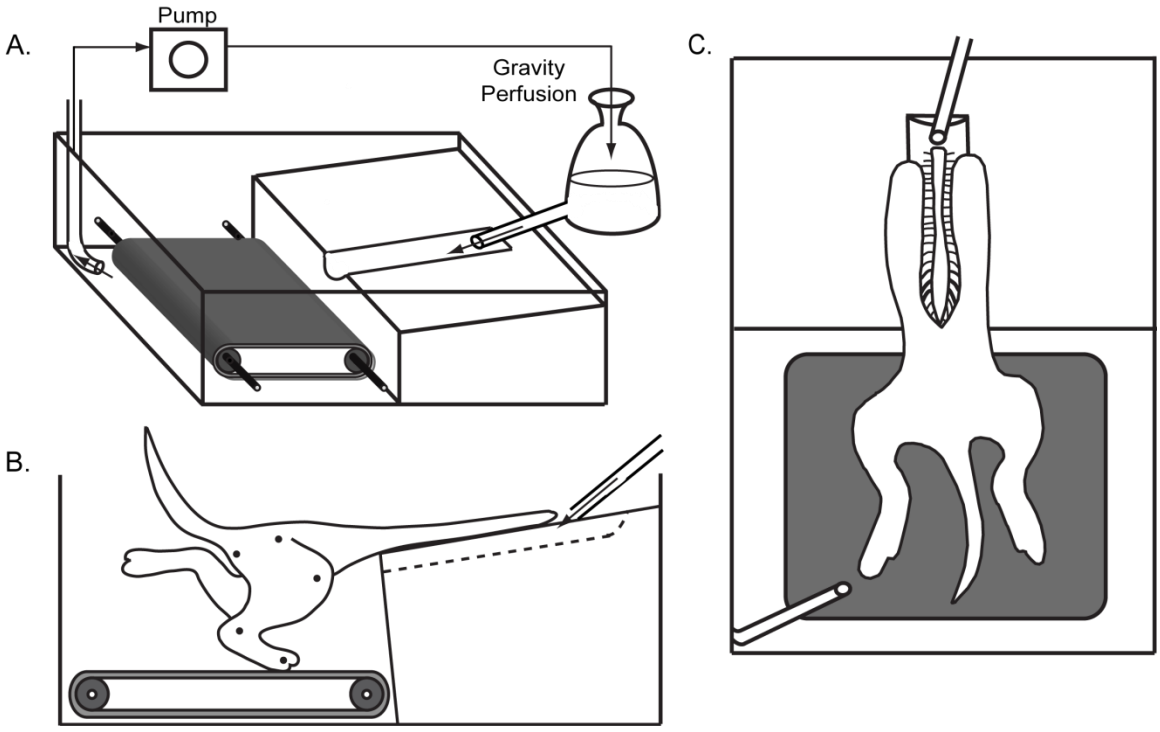

Figure 2.1 : SCHP Experimental Setup

Recording chamber and perfusion system. The continuously oxygenated aCSF flows from the gravity perfusion system, through the duct under the ventral surface of the cord, and then is pumped back to the gravity perfusion system via the peristaltic pump. B: Sagittal view of the isolated cord-hindlimb preparation and treadmill. The exposed cord is secured to the Sylgard by insect pins and the hindlimbs allowed to locomote freely on a treadmill in the caudal chamber. C: Overhead view of the isolated cord-hindlimb preparation and treadmill.

using either epoxy or petroleum jelly to prevent aCSF from leaking from the chamber. The front shaft and roller were driven by a small, brushed DC motor (Tamiya Inc, GM7), whose speed was adjustable between 2-12mm/s by incrementally increasing the voltage across the motor. The back rollers were passively turned by the belt. In later experiments, a brushless DC motor and electronic speed controller (Novak, Goat Brushless Crawler System) was used to reduce motor-related noise in the electromyographic recordings.

Since much of the motor circuitry is known to lie in the ventral portion of the cord, which is partially encased by the remaining vertebral column, a cord perfusion system was added to direct flow along the ventral surface of the cord. A small duct was channeled into the top surface of the Sylgard under the cord. A gravity-fed perfusion system, with the tip of the output at the rostral end of the duct, was then used to supply continuously oxygenated aCSF at 20-30 mL/min, with or without drugs, through the duct beneath the ventral surface. Tubing attached to a peristaltic pump (Cole Palmer Masterflex) was placed in the caudal compartment to recirculate the solution to the gravity system reservoir (Fig. 2.1A). During initial setup, a biologically inert dye was used to visualize flow, and input/output locations were adjusted until diffusion appeared uniform across the ventral surface of the cord. Some experiments were carried out in the absence of the perfusion system, but success of pharmacological activation was greater with continuous perfusion.

2.2.3 Bathing Solutions

All bathing solutions were continuously oxygenated with 95% O_2, 5% CO_2. The standard bathing solution was an artificial cerebral spinal fluid (aCSF) containing (in mM): 128 NaCl, 1.9 KCl, 1.2 KH_2PO_4, 26 $NaHCO_3$, 2.4 $CaCl_2$, 1.3 $MgSO_4$, and 10

glucose at a pH of 7.4. For dissection and electromyographic electrode insertion, low calcium, high magnesium aCSF (same as normal aCSF except 0.85mM $CaCl_2$ and 6.5mM $MgSO_4$) was used to minimize movement. Finally, for pharmacological induction of locomotion, 2-4 µM N-methyl D-aspartate (NMDA) and 40-60µM serotonin (5HT) were added to the aCSF.

2.2.4 Muscle recordings and analysis

To record electromyographic (EMG) activity, monopolar Teflon-coated platinum-iridium electrodes (0.05 mm bare diameter; AM Systems) with bared tips were implanted in up to six hindlimb muscles, including right and left tibialis anterior (TA; ankle flexors), right and left lateral gastrocnemius (LG; ankle extensors), right vastus lateralis (VL; knee extensor), and right rectus femoris (RF; knee extensor/hip flexor). Once implanted, a small drop of formulated cyanoacrylate (Nexaband Liquid Tissue Adhesive, Abbott Laboratories) was placed at the point of electrode insertion to secure the wires during movement. The fine wires were flexible enough to follow the moving limbs with negligible mechanical impedance (Kiehn and Kjaerulf 1996).

The EMG activity was collected through a differential amplifier, bandpass filtered (100 to 3000 Hz), notch filtered (60Hz), digitized at 5kHz (Digidata 1322A 16-Bit DAQ, Axon Instruments), and recorded (Clampex, Axon Instruments) for offline analysis. EMG activity was analyzed using a custom program in Matlab (MathWorks Inc). Analysis relevant to the locomotor rhythm included low-pass Chebyshev filtering to create burst envelopes, burst detection, burst duty cycle, and intermuscular phasing. The phase between two muscles was defined as the time from mid-burst of the first muscle to mid-burst of the second divided by the cycle period (Grillner and Matsushima 1992), with 0

being exactly in-phase and 0.5 being 180^{o} out-of-phase. Muscle duty cycles and intermuscular phasing were compared between dorsal-up and ventral-up *in vitro* preparations and across muscles within a preparation using two-sample and paired student t-tests ($\alpha = 0.05$ unless otherwise stated) using the statistics toolbox in Matlab (The MathWorks Inc.).

2.2.5 Video recording and kinematic analysis

For sagittal plane kinematic analysis, joint centers were palpated and marked at the hip (greater trochanter), knee (lateral epicondyle), ankle (lateral malleolus), and 5^{th} metatarsophalangeal joints using waterproof black ink. Video of hindlimb locomotion was collected in the sagittal plane using a digital video camera at a rate of 60Hz. Video recordings were synchronized with EMG recordings using a trigger light in the camera field of view and a simultaneous voltage pulse sent to an EMG trigger channel. Following collection, joint positions were digitized using semi-automatic tracking (Dartfish Software). Joint angle trajectories for the right hindlimb were then calculated from joint positions. The ankle and knee angles were defined as included angles between the foot and shank segments and shank and thigh segments respectively. The hip angle was defined as the angle between the thigh and the horizontal. In all cases, increasing angle values indicate extension.

To account for slight variations in cycle time, each step cycle was time normalized. Zero percent gait cycle was defined as the onset of retraction/stance phase, which was determined from video recordings and defined as the time when the toe was in its anterior extreme position (AEP). Similarly, protraction/swing phase onset was defined as the time when the toe was in its posterior extreme position (PEP). Once normalized,

joint angular trajectories were averaged across cycles (n = 10-23 cycles) to compute average trajectories for each animal. Average trajectories plus and minus standard deviations are presented. Stride period was defined as the time from one ipsilateral AEP event to the next, with stride frequency being the inverse of stride period. These and all subsequent kinematic analyses were performed using custom programs in Matlab.
All statistical analyses were performed using JMP statistical software (SAS) or the statistics toolbox in Matlab. Mean stride frequencies at each speed were compared using a one-way analysis of variance (ANOVA; $\alpha = 0.05$). The effect of both time and treadmill speed on stride frequency were examined using a multiple linear regression. Coefficients were tested for significant difference compared to zero ($\alpha = 0.05$).

2.2.6 Ventral-up setup

For comparison, some preparations were oriented ventral-up with their hindlimbs allowed to air-step above the cord. Procedures for ventral-up air-stepping were similar, but were undertaken in a simple flat-bottomed Sylgard chamber. Under these conditions, a static oxygenated aCSF bath was used.

2.2.7 In vivo kinematics

In vivo kinematics from adult rat treadmill locomotion were also collected. The posterior ischium and hip, knee, ankle, and 5^{th} metatarsophalangeal joints were marked, and video of treadmill locomotion (33.2cm/s) was recorded at 60Hz. Sagittal plane kinematics were then analyzed with the same techniques described above.

2.2.8 Success rate

The success rate for dorsal-up *in vitro* locomotion with the perfusion system was

high, with 94% (15/16) locomoting in response to NMDA and 5HT. However, without the perfusion system, the success rate was much lower at only 39%. For kinematic analysis, some locomoting preparations were excluded because of significant out-of-place motion or limited paw-treadmill interaction. Also, only kinematics or only EMG activity were collected in some preparations. For ventral-up *in vitro* locomotion (static bath), the success rate was similarly high, with 84% (13/15) locomoting. Again, some were excluded for out-of-plane motion and some only used for either kinematics or EMG collection.

2.3 Results

2.3.1 Hindlimb 2D kinematics from the *in vitro* preparations

Figure 2.2 shows average kinematic trajectories for the hip, knee, and ankle joints during locomotion from representative animals in the dorsal-up (Fig. 2.2A; n = 5) and ventral-up (Fig. 2.2B; n = 3) orientations. In the dorsal-up orientation, the hip and ankle extended during retraction/stance and flexed during protraction/swing, as would be expected for stepping in the behaving rat (Gillis and Biewener 2001; Thota et al. 2005). The knee joint exhibited mostly flexion during retraction/stance, presumably supporting the weight of the hindquarters upon ground contact as well as actively retracting to accelerate the hindquarters relative to the treadmill. During protraction/swing, the knee exhibited a large extension to return to its initial position.

Overall, the joint trajectories from ventral-up air-stepping differed considerably from those seen in dorsal-up stepping. First, the hip and ankle exhibited large plateau phases at the end of retraction/stance phase extension, which were absent in dorsal-up locomotion. Most interestingly, the knee exhibited a completely different trajectory.

Rather than flexing, the knee extended during the entire retraction/stance phase, followed by rapid flexion and slight extension during protraction/swing phase (Fig. 2.2B). This difference distinguishes the two movements and results in a very different coordination and phasing between the three joints. Finally, all three joints exhibited a much larger range of motion during ventral-up air-stepping compared to dorsal-up.

2.3.2 Comparison of kinematics from *in vitro* and *in vivo* conditions

Kinematics from both *in vitro* conditions (dorsal-up treadmill locomotion and ventral-up air-stepping) compare well with their *in vivo* counterparts. Figure 2.2C shows kinematic trajectories obtained during adult *in vivo* treadmill locomotion. Despite the large age and size differences, the neonatal *in vitro* dorsal-up treadmill locomotion (Fig. 2.2A) and adult *in vivo* treadmill locomotion (Fig. 2.2C) conditions produced similar kinematics. Neither exhibited the extended plateau phases observed during air-stepping and all three joint trajectories followed similar patterns. In both cases, the knee underwent a large flexion phase during retraction/stance that was absent in air-stepping trajectories. It should be noted that there is a difference between the ankle trajectories, with the *in vivo* exhibiting an early flexion phase (sometimes termed E2 phase) during retraction/stance that is absent *in vitro*. The *in vivo* knee trajectory also has an additional flexion phase near the transition at start of swing that is not present *in vitro*. These absences *in vitro* likely result from the smaller size and added weight support of the sylgard step. Nonetheless, the differences are small compared to the near reversal in knee joint trajectory between ventral- and dorsal-up *in vitro* conditions.

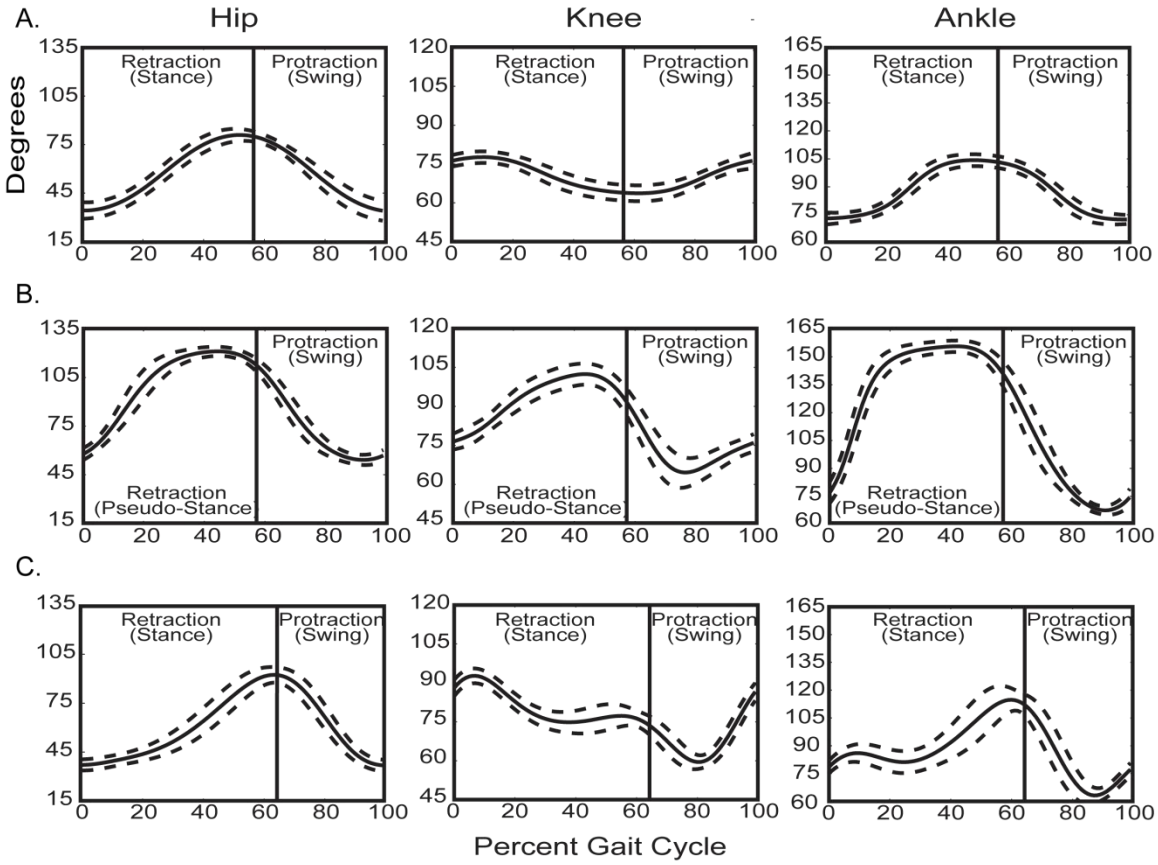

Figure 2.2 : In Vitro and In Vivo Kinematics

A: Dorsal-up *in vitro* kinematics from locomotion induced by 2-4µM NMDA, 40-60µM 5HT. Solid line: Average (n = 17 cycles) angular trajectories at the hip (left), knee (center), and ankle (right) plotted over the gait cycle. Dashed lines: Average trajectory plus or minus one standard deviation plotted over the gait cycle. 0% gait cycle represents the onset of retraction/stance phase. The solid vertical line represents the average percentage gait cycle at which the onset of protraction/swing phase occurred. B: Ventral-up *in vitro* kinematics from locomotion induced by 2-4µM NMDA, 40-60µM 5HT (Average of n = 20 cycles). C: In Vivo kinematics from adult rat during treadmill locomotion (Average of n = 17 cycles).

Similarly, the *in vitro* air-stepping trajectories (Fig. 2.2B) were similar to those previously reported from *in vivo* neonatal air-stepping (Stehouwer et al. 1994). The most obvious similarities include the presence of extension plateau phases at the ankle and hip joints as well as the absence of knee flexion during retraction/stance phases, which reflects the absence of ground interaction and need for weight support.

2.3.3 Comparison of EMG patterns from the dorsal-up and ventral-up *in vitro* preparations

To gain more direct insight into the role of sensory feedback during locomotion, I also looked at EMG activity during dorsal-up and ventral-up *in vitro* locomotion. Figure 2.3 shows representative EMG activity during locomotion from a dorsal-up and ventral-up *in vitro* preparation. Gray shading indicates retraction/stance phases. In both conditions, the EMG activity shows the expected alternation between ipsilateral ankle flexors and extensors (i.e. right LG and right TA) or between contralateral ankle flexors (i.e. right TA and left TA). However, the intermuscular phasing and relative duty cycles differed significantly between the dorsal-up and ventral-up conditions. First, the phasing between TA, an ankle flexor, and VL, a knee extensor, was significantly different ($p=0.002$) between dorsal-up (0.375 ± 0.057, $n=4$) and ventral-up (0.0961 ± 0.101, $n=5$). The phasing between TA and RF, a knee extensor/hip flexor, showed a similar trend with the dorsal-up phase (0.207 ± 0.094, $n=4$) being greater than ventral-up (0.164 ± 0.119, $n=4$), but this difference was not statistically significant.

Muscle duty cycles also showed significant differences between the *in vitro* conditions. During dorsal-up locomotion, the duty cycle of the extensors VL and LG were 0.52 ± 0.064 and 0.56 ± 0.073 respectively, while the duty cycle of the flexor TA

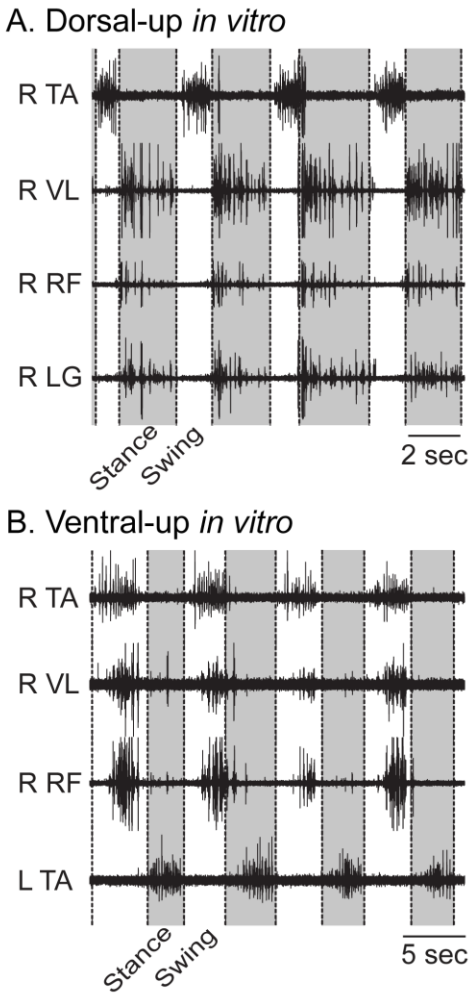

Figure 2.3 : In Vitro EMG Activity

EMG activity during *in vitro* (A) dorsal-up and (B) ventral-up locomotion induced by 2-4µM NMDA, 40-60µM 5HT. Shaded regions represent stance or pseudo-stance phases, and white regions represent swing. Muscles from top to bottom: right vastus lateralis (R VL), right rectus femoris (R RF), right lateral gastrocnemius (R LG in dorsal-up), left tibialis anterior (L TA in ventral-up).

was 0.37 ± 0.098. The duty cycles of both extensors were significantly longer than the the flexor duty cycle (VL $p<0.01$, n=4; LG $p<0.05$, n=5). During ventral-up locomotion, the duty cycle of VL was 0.34 ± 0.12 and TA was 0.47 ± 0.094. The ventral-up duty cycles was thus reversed compared to dorsal-up, with the duty cycle of TA being significantly longer than that of VL ($p<0.01$, n=5). In addition, the duty cycle of VL was significantly longer during dorsal-up locomotion compared to ventral-up ($p<0.05$), while the duty cycle of TA tended to be shorter during dorsal-up locomotion ($p=0.06$).

2.3.4 Effect of sensory perturbations on EMG and stride parameters

To demonstrate the efficacy of this preparation for studying locomotor circuitry under sensory modulation, EMG activity and stride parameters were examined in response to two sensory manipulations. First, in preparations (n=5) with initially weak locomotion, a stepping assistance perturbation was applied by exerting a swing assistive force on the right hindfoot. A glass probe was used to push the bottom of the right hindfoot anteriorly at the onset of each protraction/swing phase. Figure 2.4 shows an example of the muscular response to this perturbation. Prior to swing assistance, the locomotion was irregular in frequency and quite weak, with right LG, VL, and RF all failing to burst reliably (Fig. 2.4A). During swing assistance, the right LG, VL, and RF all began to exhibit regular bursting and engaged in the ongoing rhythmic pattern (Fig. 2.4B). Finally, after swing assistance was terminated, the EMG pattern was quite robust on all channels and regular in frequency (Fig. 2.4C). *It should be noted that this pattern was still slightly different from the typical dorsal-up pattern though, likely due to the weaker ground contact. A similar increase in extensor activity strength and regularity was observed in the other animals. In each case, reinforcing sensory feedback from swing

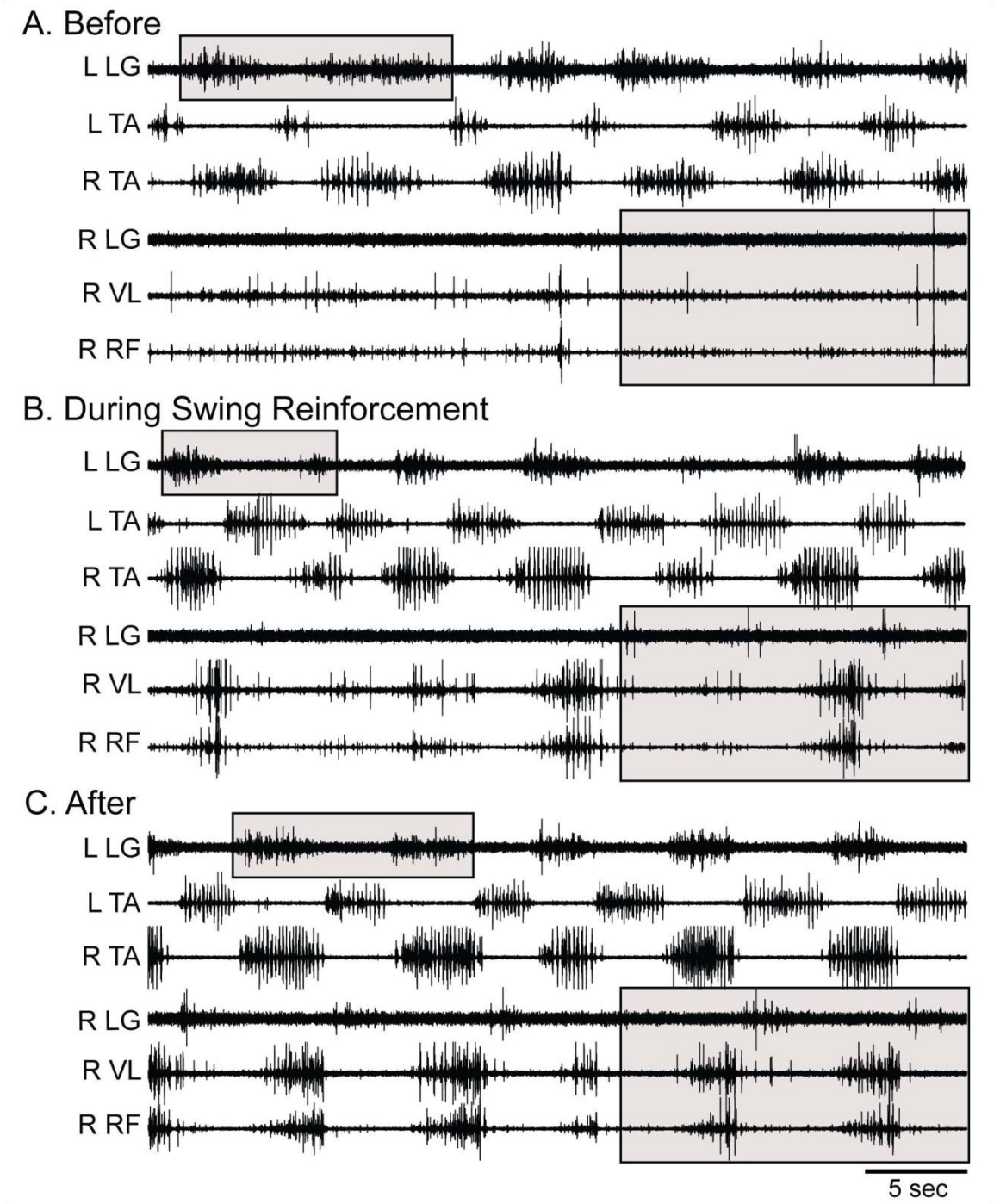

Figure 2.4 : EMG Response to Right Hindlimb Swing Assist

Muscles from top to bottom in each panel: left lateral gastrocnemius (L LG), left tibialis anterior (L TA), right lateral gastocnemius (R LG), right tibialis anterior (R TA), right vastus lateralis (R VL), right rectus femoris (R RF). A: 40 seconds of EMG activity before application of swing assistive forces to the right hindlimb. B: 40 seconds of EMG activity during swing assistance. C: 40 seconds of EMG activity after termination of swing assistance. The upper left gray boxes in each panel highlight frequency irregularity and/or regularity. The lower right gray boxes in each panel highlight the gradual engagement of the R LG, R VL, and R RF in the rhythm in response to swing assistance.

assistance increased robustness of the centrally-generated motor program. *Similarly, when drugs failed to initiate locomotion, alternating cyclical assistance on both limbs actually initiated strong locomotion for the first time (n=6 bouts in n=4 animals). Unassisted locomotion then persisted after bilateral assistance was terminated.

Secondly, the speed of the treadmill was changed during ongoing locomotion to determine if this change in sensory feedback could alter hindlimb stride frequency. Such responses have been shown previously in more intact, older animals (Forssberg and Grillner 1973; Grillner and Rossignol 1978c; Musienko et al. 2007; Pearson 1995). As treadmill speed increased from approximately 4 to 11mm/s, stride frequency increased by 12.1% from a mean of 0.257Hz to 0.288Hz (Fig. 2.5). One-way analysis of variance (ANOVA) showed that the stride frequencies were significantly different between treadmill speeds ($p<0.001$). To ensure that these changes were not simply due to drifts in frequency over time, a multiple linear regression model was used to quantify the effects of both time and treadmill speed on stride frequency. The regression analysis showed that the effect of time was not significant ($p = 0.5$), while the effect of treadmill speed was statistically significant ($p<0.001$). Two other animals also exhibited the trend of increasing stride frequency across a range of treadmill speeds. However, in these two animals, multiple linear regression revealed a stronger influence of time. Due to the compounding factor of temporal drift, the changes in stride frequency could not be attributed to treadmill speed alone. It was noted that the later two animals appeared to have less forceful interactions with the treadmill belt, while the paw of the first animal appeared to cause larger belt deflections during the stance phase. Thus, strong paw-belt interaction may be required to achieve a strong speed entraining effect and alteration of

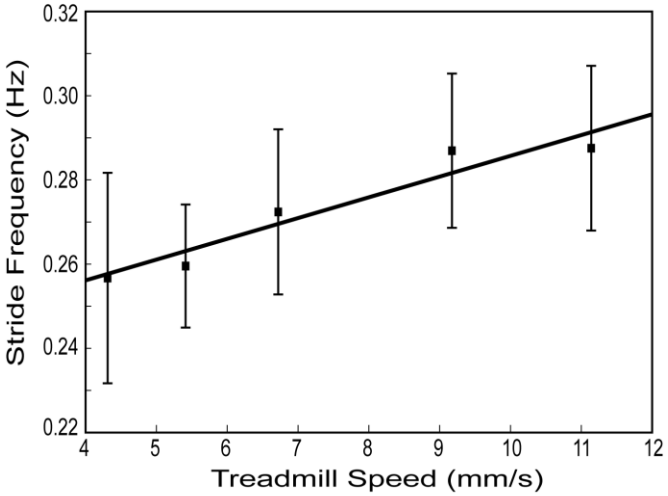

Figure 2.5 : Stride Frequency versus Treadmill Speed

Stride frequencies are represented as mean (■) plus and minus standard deviation (indicated by error bars) at each treadmill speed. The regression line shows the positive correlation of stride frequency with treadmill speed: y = 0.004932*x + 0.2364.

temporal features via belt-related sensory feedback.

2.4 Discussion

The kinematic data is this study is the first biomechanical characterization of mammalian hindlimb locomotion generated *in vitro*. Importantly, even though locomotion is neurochemically induced and undertaken in neonates, the preparation can produce task-appropriate kinematics and generate locomotor behavior similar to the normal adult rat. While some prior work has described pharmacologically induced "stepping-like movement" in earlier hindlimb-attached *in vitro* preparations (Atsuta et al. 1988; Kudo and Yamada 1987; Smith et al. 1988), no effort has been made to quantify the kinematics of this behavior and, therefore, no data is available for comparison to locomotor behaviors normally exhibited by intact rodents. Additionally, only air-stepping movements have been reported; *in vitro* locomotion has not been studied under behaviorally-relevant mechanosensory conditions. The biomechanical characterization presented here also offers a better understanding of the type of behavior being elicited by NMDA and 5HT acting on the spinal cord and further highlights the role of mechanosensory feedback in altering centrally-generated locomotor output. Interestingly, previous EMG activity from restrained hindlimbs suggested that serotonin evokes swimming-like motor output (Kiehn and Kjaerulf 1996). The results emphasize that mechanosensory input plays a large role in movement patterning and show that 5HT/NMDA can lead to stepping-like movements when given the appropriate mechanical environment.

2.4.1 Kinematics confirm the behavioral relevance of the preparation

The kinematic dissimilarities between the *in vitro* dorsal- and ventral-up

conditions demonstrate the preparation's ability to produce multiple kinematic behaviors which are largely influenced by the mechanical environment and, likely, sensory feedback. Additionally, they show that the same neurochemicals, i.e. 5HT and NMDA, can produce different movement patterns depending on the mechanosensory context. When compared to their *in vivo* counterparts, the kinematics of the *in vitro* preparations strongly resembled the patterns produced in the corresponding mechanical conditions *in vivo*. The dorsal-up treadmill locomotion joint angle trajectories (Fig. 2.2A) were comparable to those typically seen in adult treadmill locomotion *in vivo* (Fig. 2.2C), with the exception of two inflections absent *in vitro.* The slight differences can likely be attributed to discrepancies in age and size and obvious differences between *in vitro* and *in vivo* preparations. Regarding the ventral-up air-stepping (Fig. 2.2B), the patterns were strikingly similar to the air-stepping patterns previously reported in neonatal *in vivo* air-stepping (Stehouwer et al. 1994). In the *in vivo* study, the intact neonates were harnessed and air-stepping, while, *in vitro*, the isolated cord was ventral-up with the hindlimbs air-stepping above the body. Despite this difference in orientation, the absence of ground interaction and correspondingly reduced sensory input appears sufficient to produce comparable kinematic patterns.

Overall, the similarities between *in vitro* and *in vivo* in both the treadmill and air-stepping conditions suggest that spinal motor circuitry, even at an early developmental stage, is capable of producing task-appropriate motor patterns. Previous researchers have questioned the relevance of the neonatal model since neonates at this age do not typically walk (Smith and Feldman 1987). Regardless, when weight supported (i.e. reduced preparation with vertebral support from the Sylgard step), the neonatal spinal cord is

capable of producing adult-like movements given sufficient mechanosensory feedback.

2.4.2 Sensory input contributes to spatiotemporal features of motor output

While the kinematic comparison showed that the mechanical condition can alter kinematic patterns, kinematic measures cannot distinguish between purely mechanical effects and the effects mediated by sensory feedback pathways using kinematics alone. Thus, I compared EMG patterns between the dorsal- and ventral-up *in vitro* conditions to demonstrate the importance of sensory feedback in patterning motor output in the neonate *in vitro*. A limitation of locomotor studies in the neonatal rat spinal cord is the fatigability of afferent synaptic transmission (Lev-Tov and Pinco 1992), which could minimize the contribution of afferent input to ongoing motor output. Afferent activity is capable of resetting locomotion in the neonatal cord (Iizuka et al. 1997; Kiehn et al. 1992), but the contribution of sensory activity to ongoing locomotion remains uncharacterized in the neonate.

I observed significant differences in both muscle phasing and duty cycle between dorsal- and ventral-up patterns, suggesting that sensory feedback from the mechanical condition of the limbs strongly affects the spatiotemporal features of spinal motor output. As described earlier, the VL and TA were more out-of-phase during dorsal-up locomotion compared to ventral-up, with VL being active further into the stance phase during dorsal-up (Fig. 2.3). During dorsal-up locomotion, the limb extends against a resistance and bears the weight of the hind quarters during stance, leading to greater limb loading and likely excitatory length and force feedback that could increase extensor activity during stance (Mazzaro et al. 2005; Pearson et al. 1998; Rossignol et al. 2006). Such feedback would be very small, if present at all, in the ventral-up condition at the

limbs are not extending against a surface. Thus, this sensory feedback pathway might explain the shift towards increased stance-phase activity of VL during dorsal-up locomotion.

I further observed a significant difference in relative extensor and flexor duty cycles. During ventral-up *in vitro* locomotion, the flexor duty cycle exceeded the extensor duty cycle (flexor-dominated) (Juvin et al. 2007). During dorsal-up *in vitro* locomotion, the cycle became extensor-dominated, with the extensor duty cycles exceeding the flexor. Such extensor-dominated muscle activation patterns are typical of intact, behaving mammals, particularly at slower speeds (Engberg and Lundberg 1962; Forssberg and Grillner 1973; Thota et al. 2005). In contrast, the reduction of sensory feedback in the ventral-up *in vitro* condition (less ground interaction and resistance) likely lead to the observed flexor- rather than extensor-dominance in that condition. Similarly, during fictive locomotion where sensory feedback is absent, muscle activation patterns tend to be flexor-dominated as well (71% experiments) (Yakovenko et al. 2005). In sum, these results imply that sufficient and appropriate sensory feedback may be necessary for establishing the extensor-dominance observed during *in vivo* and dorsal-up *in vitro* locomotion. The results also emphasize the importance of appropriate sensory feedback for achieving behaviorally-relevant locomotor function.

Finally, I considered changes in EMG activity and stride parameters in response to mechanosensory perturbations. First, in response to stepping assistance on the right hindlimb (i.e. applying a swing-assistive force to the limb), the weak and disorganized motor pattern became highly regular and robust across all recorded muscles, showing that appropriate sensory inputs can reinforce ongoing locomotion (Fig. 2.4). *Bilateral

assistance actually initiated strong locomotor patterns when drugs were insufficient. Thus, locomotor-like sensory input can not only reinforce locomotion but also facilitate activation of the CPG. Second, the observed increases in stride frequency with belt speed resulted from changes in sensory feedback, perhaps from stretching of the hip flexors or unloading of the limb, that can initiate swing phase (Pearson et al. 1998). Together, these responses confirm that sensory feedback can cause major alterations in both the spatial and temporal features of spinal locomotor output in reduced *in vitro* models, highlighting the importance of retaining appropriate sensory feedback when studying spinal motor circuits *in vitro*. *The reinforcing perturbations also suggest that retaining sensory feedback may create a more robust preparation for studying locomotion.

2.5 Conclusions

In conclusion, this model provides a platform for studying the neurophysiology of spinal locomotor circuitry in a behaviorally-relevant context, which includes the vital influences of sensory feedback. By bringing the traditional *in vitro* isolated spinal cord preparation neuromechanically closer to reproducing *in vivo* locomotion, the dorsal-up *in vitro* model has the potential to advance the study of neural control of locomotion and the spinal circuits that govern limb movement. The critical interplay between the CPG and proprioception has been the topic of much research, dating back to early commentary by Sherrington near the turn of the century (Mott and Sherrington 1895), but, as discussed in an editorial focus in this journal in 2004, "such questions are difficult to address because they require the analysis of the functional role of neural components in a behaving animal (Cattaert 2004)." The dorsal-up *in vitro* preparation helps overcome these challenges by allowing us to readily study neural activity with intact sensory feedback from ongoing

limb movements.

One of the greatest advantages of the dorsal-up *in vitro* preparation is the potential for studying interneuronal activity and CPG function during natural, sensory-influenced behavior. As shown in the mudpuppy, once the moving limb is mechanically isolated from the cord, even intracellular recordings can be achieved in *in vitro* non-fictive preparations (Cheng et al. 2002; Wheatley et al. 1994a; Wheatley and Stein 1992). *I recently performed successful, stable intracellular patch clamp recordings from seven dorsal-horn and two ventral horn interneurons in four dorsal-up SCHPs to confirm this capability (Appendix A). Additionally, the *in vitro* spinal cord offers exquisite neurochemical and ionic control of the neuronal environment in the absence of a blood-brain barrier. By combining neural accessibility and manipulability with behavioral observability and sensorimotor integration, this novel methodology greatly expands our ability to investigate spinal mechanisms that control locomotion and to elucidate the task-specific functioning of the CPG.

CHAPTER 3

EFFECTS OF HINDLIMB MECHANICS ON REGULATION OF SENSORY INFLOW BY PRESYNAPTIC INHIBITION

3.1 Introduction

During locomotion, sensory feedback plays a major role in determining the spatiotemporal features of muscle activation and limb movement. Sensory signals can alter the timing of phase transitions and flexor-extensor duty cycles (Hayes et al. 2009a; Pearson 1995; Pearson et al. 1998; Whelan et al. 1995a; b), modify extensor magnitude during stance (Donelan and Pearson 2004; Hayes et al. 2009a; Hiebert and Pearson 1999; Pearson et al. 1998; Rossignol et al. 2006), and reset ongoing locomotion in a phase-dependent manner (Conway et al. 1987; Iizuka et al. 1997; Kriellaars et al. 1994; Pearson et al. 1998). Sensory feedback can also reinforce weak locomotion and refine muscle activation to meet task demands (Hayes et al. 2009a; Pearson et al. 1998).

Precisely because sensory feedback wields such strong influence on motor behavior, it must be tightly regulated to allow for refinement of motor output without unwanted interference. Both presynaptic and postsynaptic inhibition regulate the effectiveness of sensory input onto central circuits (Rudomin et al. 1987; Solodkin et al. 1984). Presynaptic inhibition of afferents is "more powerful than postsynaptic inhibition in depressing the central excitatory actions of almost all primary afferent fibers (Eccles 1964)." Compared to postsynaptic inhibition, presynaptic inhibitory actions are preemptive, longer lasting, and more selective. Presynaptic inhibition occurs at the spinal terminals of afferents before the first synapse in the spinal cord, so it is the first site for

regulating sensory inflow and, thus, prevents *any* undesirable effects on spinal neurons. Additionally, presynaptic inhibition exerts longer lasting effects, reducing reflex effectiveness for hundreds of milliseconds (300-400msec) while postsynaptic inhibition lasts only tens of milliseconds (~10-30msec) (Eccles et al. 1962c; Gossard and Rossignol 1990). Presynaptic inhibition can also be highly selective by inhibiting specific intraspinal terminals without affecting other branches of the same afferent (Eguibar et al. 1994; Eguibar et al. 1997b). In contrast, postsynaptic inhibition alters responses to *all* inputs to a postsynaptic cell by changing the postsynaptic cell's excitability. While postsynaptic changes are certainly important (e.g. (Kiehn et al. 2000)) and co-exist with presynaptic effects (Solodkin et al. 1984), presynaptic inhibition clearly offers a highly selective and effective mechanism for sensory regulation.

Presynaptic inhibition can be activated by homonymous afferents, heteronymous afferents, descending systems, or spinal circuits, such as the locomotor circuitry, typically via $GABA_A$ergic pathways (for review see (Rudomin 2009; Rudomin and Schmidt 1999)). When $GABA_A$ receptors on primary afferent terminals are activated, chloride flows out of the terminals[1]. The chloride efflux initiates a primary afferent depolarization (PAD) that then travels electronically back out the dorsal root toward the periphery. This depolarization reduces the transmitter released in response to an incoming action potential by inactivating sodium and calcium channels and/or by shunting. In this way, PAD reduces the central actions of incoming sensory events (Eccles et al. 1961b; Eccles et al. 1962a; Eccles et al. 1962b). Further, because PAD travels back out in the dorsal

[1] The reversal potential of chloride is maintained much higher in primary afferents by a sodium-potassium-chloride co-transport pump, NKCC1.

root, presynaptic inhibition can be monitored as a dorsal root potential (DRP), which is the summed back-propagated PAD from many axons recorded at the dorsal root entry zone (Fig. 3.1).

From fictive locomotion, we know that DRPs, as well as the corresponding presynaptic inhibition levels, are rhythmic during locomotion with maximum inhibition occurring during flexion (e.g. (Duenas and Rudomin 1988; Gossard et al. 1991)). H-reflex patterns have also been regularly attributed to presynaptic inhibition as the monosynaptic reflex is most depressed during flexion, but pre- and post-synaptic sources cannot be distinguished from H-reflexes alone (for review see (Brooke et al. 1997; Stein 1995)). Due to interactions with spinal and supraspinal locomotor circuits as well as multimodal interactions, the effectiveness of specific afferents for generating inhibition or eliciting reflexes changes significantly across locomotor phase and between tasks. Given this, it is vital to study the patterns of locomotion in the most behaviorally relevant conditions possible and with the most natural patterns of afferent interactions possible.

However, it has been difficult to study both centrally-evoked and afferent-evoked presynaptic inhibition during non-fictive locomotion because it is "almost technically *impossible* to record PADs during *real* walking (Menard et al. 1999)" due to the sensitivity of DC recordings to cord movement. In fact, there is only one brief report in the literature of DRPs recording during non-fictive locomotion (Yakhnitsa et al. 1988). The dorsal-up spinal cord hindlimb preparation (SCHP) developed in Chapter 2 now allows us to mechanically isolate the spinal cord from the limbs and, thus, provides sufficient stability for DC DRP recordings. The ability to stabilize the cord, while

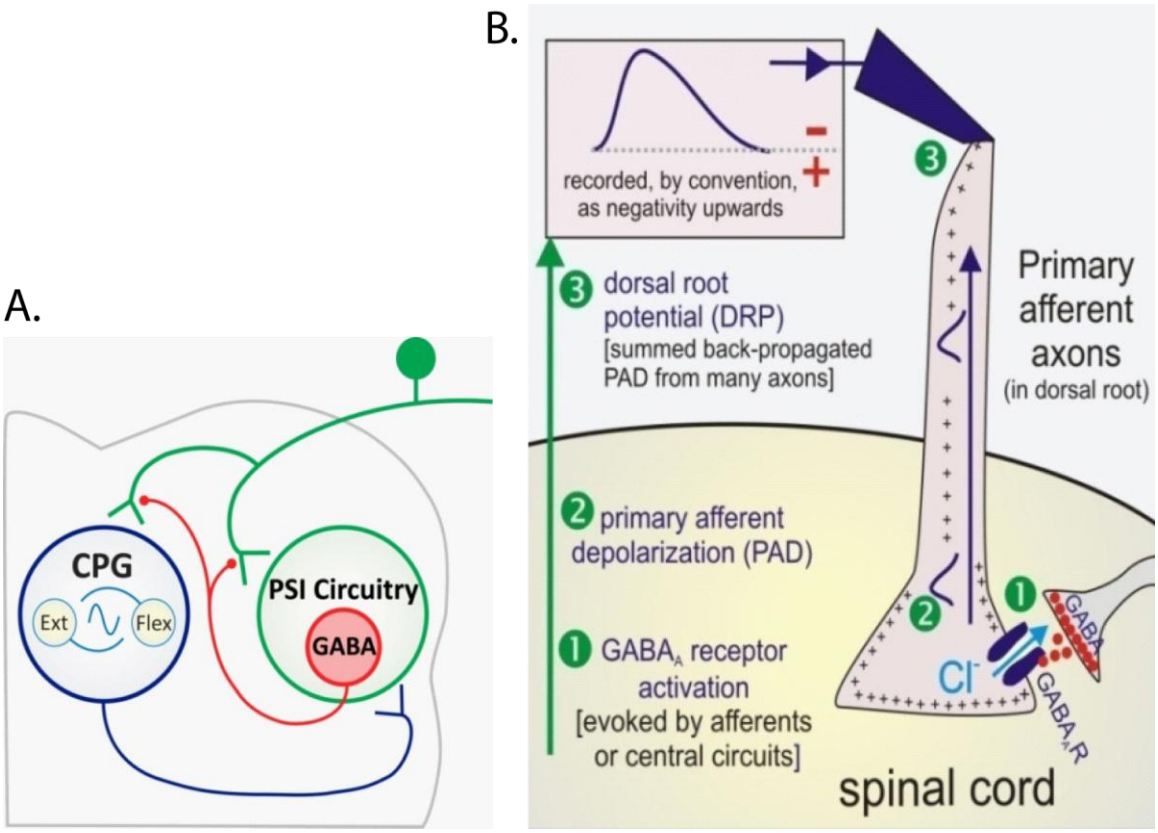

Figure 3.1: Mechanisms of Presynaptic Inhibition

A: Presynaptic inhibition (PSI) can be evoked by homonymous afferents, heteronymous afferents, or central circuits such as the spinal locomotor circuitry. B: Measurement of and mechanism underlying $GABA_A$-mediated presynaptic inhibition by primary afferent depolarization (modified from (Hochman et al. 2010)). The order of events is numbered 1-3. Following activation by one of the events shown in A, $GABA_A$ergic neurons activate $GABA_A$ receptors are primary afferent terminals in the spinal cord. Because the chloride gradient is maintained to favor outward flow in afferents, chloride effluxes resulting a depolarization wave that travels antidromically into the dorsal root. The depolarization wave can be then be monitored as a dorsal root potential (DRP) at the dorsal root entry zone.

retaining sensory feedback and intact limb movement, make the SCHP a powerful model for studying sensory regulation during locomotion via presynaptic inhibition.

Most of the investigations on afferent-evoked presynaptic inhibition have focused on ipsilateral effects with little attention to the contralateral afferents. A small number of early studies found that stimulation of group I and flexor reflex afferents produced a contralateral DRP along with the larger ipsilateral DRP (Devanandan et al. 1965; Gossard and Rossignol 1990; Jankowska et al. 1966), demonstrating that contralateral afferents could contribute to sensory regulation. Despite this finding, no literature has addressed the contribution of contralateral presynaptic inhibition to sensory regulation during locomotion nor investigated the impact of contralateral sensorimotor state on presynaptic inhibition.

Due to the nature of locomotion, the nervous system must control multiple limbs in a coordinated fashion through central circuits, sensory feedback interactions, and/or mechanical coupling. Therefore, contralateral sensory inputs, as well as contralateral presynaptic inhibition, may likely play an important role in interlimb coordination. Studies on H-reflex modulation during human walking and cycling suggest that contralateral limb sensorimotor state influences both the sensory sensitivity and resulting behavior of the ipsilateral limb. For example, unilateral passive and active pedaling leads to a constant downregulation of H-reflex gain on the non-moving limb (McIlroy et al. 1992). These effects persist in spinal cord injury patients and spinal dogs, confirming their spinal origin (Brooke et al. 1995b; Misiaszek et al. 1996). When the contralateral limb is still, the absence of contralateral movement- and force-related feedback alters both the muscle activation patterns and net work produced by the ipsilateral limb (Ting et

al. 1998; Ting et al. 2000). These observations have been attributed to central interlimb coupling, postsynaptic excitability changes, and presynaptic inhibition, but direct measurements were not possible. The SCHP offers us the unique opportunity to investigate both the contralateral and ipsilateral contributions to presynaptic inhibition during non-fictive locomotion, while manipulating the mechanics and neural system in ways otherwise not possible.

In this study, I characterized the patterns of presynaptic inhibition during non-fictive locomotion in the SCHP in relation to both ipsilateral and contralateral hindlimb mechanics. I hypothesized that the movement and loading of the contralateral limb would influence the patterns of presynaptic inhibition on the ipsilateral limb and, thus, the magnitude and timing of sensory information allowed into the spinal cord. To test this hypothesis, I recorded DRP activity as a measure of PAD-evoked presynaptic inhibition and compared the spatiotemporal dependence of DRP patterns on ipsilateral and contralateral limb force and kinematics. I then performed mechanical perturbations on each limb to isolate the influence of the individual limbs and distinguish between movement- and force-related feedback. Because both central circuits and sensory feedback can influence presynaptic inhibition, I also considered the dependence of presynaptic inhibition on motor output, as monitored at the ventral roots, and performed deafferentations to distinguish central and sensory sources. Finally, I considered the functional implications of presynaptic inhibition and its potential influence on motor behavior. I found that the mechanics of the contralateral limb, particularly limb loading, plays a pivotal role in regulating ipsilateral sensory inflow via contralateral afferent-evoked presynaptic inhibition. A portion of these results have been presented in abstract

form (Hayes et al. 2009b; Hayes and Hochman 2009).

3.2 Methods

All procedures described here were approved by the Emory University Institutional Animal Care and Use Committee. A total of fifteen neonatal rats were used in these studies. Over 700 step cycles from ten animals, were analyzed to test the central hypothesis of dependence of the DRP on ipsilateral and contralateral limb loading and movement. Mechanical perturbations were then performed in nine animals and neural perturbations in seven animals. The sample size is reported below for each condition.

3.2.1 *In vitro* spinal cord-hindlimb preparation (SCHP)

Studies were undertaken in the *in vitro* dorsal-up SCHP, as presented in Chapter 2 and described previously (Hayes et al. 2009a). Briefly, neonatal rats postnatal days 1-4 were decapitated and eviscerated. The spinal cord, caudal vertebral column, pelvis, and hindlimbs were isolated. All skin was removed except that covering the dorsal and plantar surfaces of the paws. The preparation was then transferred to a custom-built perfusion chamber. The cord was mounted dorsal-up on a Sylgard step and securely stabilized with insect pins through the ribs and remaining paraspinal tissues, with hindlimbs hanging pendant to step unrestrained on force platforms (described below, Fig. 3.2).

3.2.2 Bathing solutions

All bathing solutions were continuously oxygenated with 95% O_2, 5% CO_2. The standard bathing solution was an artificial cerebral spinal fluid (aCSF) containing (in mM): 128 NaCl, 1.9 KCl, 1.2 KH_2PO_4, 26 $NaHCO_3$, 2.4 $CaCl_2$, 1.3 $MgSO_4$, and 10

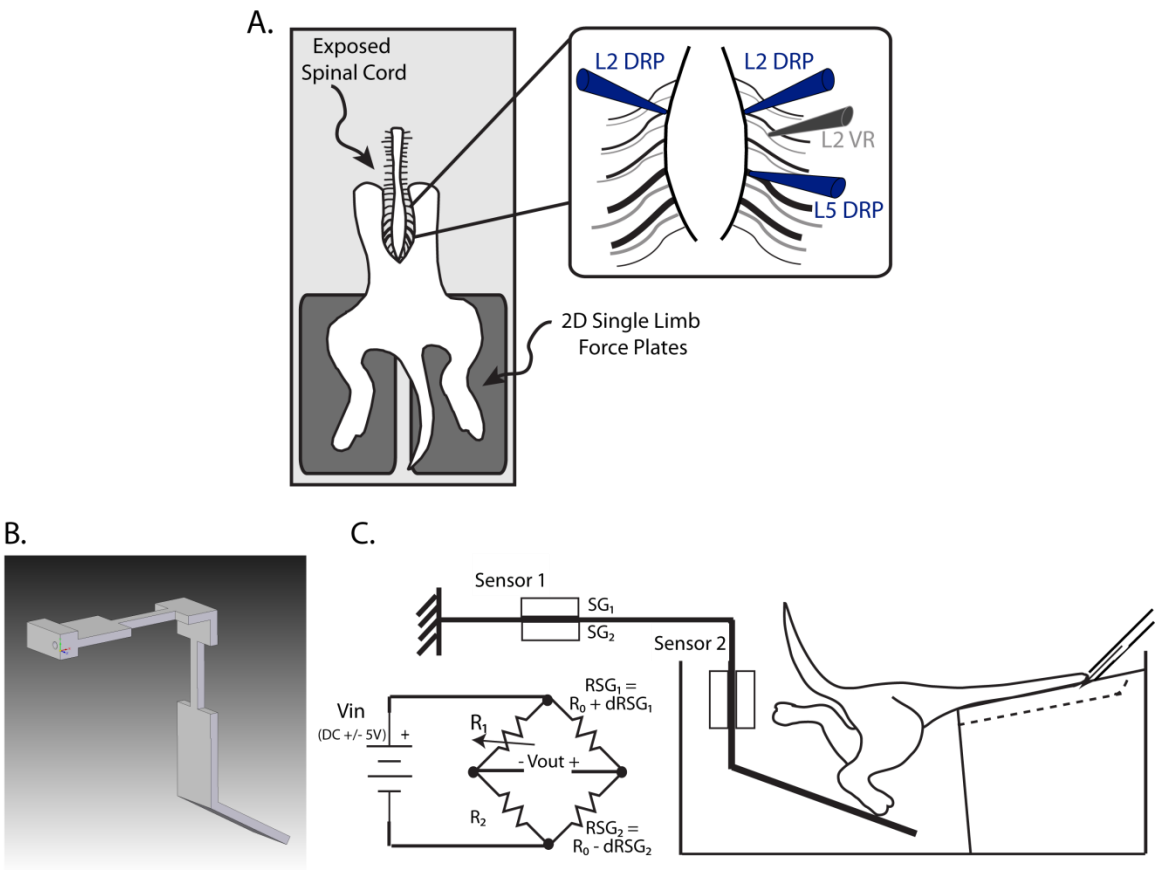

Figure 3.2: Experimental setup and methodology

A: Overhead view of the *in vitro* spinal cord-hindlimb preparation (SCHP) with exposed spinal and each intact hindlimb free to walk on a separate 2D force platform. Inlay shows the recording configuration. Dorsal root potentials (DRPs) were recorded near the dorsal root entry zones of L2 and L5 dorsal roots using glass suction electrodes. Activity in the L2 ventral root (VR) was also recorded. B: Design schematic of a single limb force platform used to monitor hindlimb forces. C: Sagittal view of hindlimb-force platform interaction and wheatstone bridge circuitry. Strain produced by strain gauges SG1 and SG2 of Sensor 1 and fed into the wheatstone bridge circuit. Strain sensed by Sensor 2 is fed into a separate but identical wheatstone bridge circuit. Output voltages are amplified by a DC amplifier and then converted to vertical and fore-aft forces in offline analysis.

glucose at a pH of 7.4. For dissection and electrode placement, low calcium, high magnesium aCSF (same as normal aCSF except 0.85mM $CaCl_2$ and 6.5mM $MgSO_4$) was used to minimize movement. Solutions were provided through a gravity-fed perfusion system and recirculated by a peristaltic pump. To pharmacologically induce locomotion, 4-6 µM N-methyl D-aspartate (NMDA) and 10-80µM serotonin (5HT) were added to the aCSF. In thirteen experiments,10-40 µM of dopamine (DA) was added as well.

3.2.3 Force platforms for monitoring limb endpoint forces

In ten experiments, limb endpoint forces were measured. Vertical and fore-aft forces were monitored using two 2D force platforms, one for each hindlimb (Fig. 3.2, designed after (Biewener and Full 1992; Chang et al. 1997; Heglund 1981)). The platforms were designed in ProEngineer, printed on an Objet 3D printer, and composed of an acrylic-based photopolymer. Force was transduced via Omega Engineering SGD-1.5/120-LY11 strain gauges. The strain gauge outputs were fed into a Wheatstone bridge circuit (Figure 2C) and DC amplifier. The amplifier included voltage regulators (National Semiconductor LM337/317) on the bridge excitation inputs and a variable gain precision instrumentation amplifier (National Instruments AD524). The output of the amplifier was digitized at 5kHz and recorded (Digidata 1322A 16-Bit DAQ, Axon Instruments) for offline calibration and analysis.

The force platforms were calibrated by applying *n* known weights and the influence matrix [I] was calculated according to:

$$[V_{2xn}] = [I_{2x2}] \,.\, [L_{2xn}] \text{ such that } [I_{2x2}] = [V_{2xn}].\, [L_{2xn}]^{-1}$$

where [V] is the voltage data in response to the known applied loads in µV, [L] is the known loads in mN, [I] is the influence matrix describing the relationship, and n is the

number of known weights (see Appendix B). After calibration, vertical and fore-aft forces from locomotor trials were computed from the recorded voltage traces according to:

$$[F_{2xn}] = [I_{2x2}]^{-1}. [V_{2xn}] \text{ where } [I_{2x2}]^{-1} = \{[V_{2xn}]. [F_{2xn}]^{-1}\}^{-1}$$

where [F] is the force matrix that includes both vertical and fore-aft forces computed from the conversion matrix $[I]^{-1}$ (Chang et al. 1997).

Following collection, forces were exported to Matlab for calibration and analysis. Ground reaction forces during each locomotor cycle were initially identified by a threshold detector. Their onset and offset times were more finely discriminated using their second derivatives to detect the maximum inflection points. Force magnitude was quantified by the area under the curve, peak-to-peak amplitude, and the mean amplitude during each event, all relative to baseline. This paper focuses on the relationship to vertical forces, defined as parallel to gravity. Thus, all subsequent references to limb endpoint force refer to vertical forces.

Two of ten force experiments reported here were carried out using a single 1D force platform shared by both hindlimbs. Each force event was labeled as right or left using the video kinematic data. A similar 1D calibration and conversion of voltage to vertical force was performed.

3.2.4 Kinematics

For sagittal plane kinematic analyses, joint centers were palpated and marked at the hip (greater trochanter), knee (lateral epicondyle), ankle (lateral malleolus), and 5th metatarsophalangeal joints using waterproof black ink. Video of hindlimb locomotion was collected in the sagittal plane using a digital video camera at a rate of 30 or 60Hz.

Video was synchronized with electrophysiological recordings using a trigger light in the field of view and a simultaneous voltage pulse sent to a trigger channel in the data acquisition system. Following collection, joint positions were digitized using semi-automatic tracking (Dartfish Software) and joint angle trajectories computed for the right hindlimb. The ankle and knee angles were defined as included angles between the foot and shank segments and shank and thigh segments respectively. Hip angle was defined as the angle between the thigh and the horizontal. In all cases, increasing values indicate extension (0^o max flexion and 180^o max extension). All further kinematic analyses were performed in Matlab.

3.2.5 Ventral root and dorsal root potential recordings

Activity in the right lumbar ventral root L2 was recorded as a monitor of spinal motor output using *en passant* glass suction electrodes (Fig. 3.2). The L2 ventral root was chosen because its bursting activity typically corresponds to flexor muscle activation (Kiehn and Kjaerulf 1996), providing an approximate marker of the flexion phase. Ventral root recordings were passed through an AC-coupled differential amplifier, bandpass filtered (100 to 3000Hz), notch filtered (60Hz), and digitized at 5kHz (Digidata 1322A 16-Bit DAQ, Axon Instruments). Following collection, ventral root recordings were rectified and low pass Chebyshev filtered to create a burst envelope and then bursts were detected using a threshold detection graphical user interface in Matlab (Gozal 2010). Their onset, offset, and peak times, as well as the area under the low-passed envelope, were calculated.

Throughout these experiments, DRPs were used to monitor both the timing and magnitude of presynaptic inhibition of primary afferent inflow (Duenas and Rudomin

1988; Gossard and Rossignol 1990; Ménard et al. 2003). Increases in DRP amplitude indicated increases in presynaptic inhibition and vice versa. DRPs were recorded with *en passant* glass suction electrodes placed at the entry zones of dorsal roots L2 (and occasionally L5) on the ipsilateral and contralateral sides. Recordings were collected through a DC amplifier or AC amplifier with a high-pass cutoff frequency ≤ 0.10Hz and digitized at 5kHz. Using custom software in Matlab, DRPs were initially identified using a threshold detector. As above, their onset and offset times were then more finely discriminated using their second derivatives to identify the maximum inflection points. The magnitude of the DRP was then characterized by the area under the curve, the peak-to-peak amplitude, and the mean voltage deflection, all relative to a locally detrended baseline to account for DC drift.

Throughout this study, ipsilateral indicates the side of the recorded DRP (iDRP) and contralateral indicates the side contralateral to the DRP. In the figures, ipsilateral forces are represented in green while contralateral forces are represented in red.

3.2.6 Data Analysis

All subsequent analyses were performed using custom software in Matlab. Statistics were performed using the statistics and circular statistics toolboxes (Berens 2009). Differences were considered significant if $p \leq 0.05$ unless otherwise stated.

3.2.6.1 Dependence of the DRP on ipsilateral and contralateral hindlimb forces

To test the hypothesis that contralateral limb loading influences ipsilateral presynaptic inhibition, the spatiotemporal dependence of the L2 DRP on ipsilateral and contralateral force was compared. For each step cycle delineated by ventral root or kinematic events, the corresponding DRP was detected. If no DRP occurred during the

cycle, a deletion was noted and the area, peak, and mean were set to zero. The preceding and/or coincident ipsilateral and contralateral force events were then detected for each DRP or DRP deletion. Ipsilateral and contralateral force deletions were also noted.

To quantify the dependence of the DRP magnitude on limb endpoint force, the DRP area, peak-to-peak amplitude, and mean amplitude were plotted against the corresponding ipsilateral and contralateral force values for each cycle. Linear regressions and the Pearson correlation coefficient (R) were computed. Student t-tests were then performed to test the significance of the correlation.

To examine the temporal relationship, the absolute time delay between force onset and DRP onset was measured for each cycle. The phase between DRP onset and force onset was defined as the delay divided by the cycle period and multiplied by 360^o, such that 0^o represented exactly in-phase and 180^o represented out-of-phase. For each preparation, the temporal relationship could be graphically summarized on the unit circle by a vector at the mean phase angle $\bar{\theta}$ with length equal to r. The value of r indicates the concentration of cycle phase angles about the mean phase angles and ranges from 0 to 1 (Kjaerulff and Kiehn 1996). Rayleigh's test for circular uniformity (Zar 1974) was then used to determine whether r was high enough to indicate a significant relationship between the DRP and ipsilateral or the DRP and contralateral force. Phasing was also examined to determine if the ipsilateral or contralateral force just preceded the DRP onset, indicating that the force could potentially evoke the DRP.

In addition, the Wallraff procedure for comparing angular dispersion was used to compare the temporal coupling of the DRP to the ipsilateral force and to the contralateral force (Wallraff 1979; Zar 1974). Angular distances for each cycle were computed as the

cycle phase angle minus the mean phase angle. The angular distances were then pooled and two-sample Mann-Whitney tests were applied to compare angular dispersion between the DRP-ipsilateral force phasing and the DRP-contralateral force phasing. Higher angular dispersions indicated less coupling between variables, while lower angular dispersions indicated tight coupling between variables.

3.2.6.2 Dependence of the DRP on motor output

Similar procedures were used to examine the spatiotemporal dependence of the L2 DRP on L2 ventral root motor output (n = 10). After identifying the DRP and L2 ventral root for each cycle, linear regressions and the Pearson correlation coefficient were used to characterize the relationship between DRP and ventral areas and peaks. The temporal relationship was characterized by the phase angle, concentration about the mean angle (r), and angular dispersion. Again, high r and low angular dispersion for the DRP-ventral root phasing indicated a tight coupling between the DRP and motor output, while low r and high angular dispersion indicated that the DRP timing was not dependent upon motor output. As described above, the Wallraff procedure and Mann-Whitney tests were used to compare angular dispersion between DRP-force phasing and DRP-ventral root phasing to determine whether DRP timing was more dependent on limb endpoint force or motor output. The relationships between the L2 DRP and ipsilateral and contralateral kinematics were also examined by plotting DRP area against the corresponding hip, knee, and ankle range of motion and area under the joint angle trajectory for a given cycle.

3.2.6.3 Impact of presynaptic inhibition on motor behavior

To understand the impact of presynaptic inhibition on subsequent motor behavior, the timing and magnitude of ipsilateral ankle and hip kinematic events were related to the

coincident and/or preceding DRP in preparations in which right L2 DRP and right kinematics were both available (n = 4). The phasing between the DRP and ankle and hip peak angular velocity and acceleration was also examined to see if the DRP coincided with or just preceded these events, suggesting that the DRP could play a role in either their timing or their magnitude. The impact of DRP deletions on ipsilateral kinematics and ventral roots was also considered.

3.2.7 Mechanical Perturbations

In nine rats, force platforms were removed for one to two minutes to determine whether the loss of ground contact force, either ipsilateral or contralateral, influenced the magnitude or consistency of the DRP. Ipsilateral and contralateral platforms were removed independently to isolate the effects of force from each limb.

3.2.8 Dorsal root and peripheral nerve transections

Neural cuts were performed in a total of seven rats. In four rats, DRPs were compared before and after lumbar dorsal root rhizotomy to distinguish afferent-evoked and centrally-evoked DRPs. For these experiments, care was taken to fully expose all dorsal roots of interest during the initial dissection. After collecting control data, aCSF was exchanged for low calcium high magnesium aCSF to avoid central sensitization by noxious inputs. The dorsal roots were then completely transected and the preparation returned to regular aCSF. Following a thirty minute wash in regular aCSF, deafferented data were collected and compared. To ensure that the effects were not simply due to low calcium high magnesium aCSF, dorsal root rhizotomies were performed in regular aCSF in two experiments.

In a separate three rats, the medial and lateral plantar nerves were cut, removing

most of the cutaneous innervation on the plantar surface of the paw. The plantar nerves are cutaneous nerves that innervate the plantar surface of the paw and digit pads as well as intrinsic musculature in the foot (Bouyer and Rossignol 2003a; Greene 1963). During the initial dissection for these experiments, the medial and lateral plantar nerves were exposed by gently opening the space between the calcaneal tendon and tibia on the lateral aspect and removing any overlaying fascia. This sham exposure ensured that no additional biomechanical disturbances were made between control and cutaneous dennervation trials. After collecting control data, aCSF was exchanged for low calcium high magnesium aCSF, and the plantar nerves completely transected. Following a thirty minute wash in regular aCSF, dennervation data were collected and compared.

3.3 Results

3.3.1 Rhythmic, $GABA_A$-dependent DRPs observed during non-fictive *in vitro* locomotion

As seen during fictive locomotion, DRPs in dorsal root L2 were rhythmic during locomotion (n=15), with the maximum depolarization occurring during the flexion phase (Fig. 3.3A). Often, extensor-phase depolarizations were also distinguishable in the L2 root, but they were significantly smaller and less consistent and, thus, not addressed here. In three experiments, DRPs were also recorded from dorsal root L5. L5 DRPs were always in-phase with the L2 DRP with their maximum during the flexion phase (Fig 3.4).

Application of 6-10μM of bicuculline, a $GABA_A$-receptor antagonist, abolished or greatly reduced the locomotor-related rhythmic DRPs (n=3/3, Fig. 3.3B). This observation confirmed that the rhythmic oscillations in dorsal root membrane potential were $GABA_A$-receptor dependent and reporting the GABAergic primary afferent

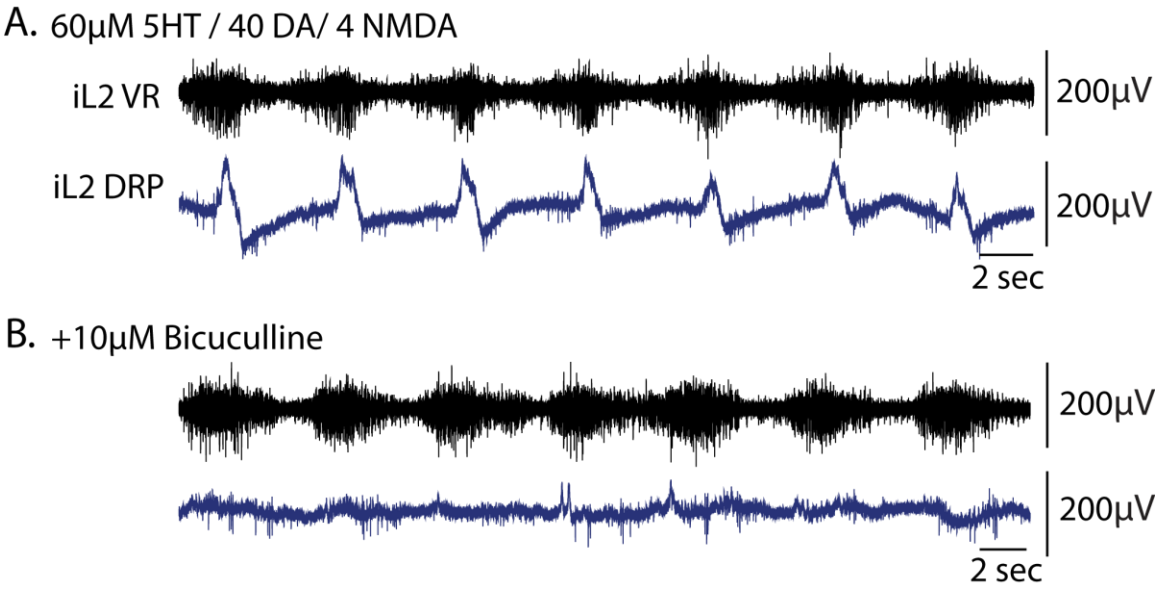

Figure 3.3: Rhythmic DRPs during locomotion are $GABA_A$ receptor dependent
Rhythmic DRPs from the L2 dorsal root (iL2 DRP) are shown during locomotion induced by 4µM NMDA, 60 µM serotonin (5HT), and 40 µM dopamine (DA). L2 Ventral root activity (iL2 VR) is shown as a reference for the flexion phase. A: During locomotion, DRPs are rhythmic with peaks occurring during the ipsilateral flexion phase. B: Application of 10 µM bicuculline, a $GABA_A$ receptor antagonist, nearly abolishes the DRPs, confirming that they are mediated by $GABA_A$ergic pathways

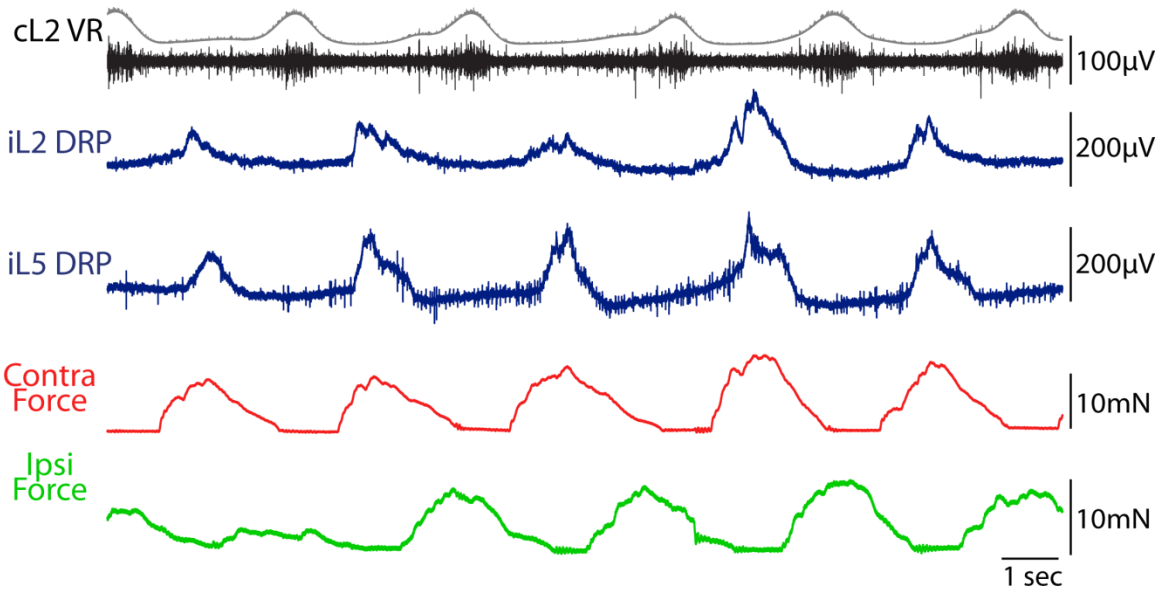

Figure 3.4: DRPs recorded from the L2 and L5 dorsal roots during locomotion are in-phase
Representative patterns for L2 and L5 DRPs (iL2 DRP, iL5 DRP, blue) during locomotion are shown relative to contralateral L2 ventral root activity (cL2 VR, black) as well as the ipsilateral (green) and contralateral force (red) profiles. The rectified and integrated burst envelope (gray) is overlaid on the ventral root to emphasize burst timing. L2 and L5 DRPs were always in phase during locomotion, suggesting that the patterns observed in L2 represented a distributed pattern of flexor-phase presynaptic inhibition in multiple lumbar segments.

depolarizations characteristic of presynaptic inhibition.

3.3.2 DRPs scale with contralateral limb endpoint force

Figure 3.5 shows the three typical locomotor patterns of L2 DRPs in relationship to L2 ventral root and ipsilateral and contralateral forces. As shown in panel A, variations in contralateral force predicted both the amplitude and timing of the ipsilateral DRP. When the contralateral force was small, the DRP was small; when the contralateral force increased, the DRP amplitude increased as well. Most importantly, when the contralateral force was delayed or absent, no DRP occurred. In contrast, ipsilateral force magnitude and timing did not appear to affect the DRP. Panel B shows a similar relationship, but during highly consistent locomotion on both limbs.

In the presence of dopamine, the locomotor pattern occasionally waxed and waned (n = 3/13 experiments with DA), leading to locomotor bouts in which one limb reached peak strength while the other limb weakened or exhibited deletions. During these bouts, the L2 DRP only occurred in cycles with a contralateral force, independent of ipsilateral force magnitude (Fig. 3.5C). Even in the absence of ipsilateral force, either due to a pause in locomotion or a lack of paw-plate interaction, an L2 DRP still occurred as long as a significant contralateral force was present. These bouts further highlighted the dependence of the L2 DRP on contralateral limb force and its independence from ipsilateral limb movement and force.

To quantify this magnitudinal relationship, L2 DRP area, peak amplitude, and mean amplitude were plotted against the corresponding values for the ipsilateral and contralateral forces for each cycle. In all preparations examined, DRP area correlated significantly with contralateral force (n = 10/10 at $p < 0.05$ with 8 at $p < 0.001$, see Table

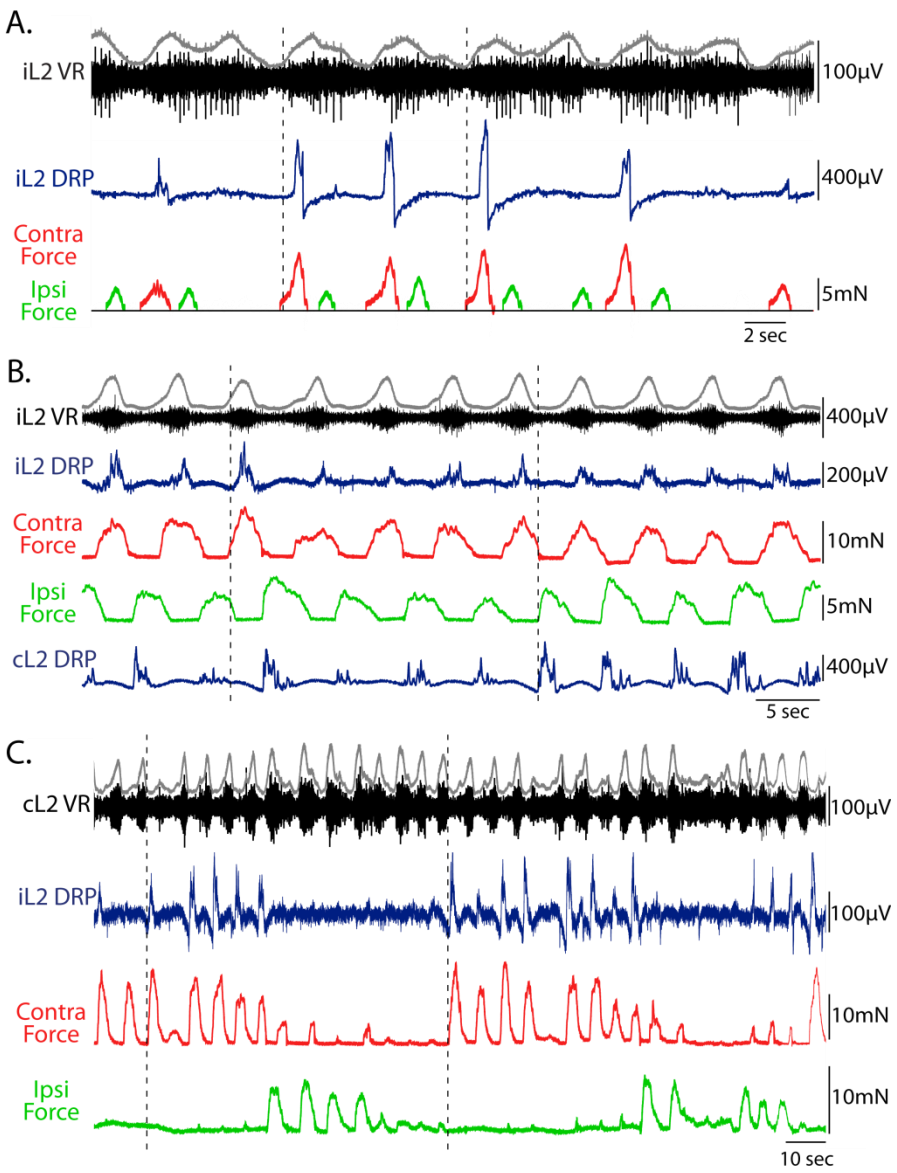

Figure 3.5: Representative DRP patterns during three locomotor conditions
DRPs (iL2 DRP, blue) are shown relative to ipsilateral or contralateral ventral root (iL2 VR or cL2 VR, black), contralateral forces (red), and ipsilateral forces (green). Ipsilateral (i) always indicates the side of the iL2DRP. Dashed vertical lines emphasize the phasing of the DRP relative to contralateral force. A: Single force platform condition. Contra- and ipsi-lateral force events were distinguished with video recordings. DRPs occurred only when a contralateral force was exerted, such that no DRP occurred when the contralateral limb failed to touch the plate. DRPs were largest in the presence of large contralateral forces, but their magnitude was independent of ipsilateral force. B: Two force platform condition with consistent cycle-to-cycle forces. Forces vertical to the plate are shown. DRPs consistently occurred immediately followed contralateral force onset and scaled with contralateral force amplitude. C: Waxing and waning locomotor patterns occasionally induced by dopamine (n=3/13 with DA). DRPs only occurred during contralateral force bouts, independent of ipsilateral force and contralateral motor output.

3.1), while none showed a significant positive correlation with ipsilateral force area. One preparation did exhibit a significant *inverse* relationship ($R < 0$) between DRP and ipsilateral force area, most likely due to the inverse relationship between ipsilateral and contralateral force magnitudes seen in that animal. Significant correlations were also observed between DRP and contralateral force peak ($n = 9/10$ at $p < 0.05$, with 6 at $p < 0.001$) and mean ($n = 8/10$ at $p < 0.05$, with 6 at $p < 0.001$) with no significant positive correlations to ipsilateral force peak or mean. All statistics are reported in Table 3.1. Representative regressions are shown in Figure 3.6.

Table 3.1 : Linear regression results for DRP as a function of force magnitude

Exp. Number	Area		Peak		Mean	
	Ipsi	Contra	Ipsi	Contra	Ipsi	Contra
1	-0.114 (p=0.389)	0.842 (p< 0.0001)	0.0390 (p=0.769)	0.873 (p<0.0001)	0.0614 (p=0.644)	0.677 (p<0.0001)
2	-0.139 (p=0.302)	0.840 (p<0.0001)	-0.0179 (p=0.895)	0.287 (p<0.05)	-0.119 (p=0.380)	0.567 (p<0.0001)
3	0.269 (p=0.0564)	0.743 (p<0.0001)	0.201 (p=0.157)	0.639 (p<0.0001)	0.450 (p<0.001)	0.678 (p<0.0001)
4	-0.00430 (p=0.979)	0.340 (p<0.05)	-0.0664 (p-0.6799)	-0.0475 (p=0.768)	0.0737 (p=0.647)	0.156 (p=0.331)
5	-0.206 (p=0.359)	0.705 (p<0.001)	-0.193 (p=0.390)	0.587 (p<0.05)	-0.201 (p=0.370)	0.0205 (p=0.926)
6	-0.00960 (p=0.960)	0.677 (p<0.0001)	0.0477 (p=0.803)	0.739 (p<0.0001)	0.0432 (p=0.821)	0.514 (p<0.05)
7	-0.465 (p<0.01)	0.571 (p<0.001)	-0.334 (p=0.0577)	0.569 (p<0.001)	-0.282 (p=0.112)	0.448 (p<0.01)
8	0.0389 (p=0.746)	0.315 (p<0.01)	0.0196 (p=0.870)	0.398 (p<0.001)	0.0999 (p=0.404)	0.419 (p<0.001)
9	0.0642 (p=0.595)	0.616 (p<0.0001)	0.0633 (p=0.600)	0.528 (p<0.0001)	0.112 (p=0.352)	0.648 (p<0.001)
10	0.0424 (p=0.724)	0.767 (p<0.0001)	-0.0289 (p=0.809)	0.371 (p<0.01)	-0.0210 (p=0.861)	0.5756 (p<0.0001)

For each experiment, DRP amplitude was plotted as a function of force area, peak, and mean cycle-to-cycle DRP amplitude. This table reports the Pearson Correlation Coefficient R and p-value (shown in parenthesis) representing the significance of each regression.

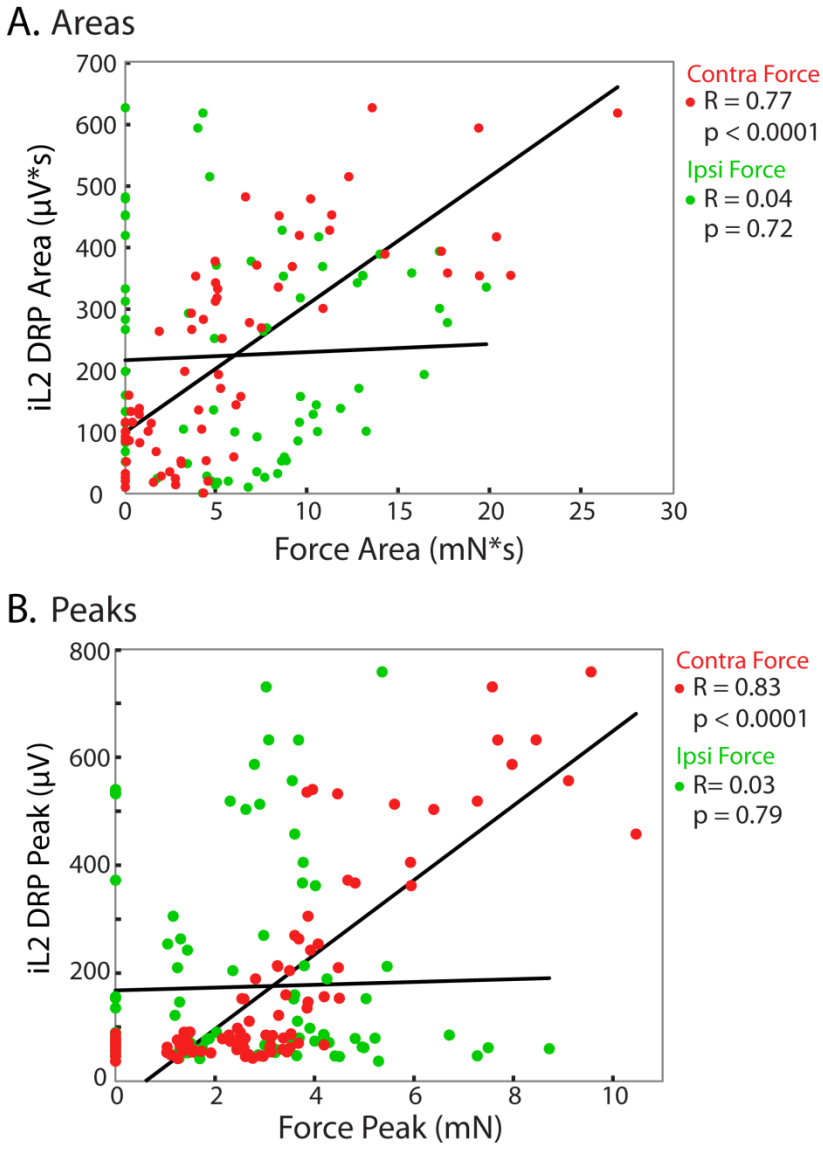

Figure 3.6: DRP scales with contralateral force, but not ipsilateral force

A: Linear regression relating DRP area to ipsilateral (green) and contralateral (red) force area from a single representative animal. Each point represents the values for a single cycle (n=72 cycles). The Pearson Correlation Coefficients (R) quantifies the linear dependence of DRP area on force area. R values near +1 indicate a strong positive correlation, values near 0 indicate no linear correlation, and values near -1 indicate a strong negative correlation. P-values (p) indicate whether the DRP shows a significant linear relationship with force. B: Linear regression relating DRP peak to ipsilateral and contralateral force peak from a second representative animal (n=95 cycles). In both cases, DRP magnitude scales with contralateral force, but is independent of ipsilateral force. When no contralateral force occurs for a given cycle (red points lying on the y-axis), the DRP is small or zero. The absence of an ipsilateral force (green points lying on the y-axis) does not affect DRP magnitude as it can be large or smaller even when no ipsilateral force occurs.

3.3.3 Contralateral limb force precedes and is tightly coupled with DRP onset

In order for the contralateral limb to actually evoke or influence DRP magnitude, and thus the amount of presynaptic inhibition on the ipsilateral limb, contralateral force must precede the onset of the ipsilateral L2 DRP each cycle. To test this, the temporal phasing and coupling of the DRP to i) contralateral force, ii) ipsilateral force, and iii) motor output were compared. Figure 3.7A shows the phasing of the ipsilateral and contralateral force onset relative to DRP onset for a representative bout of locomotion, with the contralateral force immediately preceding the DRP and the ipsilateral force showing a more varied and out-of-phase relationship. Examination of delays and phasing across all experiments confirmed that the mean onset of contralateral force always just preceded the onset of the DRP (n = 10/10, Fig. 3.7B). The mean phase angle of contralateral force onset relative to DRP onset was -26.06^{o} (r = 0.86) with a mean delay of 411msec ± 120msec, while the ipsilateral mean phase angle was 158.16^{o} (r = 0.55) with a mean delay of 2.90sec ± 180msec.

As evidenced by low angular dispersions about the mean, L2 DRP onset was tightly coupled in time with contralateral force onset. Rayleigh's test confirmed significant coupling with contralateral force. The Wallraff procedure and Mann-Whitney tests revealed that the angular dispersion for contralateral force-DRP phasing was significantly lower than for ipsilateral force (n=10/10), reflecting a stronger temporal dependency on contralateral force.

The temporal relationship between L2 motor output and L2 DRP was also examined. As seen in Figure 3.7 C and D, ipsilateral L2 DRP onset was significantly less coupled with either L2 ventral root motor output (ipsilateral ventral root (n = 4/4),

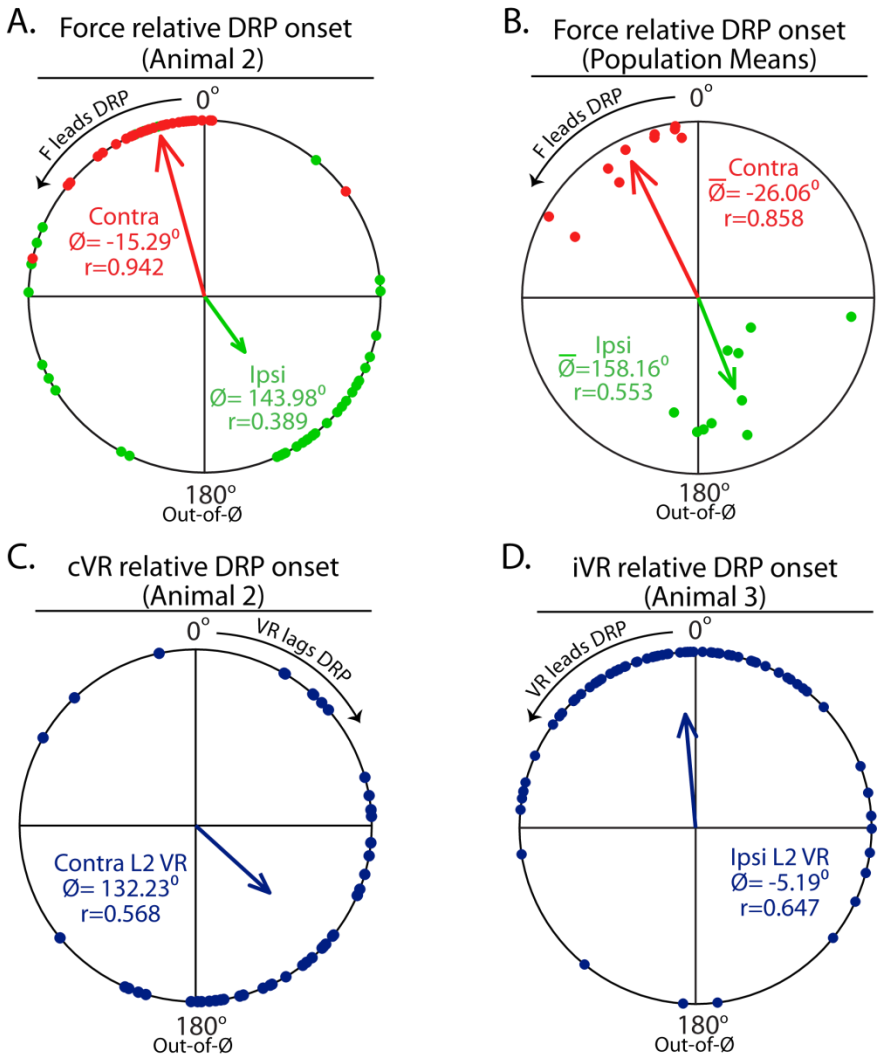

Figure 3.7: Phase relationships between force and ventral root onset relative to ipsilateral DRP onset

In all phase plots, 0^o represents the onset of the ipsilateral DRP. The cycle progresses clockwise from 0^o (in-phase) to 180^o (out-of-phase) to 360^o / 0^o. Points to the northwest precede DRP onset. Points to the northeast lag DRP onset. Arrow length represents the concentration (r) about the mean angle (Ø). Higher values and longer arrows indicate that the events are coupled in time and tend to occur at the same time relative to each other in each cycle. A: Contralateral (red) and ipsilateral (green) force onset relative to ipsilateral DRP onset. Contralateral force consistently precedes the DRP onset. Ipsilateral force is typically out-of-phase with contralateral force and ipsilateral DRP. However, when this timing varies, the DRP continues to follow contralateral force independent of ipsilateral force timing. B: Mean phase angle for contralateral and ipsilateral force onset relative to DRP onset for all animals. Each dot is plotted at the mean angle and at radius r for a single animal. Arrow length indicates the pooled r value and weighted mean angle for all animals. C: Contralateral L2 ventral root burst onset relative to DRP onset in the same animal as A. D: Ipsilateral L2 ventral root burst onset relative to DRP onset in another representative animal.

contralateral ventral root (n = 5/6)). Rayleigh's test p-values for L2 motor output-DRP coupling were at least an order of magnitude smaller than for contralateral force-DRP coupling. In 4/6 experiments with contralateral ventral root recordings, angular dispersion were significantly higher for contralateral L2 motor output-DRP phasing compared to contralateral force-DRP phasing. Angular dispersion for ipsilateral L2 motor output were also higher compared to contralateral force-DRP phasing in 4/4 experiments, but only statistically significant for 1/4.

In sum, neither ipsilateral force nor motor output timing appears to determine the timing of presynaptic inhibition during non-fictive locomotion. Rather, the timing of presynaptic inhibition is tightly coupled to contralateral limb endpoint force.

3.3.4 Relationship to locomotor frequency

Figure 3.8 shows the relationship between L2 DRP area and locomotor frequency, as defined by ventral root bursting. DRP area consistently increased with locomotor frequency. The relationship was well fit with an exponential curve (n = 10/10 with $R^2 > 0.85$, n = 6/10 with $R^2 > 0.94$). Therefore, as locomotor frequency increases, the magnitude of the DRP increases, meaning that less sensory feedback in the inhibited afferent pathways is allowed access to spinal circuits during faster locomotion.

3.3.5 Relationship to hindlimb kinematics

No cycle-to-cycle relationships were observed between contralateral ankle, knee, and hip range of motion and the resulting L2 DRP pattern. Neither range of motion nor area under the angular trajectory appeared to influence the magnitude of the DRP. Similarly the magnitude of the concurrent ipsilateral flexion and extension did not appear to influence DRP magnitude.

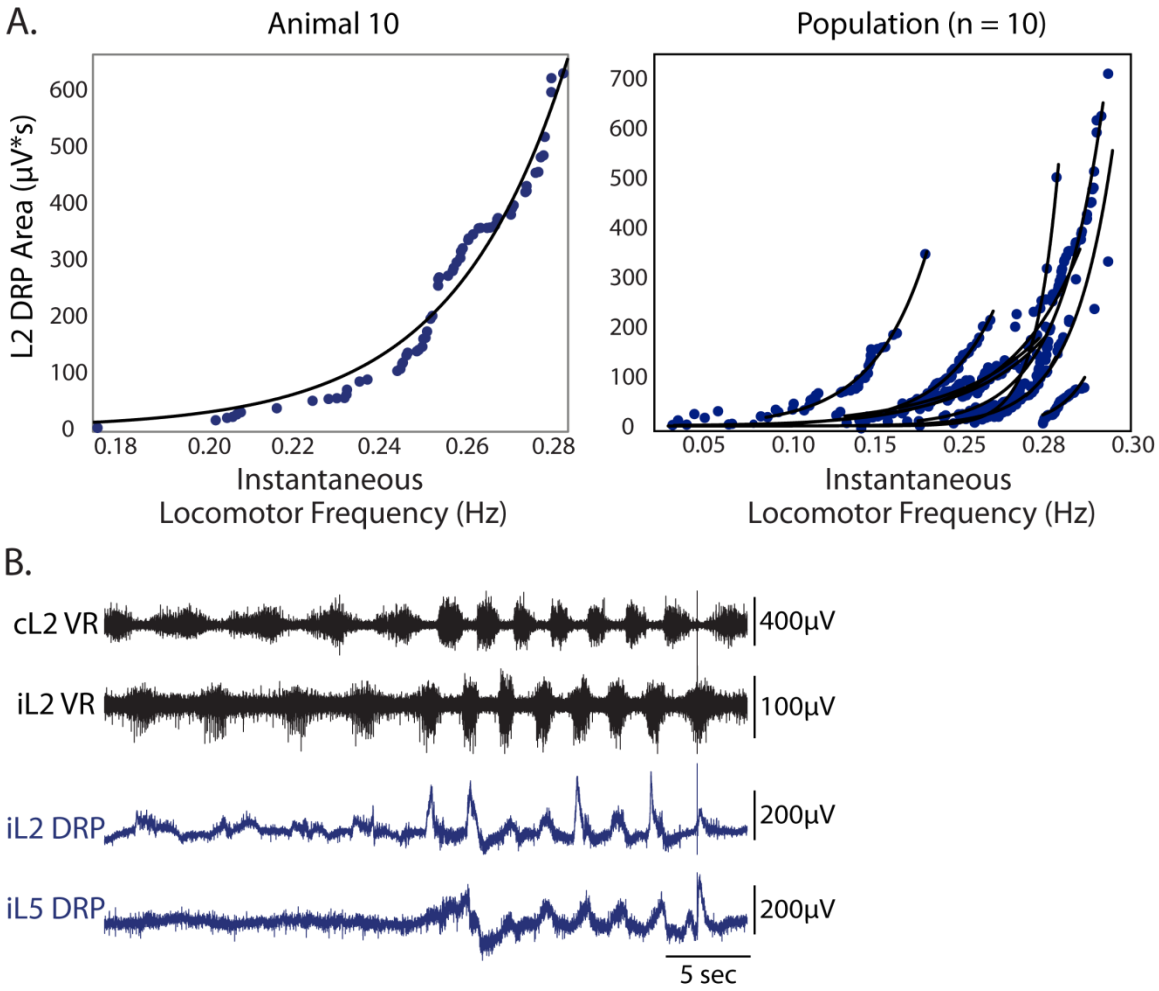

Figure 3.8: Relationship of DRP magnitude to locomotor frequency

A: The left panel shows DRP area versus instantaneous locomotor frequency fitted by an exponential curve ($y=ae^{bx}$ where y=DRP area, x= frequency) for a representative animal, while the right panel shows the exponential fit for ten animals. As seen in both panels, DRP area increases with increasing locomotor frequency such that more swing-phase sensory inflow is inhibited at higher speeds. B: In another animal, the paw stuck to the plate in the middle of a locomotor bout. This natural perturbation resulted in a rapid increase in frequency and force. As a result, both the L2 and L5 DRP rapidly increased. This was an unusual and extreme case, but it highlights the increase in presynaptic inhibition with locomotor frequency and force

Within a step cycle, the DRP occurred during early ipsilateral flexion phase in all animals. Ankle peak acceleration either preceded (n = 1/4) or nearly coincided with the ipsilateral DRP (phase ~ 0^o n = 2/4). Ankle peak velocity tended to occur after the DRP (n = 2/4) or centered around zero degrees (n = 1/4), suggesting that the DRP could influence ongoing flexion. Kinematic and DRP timing in the fourth animal exhibited little coupling with r values all below 0.44, likely due to the irregular waxing and waning pattern seen in this animal.

3.3.6 Impact of DRPs on ipsilateral motor output

While the magnitude of the DRP did not scale with ipsilateral or contralateral kinematics on a cycle-to-cycle basis, when a DRP was intermittently absent or more than double the mean amplitude, a corresponding change was seen in ipsilateral motor output. A total of four animals had right L2 DRP to compare with right L2 ventral root recordings and right hindlimb kinematics. Three of these animals showed sufficient variation in DRPs to ascertain an effect, while the fourth showed little variation in DRP, kinematics, or ventral root activity.

In the first animal, when a DRP was absent, the ipsilateral hip and ankle paused in extension and failed to flex. This occurred in 91% (10/11) of these cycles (Fig 3.9). In contrast, when a DRP was present, the hip and ankle successfully flexed in 64/66 cycles with only 3% exhibiting flexion failure in the presence of a DRP. While presynaptic inhibition is clearly not the only contributor to flexion, this finding implies that contralaterally-generated presynaptic inhibition may reduce inhibition of ipsilateral flexion; in the absence of this presynaptic inhibition, signals can impede flexion.

For animals two and three, similar effects of the DRP were seen in the ipsilateral

L2 ventral root, which is composed primarily of flexors including motoneurons from iliopsoas, pectineus, and tibialis anterior (Nicolopoulos-Stournaras and Iles 1983). In the second animal (see Fig. 3.4), when the DRP peak magnitude exceeded double the mean value, the ipsilateral L2 ventral root burst area and duration were significantly larger ($p < 0.05$). Finally, the third animal exhibited the dopaminergic waxing and waning pattern described in Section 3.3.2 and Figure 3.4C. As a result, the largest DRPs occurred during contralateral force when the ipsilateral limb and ventral root were nearly quiescent. However, the presence of the L2 DRP appeared to sculpt ventral root activity, bringing out small flexor bursts of activity when the ventral root was otherwise inactive (Fig. 3.10). Thus, even during quiescence, the DRP may reduce inhibition of flexor motoneuron activation.

An effect was difficult to ascertain in the fourth animal because locomotion was highly consistent, providing no variation in DRP size or occurrence. Every cycle had a DRP and accompanying ventral root activity as well as hip and ankle flexion. Importantly though, this observation is consistent with presynaptic inhibition preserving swing progression.

Although not conclusive, these observations provide evidence that presynaptic inhibition may inhibit sensory signals that could otherwise reduce or impede flexion activity during the swing phase. In this way, presynaptic inhibition may act to preserve flexion and swing. Alternative explanations for the observed behaviors are explored in the discussion.

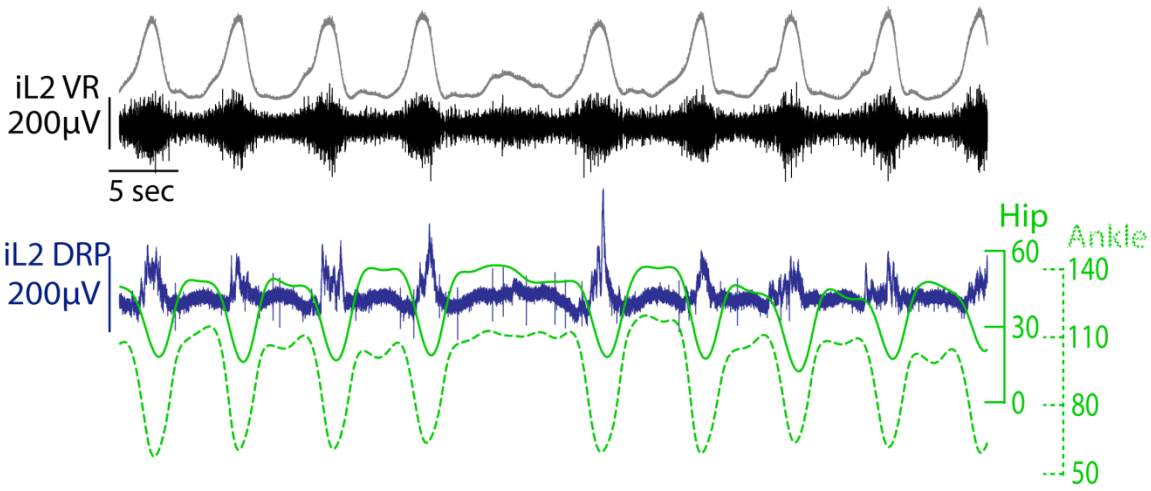

Figure 3.9: Effect of DRP on ipsilateral hip and ankle kinematics

Top traces: Ipsilateral L2 ventral root activity (iL2 VR, black) with rectified and integrated envelope (gray) to emphasize bursting patterns. Bottom traces: Ipsilateral hip (green) and ankle (dashed green) joint angle trajectories overlaid on the ipsilateral L2 DRP (iL2 DRP, blue). Joint flexion is down and extension is up. When the ipsilateral DRP is absent, hip and ankle joint flexion stalled, suggesting that presynaptic inhibition normally aids or preserves ipsilateral flexion.

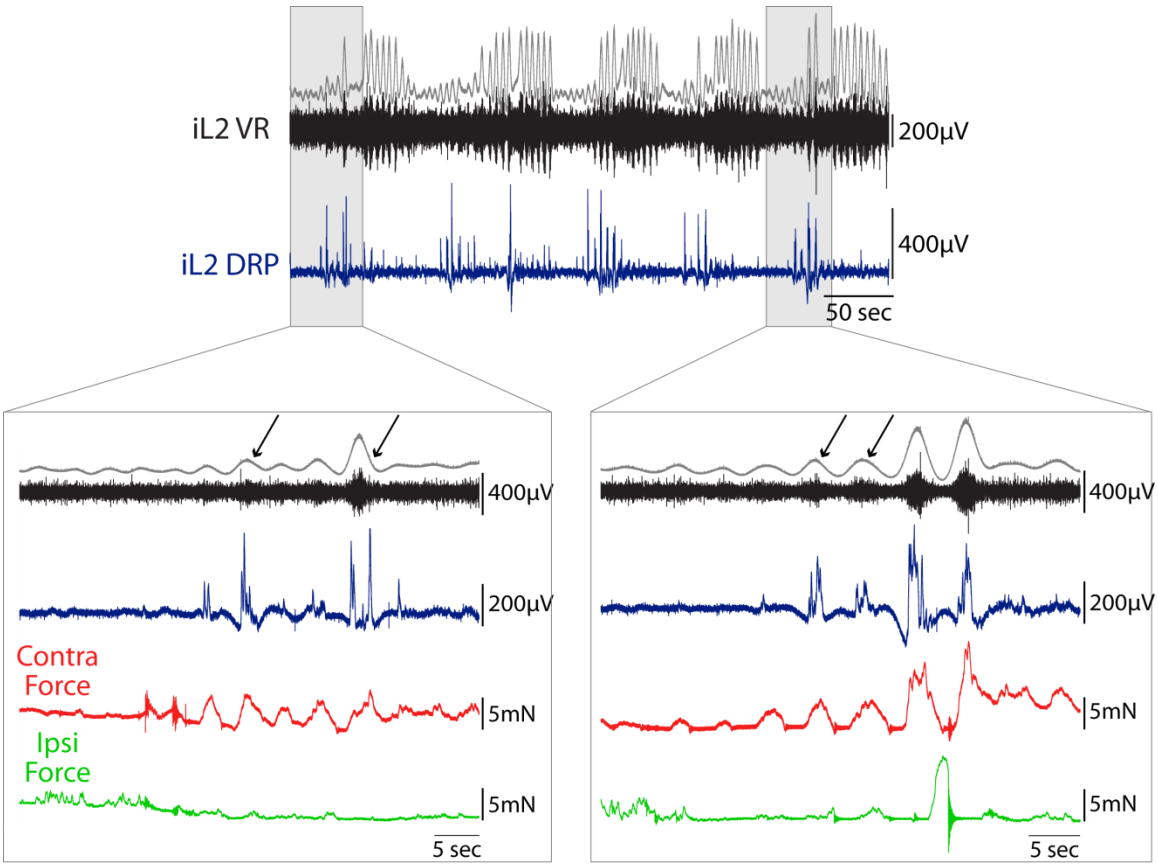

Figure 3.10: Effect of DRP on ipsilateral motor output during dopaminergic waxing and waning locomotion

The upper traces show the L2 DRP relative to ipsilateral L2 ventral root activity (black with gray rectified and integrated envelope) during a waxing and waning locomotor bout as seen in Figure 3.5C. The inlay boxes show zoomed in periods during ipsilateral quiescence. Because the DRP responds to contralateral force, DRPs often occur during ipsilateral quiescence. Even when the ipsilateral limb is quiescent and no significant ipsilateral limb movement or force is seen, the DRP can sculpt ipsilateral ventral root activity to elicit small flexion activity (arrows) during an otherwise silent period, further implying that presynaptic inhibition affects ipsilateral flexor motor output.

3.3.7 Perturbation responses

3.3.7.1 Response to ipsilateral and contralateral plate removals

To determine if significant contralateral force was necessary for cycle-to-cycle generation of the large L2 DRPs observed during non-fictive locomotion, ipsilateral and contralateral plates were removed separately. Ipsilateral DRPs continued unchanged when the ipsilateral plate was removed (n=6/7, Fig 3.11B), but were greatly reduced or abolished immediately upon contralateral plate removal (n=7/8, Fig. 3.11A). Importantly, these changes were seen without any significant (or even slight) changes in locomotor frequency, excluding frequency as a confounding factor. In the absence of the force platform, the limb still experienced some force-feedback as it stepped through the aCSF, but the endpoint force experienced by the limb was obviously greatly reduced in the absence of the plate and resulted in a loss of ipsilateral L2 DRP. The responses to plate removal confirm an essential role of contralateral endpoint force in ipsilateral DRP generation.

3.3.7.2 Contralateral lumbar dorsal root rhizotomy, but not plantar nerve transection, abolish rhythmic DRPs

Because central circuits are capable of producing rhythmic presynaptic inhibition in the absence of afferent activity (Dubuc et al. 1988; Gossard et al. 1991), contralateral lumbar dorsal roots were rhizotomized to confirm that contralateral afferents were responsible for evoking the force-related DRPs observed during non-fictive locomotion. In 3/4 experiments, the force-related DRPs were abolished or reduced in number and consistency when a minimum of L3-L5 dorsal roots were rhizotomized (Fig. 3.12A and B). Some DRPs persisted, but were quite inconsistent and unrelated to contralateral force.

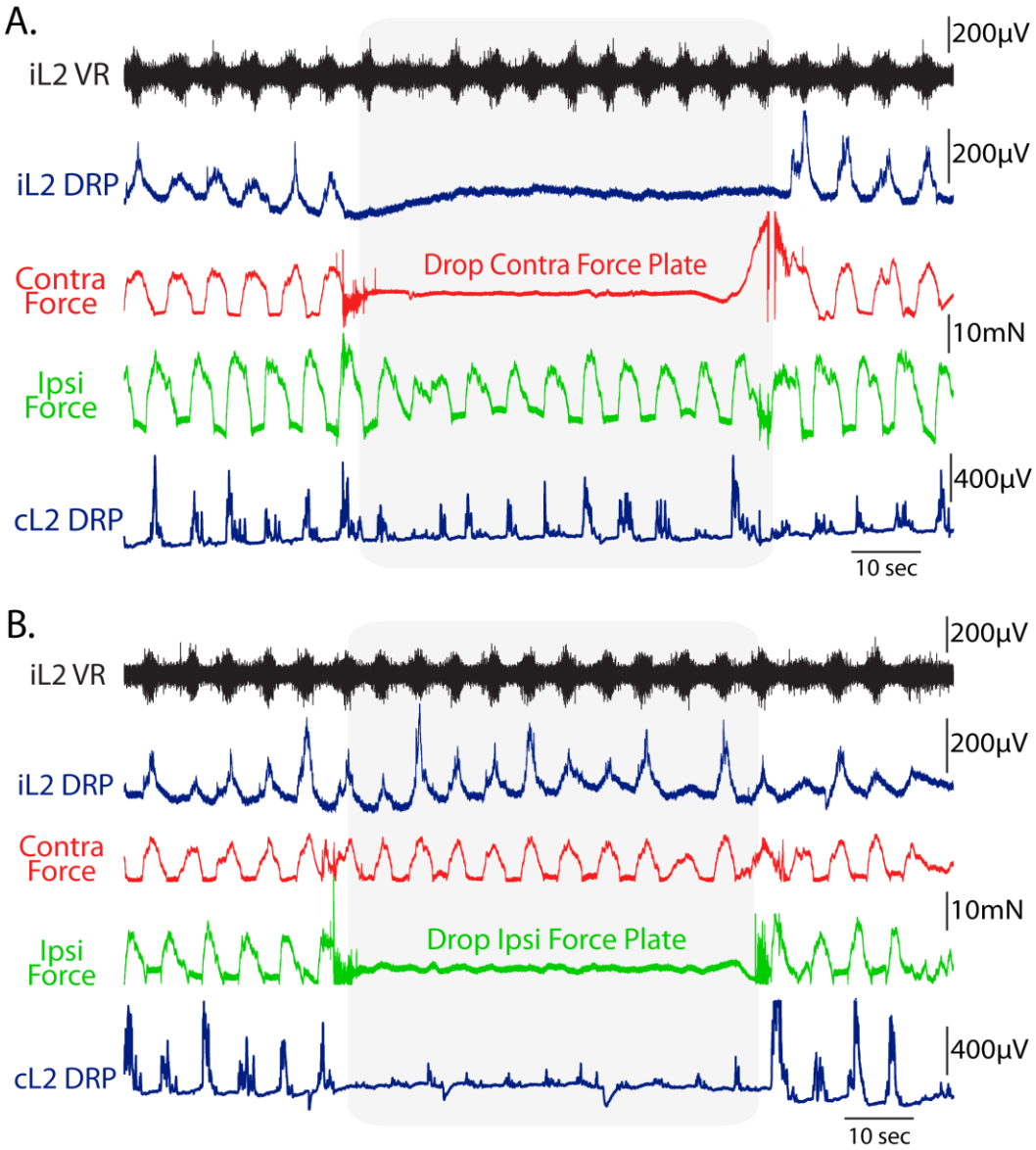

Figure 3.11: Response to contralateral and ipsilateral plate removals

Ipsilateral and contralateral DRPs (iL2 DRP, cL2 DRP, blue) are shown with ipsilateral ventral root activity (iL2 VR, black), contralateral force (red), and ipsilateral force (green). Gray boxes highlight the period of contralateral (A) and then ipsilateral (B) plate removals. Note that there was not a significant change in locomotor frequency before, during, or after plate removal. A: When the contralateral plate is removed, reducing contralateral limb loading, the ipsilateral L2 DRP is nearly abolished. The DRPs return as soon as the contralateral plate is restored. This result demonstrates that sufficient contralateral limb loading is required to generate the large DRPs typically seen during nonfictive locomotion. The contralateral L2 DRP is largely unaffected by the plate removal, as its opposite force remains. B: When the ipsilateral plate is removed, the contralateral DRP is greatly reduced while the ipsilateral DRP is largely unchanged. Note that small contralateral DRPs remain, which are likely centrally-generated as in fictive locomotor literature or generated by residual ipsilateral and/or contralateral input. Yet, the largest contralateral force-sensitive component of the DRP requires significant contralateral force.

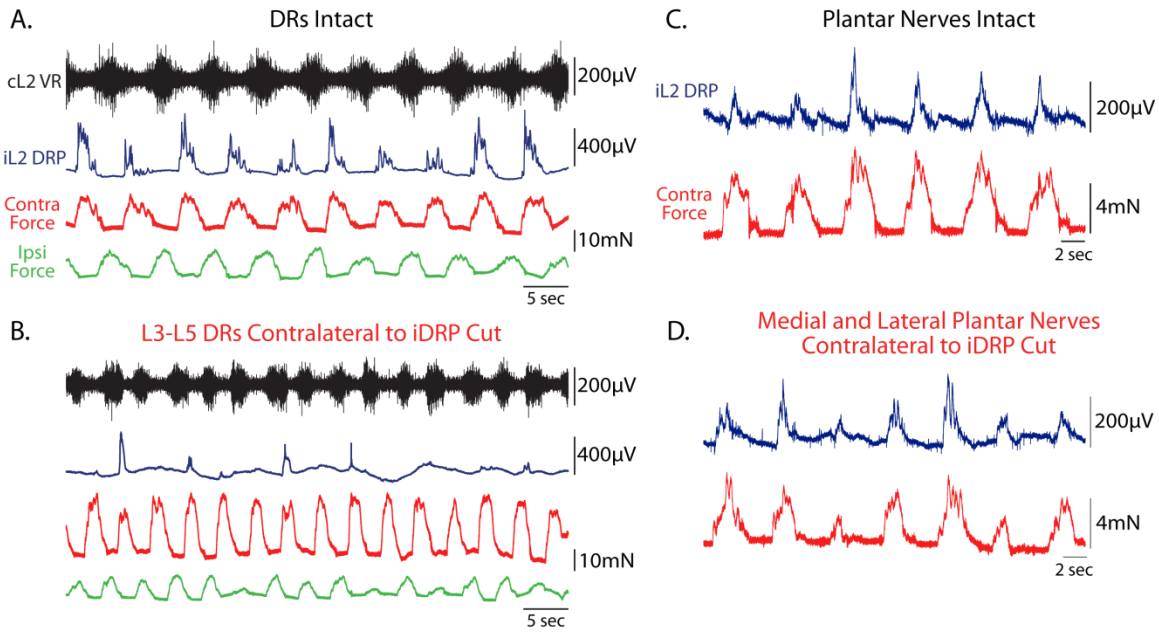

Figure 3.12: Response to contralateral dorsal root and planter nerve transections
A: L2 DRP relative to ipsilateral ventral root, contralateral force, and ipsilateral force with intact dorsal roots during locomotion. B: Following rhizotomy of L3,L4, and L5 dorsal roots contralateral to the DRP, the DRP was significantly reduced and inconsistent despite high contralateral forces. Thus, these DRPs are generated by contralateral afferent input rather than central circuits. Note that the increase in frequency results from the addition of 2 µM NMDA to induce locomotion without intact roots and did not occur when drug concentrations were held constant. C: L2 DRP and contralateral force before plantar nerve transection. D: Following transection of the contralateral medial and lateral plantar nerves, the DRP persisted and continued to scale with contralateral force. Thus, the force-sensitive DRPs do depend on contralateral paw cutaneous afferent input.

In the fourth experiment, which exhibited dopaminergic waxing and waning, the pre-rhizotomy right L2 DRPs were less consistent and only occurred in the presence of the maximal left limb endpoint forces. Post-rhizotomy, larger, highly consistent right L2 DRPs emerged independent of the presence or absence of left force. While the DRPs were not abolished by removing lumbar contralateral afferent input in this animal, their nature was clearly altered.

In contrast to dorsal root rhizotomy, a more selective removal of only paw plantar surface cutaneous afferents by contralateral plantar nerve transection did not substantially affect ipsilateral DRP generation (Fig. 3.12C and D). L2 DRPs persisted and continued to scale with contralateral force (n = 3/3). The failure of plantar nerve transection to block force-dependent DRPs demonstrates that cutaneous afferents are not required.

3.3.8 Contralateral toe contact linked to DRP generation

Contralateral toe ground contact, defined as contact at or distal to the MTP joint, was required for significant DRP generation. Occasionally during locomotion (n = 3), a portion of the paw proximal to the MTP joint rather than the toe would strike the front edge of the plate. When limited or no toe contact occurred, DRPs were reduced or absent (Fig 3.13A).

The timing of contralateral toe contact also influenced DRP onset. When a more proximal portion of the paw struck first, followed by the toe, the onset of the DRP was delayed relative to the initial force. Figure 3.13B shows examples of this pattern. Together, these results suggest that afferents at the toe activated by limb loading contribute to the contralateral afferent signals that evoke the DRP and, thereby, impact DRP magnitude and timing.

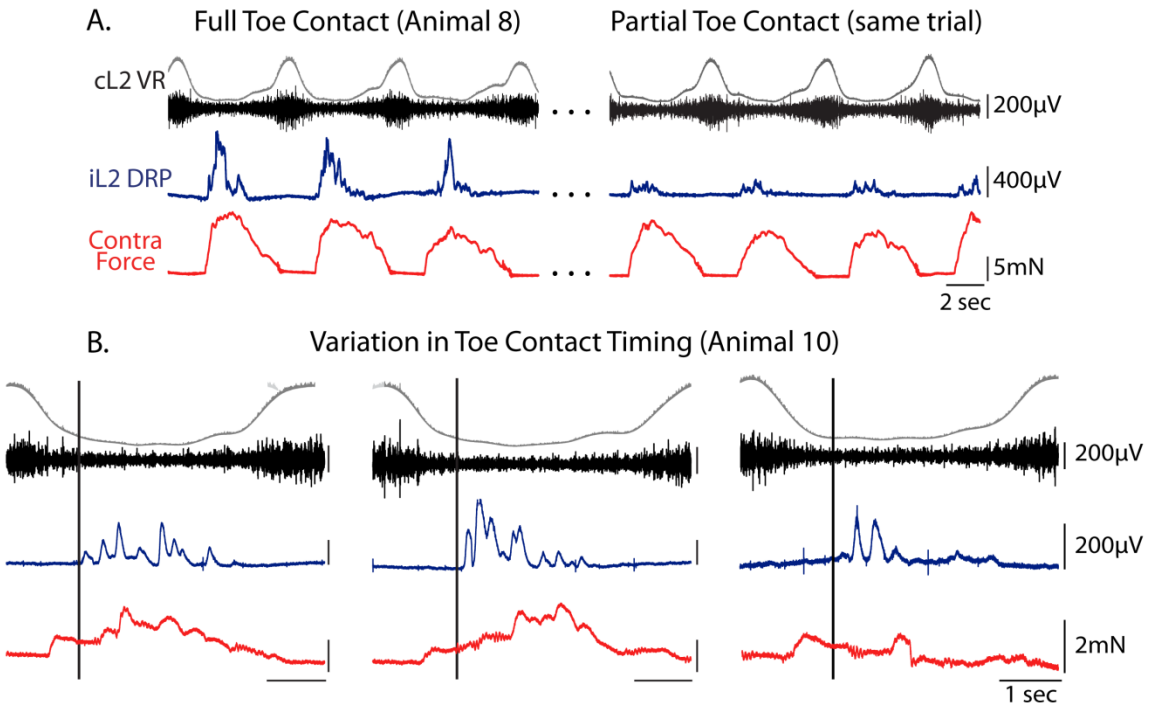

Figure 3.13: Role of contralateral toe contact in DRP generation

A: L2 DRP relative to ipsilateral ventral root (black with gray rectified and integrated envelope) during locomotion with full contralateral toe contact (MTP to toe tip, left panel). 130 seconds later in the same locomotor bout (right panel), the toe moved to the front of the force platform such that only a small portion of the toe contacted the plate. The reduction in toe contact, and likely toe afferent input, resulted in reduced DRPs. B: In another animal, toe contact occurred later relative to force onset. Three examples are shown with corner scale bars all representing 2mN and 1sec. Vertical lines indicate toe contact time. The DRP occurred immediately after the toe contacted the plate rather than at force onset

3.4 Discussion

This study reveals a previously unstudied mechanism for presynaptic inhibition during locomotion. To the best of my knowledge, no previous literature tested the impact of ipsilateral and contralateral hindlimb mechanics on presynaptic inhibition. The results demonstrate that, during non-fictive locomotion, the contralateral limb plays a pivotal role in regulating ipsilateral sensory inflow at the presynaptic terminal. Specifically, contralateral limb stance-phase force influences both the extent and timing of ipsilateral swing-phase presynaptic inhibition, thereby regulating the amount and timing of sensory inflow acting on spinal and ascending circuits. While not the primary aim of this study, preliminary observations suggest that this contralaterally-generated force-sensitive presynaptic inhibition may act to preserve swing by inhibiting unwanted inputs that counteract flexion. Without this inhibition, swing and the accompanying flexion may be susceptible to inhibition. Here I discuss the potential circuitry underlying this phenomenon and its implications for motor control.

3.4.1 Flexion-phase DRPs during non-fictive *in vitro* locomotion are largely generated by contralateral afferents via a GABAergic pathway

3.4.1.1 Contralateral afferent sources

When contralateral lumbar afferent inflow was removed by dorsal root rhizotomy or when signals related to contralateral limb loading were greatly reduced by force plate removal, the L2 DRPs ceased. Therefore, flexion-phase L2 DRPs observed during non-fictive locomotion require and are evoked by contralateral afferent signaling.

Several afferent modalities could be responsible for evoking the observed responses to limb endpoint force. Because ground contact was necessary for the strongest

L2 DRPs, I initially hypothesized that pressure-sensitive cutaneous receptors on the plantar surface of the paw might be responsible. However, removing substantial cutaneous innervation of the paw plantar surface by plantar nerve transection did not reduce the DRPs, demonstrating that cutaneous afferents are not necessary for DRP generation. Intrinsic toe muscles are also primarily innervated by the plantar nerves and, thus, not required for contralateral presynaptic inhibition.

It was also conceivable that group Ia or II muscle spindle afferents from contralateral flexors could contribute to the generation of ipsilateral presynaptic inhibition. However, DRP magnitude did not change with contralateral range of motion (muscle stretch) or slope (rate of stretch) at the ankle, knee, or hip, making a strong contribution to presynaptic inhibition generation from these muscle spindles less likely (Hiebert and Pearson 1999; Prochazka et al. 1989).

Because toe contact was required for DRP generation, toe afferents are a potential source of the contralateral presynaptic inhibition. Extrinsic toe extensors, such as extensor digitorum longus and extensor hallucis longus (EDL and EHL, toe extensors/ankle flexors), are most active during swing and maximally lengthened at the stance-to-swing transition (Loeb and Duysens 1979; Prochazka and Gorassini 1998). As a result, their Ia and Ib (and likely group II) afferents tend to fire in early swing rather than stance (Loeb and Duysens 1979; Prochazka and Gorassini 1998), making their contribution unlikely. In contrast, extrinsic toe flexors, particularly flexor hallucis longus (FHL, toe flexors/ankle extensors), are active during stance with other ankle extensors (O'Donovan et al. 1982). Even though FDL and FHL may not be true synergists in the cat (Bonasera and Nichols 1994), flexor digitorum longus (FDL) can be co-activated with

FHL and other ankle extensors in the rat (Kiehn and Kjaerulf 1996). Recordings from afferents in the moving cat show that FHL and FDL group Ia and group Ib both fire during stance particularly at toe contact (Loeb and Duysens 1979; Prochazka and Gorassini 1998; Prochazka et al. 1976), making their peak firing well-timed to evoke the observed patterns of presynaptic inhibition.

Although Ia, II, or Ib afferents from these toe flexors may contribute, Ib afferents are the more likely afferent source based on the known presynaptic inhibition pathways. Specifically, a previous study in the anesthetized cat indicated that Ib afferents, but not Ia or group II afferents, could produce contralateral presynaptic inhibition (Devanandan et al. 1965). The limited research on crossed presynaptic inhibition pathways could not identify any Ia-evoked crossed presynaptic inhibition (Devanandan et al. 1965). Rather, Ia presynaptic actions tended to be strictly ipsilateral, mirroring the largely ipsilateral and modest contralateral postsynaptic actions of Ia afferents (Harrison and Zytnicki 1984; Holmqvist 1961). Finally, increased contralateral limb endpoint force would likely lead to increased Ib firing as ankle extensor/toe flexor activity increased (Donelan and Pearson 2004; Loeb and Duysens 1979), readily explaining the scaling of presynaptic inhibition with contralateral force. In sum, Ib afferents from FHL and FDL seem the most likely afferent sources and provide a parsimonious explanation for contralateral force-sensitive presynaptic inhibition (Fig. 3.14).

Because most quadrupeds walk digitigrade (Cunningham et al. 2010), the toe muscles are also well positioned to sense ground stability and unexpected toe and ankle perturbations during stance, making their contribution to contralateral sensory regulation rather appropriate. If the landing of the stance limb is abnormal, the limb entering swing

may need to respond and compensate. Humans, on the other hand, walk plantigrade and often run digitigrade (Cunningham et al. 2010). As a result, toe-related contralateral presynaptic inhibition may contribute to sensory regulation with a different spatiotemporal profile during walking (closer to toe off) or simply contribute more significantly during running. Work on humans suggests that the monosynaptic reflex is downregulated with increasing speeds, so presynaptic inhibition may well increase during running relative to walking (Capaday and Stein 1987; Edamura et al. 1991).

3.4.1.2 $GABA_A$-receptor dependency

The L2 DRPs were also abolished by bicuculline, a $GABA_A$ receptor antagonist, confirming that the contralateral afferents act through a GABAergic pathway that requires $GABA_A$ receptor activation. This finding ensures that the rhythmic oscillations in dorsal root potential are not movement artifact, but are indeed reporting $GABA_A$-dependent primary afferent depolarization, the hallmark of classic presynaptic inhibition. Other receptors, such as 5HT3 (Lopez-Garcia and King 1996; Peng et al. 2001), AMPA (Lee et al. 2002), or NMDA (Bardoni et al. 2004) receptors, can generate primary afferent depolarizations and may contribute to the contralateral afferent-evoked presynaptic inhibition, but a large portion of the observed presynaptic inhibition arises through GABAergic transmission.

Previous work in the neonatal spinal cord showed that bicuculline blocked short-latency afferent-evoked DRPs, but lower amplitude and longer latency GABA-independent DRPs emerged at higher concentrations of bicuculline (20μM used in (Kremer and Lev-Tov 1998) compared to 6-10μM used here). GABA-independent centrally-generated DRPs also emerged during fictive locomotion in the presence of 20

μM bicuculline, but the disinhibition produced by these higher concentrations of bicuculline also altered locomotion such that all the ventral and dorsal roots bursted in synchrony. Although these findings suggested that GABA-independent mechanisms might underlie PAD in the neonatal spinal cord, my results suggest that the most prominent components of afferent-evoked DRPs during non-fictive locomotion are largely generated by GABAergic mechanisms and, thus, abolished by lower concentrations of bicuculline (6-10μM). GABA-independent PAD may only dominate in a highly disinhibited state in which GABA receptor blockage significantly reduces spinal neuron inhibition. It should be noted, though, that the small DRPs that persisted in the presence of bicuculline (see Fig. 3.3B) may reflect the GABA-independent centrally-evoked or afferent-evoked PAD mechanisms similar to those reported by Kremer and Lev-Tov (Kremer and Lev-Tov 1998).

3.4.1.3 Peripheral and central sources of onset latency

In the cat, DRPs evoked by contralateral peripheral nerve stimulation occur at a mean latency of ~10-30msec (Devanandan et al. 1965; Eccles et al. 1964; Gossard and Rossignol 1990). While the neonatal rat may exhibit slightly slower conductances and longer synaptic delays (Garraway and Hochman 2001; Takahashi 1992), central delays alone cannot sufficiently account for the relatively long observed delays between contralateral force onset and DRP generation (411msec ± 120msec, range 5.40msec to 2.98sec). Rather, the timing of contralateral afferent activation is likely responsible for the variability and relatively long delays. Contralateral afferents are likely recruited at different times in the force profile during each step, possibly even several 100msecs after force onset. For example, as shown in Figure 3.13B, the timing of toe contact strongly

influences DRP onset, such that the DRP is not generated until toe contact and subsequent toe afferent activation. Following afferent activation, transmission through a crossed polysynaptic, ionotropic $GABA_A$ergic pathway will be relatively rapid (10-30msec *in vivo*), such that this central component accounts for only a small fraction of the total delay from force onset to DRP onset. In addition, contralateral DRP generation may require central convergence of several afferent signals and temporal summation over several 100msecs.

3.4.2 Contralateral force determines both the extent and timing of ipsilateral flexion-phase presynaptic inhibition

3.4.2.1 Magnitude

As shown in Figures 3.4 and 3.5, the magnitude of the L2 DRP strongly correlates with contralateral limb endpoint force, but is independent of ipsilateral force. This relationship suggests that contralateral force plays a major role in regulating swing-phase sensory inflow on the ipsilateral side, particularly of proximal flexors, on a dynamic step-to-step basis. In this way, the amount of force experienced during contralateral stance determines the amount of sensory input allowed into the spinal cord during ipsilateral swing. If contralateral stance-phase force increases, presynaptic inhibition increases such that less sensory feedback can enter the spinal cord through the inhibited afferent pathways; if contralateral force decreases, more feedback is allowed through.

Although the DRP clearly indicates presynaptic inhibition of an afferent population, the identity of this population was not addressed in this study. Thus, the observed presynaptic inhibition may be acting across many populations and modalities to decrease all sensory input to spinal and ascending circuits. Alternatively, presynaptic

inhibition may be acting to selectively block specific pathways and redirect those inputs to distinct postsynaptic targets through non-inhibited pathways. For example, presynaptic inhibition could close an inhibitory pathway and direct feedback through an excitatory pathway. Such a mechanism could underlie the shift from inhibitory force feedback to excitatory force feedback reported previously (Hultborn 2001; McCrea et al. 1995; Pearson and Collins 1993; Quevedo et al. 2000). In fact, disynaptic excitation in flexors in higher during flexion (Quevedo et al. 2000) when presynaptic inhibition is maximum and, thus, capable of altering the balance between inhibitory and excitatory pathways. In summary, the contralateral-afferent-evoked presynaptic inhibition may serve to decrease overall sensory feedback or alter the balance of sensory pathways. In either case, the amount of sensory feedback allowed into the spinal cord through the inhibited afferents is reduced by presynaptic inhibition, even if some of the input is redirected through other non-inhibited or even facilitated pathways.

The plate removal experiments further affirm the assertion that contralateral force influences DRP generation. When the contralateral plate was removed and ground contact force absent, the large L2 DRPs were abolished. Therefore, contralateral force not only influences ipsilateral presynaptic inhibition but is actually necessary for step-to-step generation of the large L2 presynaptic inhibition described here. In some experiments, small rhythmic DRPs remained even after plate removal (see Fig. 3.11B). These remaining DRPs were likely centrally mediated, similar to the DRPs observed during fictive locomotion in the absence of rhythmic afferent inflow (e.g. (Dubuc et al. 1988)). They could also be mediated by rhythmic afferent activity related to ipsilateral or contralateral movement, but both the amplitude and patterns closely resemble those seen

during fictive locomotion. Presumably, central circuits still contribute to presynaptic shaping of sensory inflow, providing a way for locomotor and supraspinal structures to selectively control their inputs. Afferent-evoked presynaptic inhibition adds another layer of sensory regulation to help dynamically shape sensorimotor function to match environmental demands.

3.4.2.2 Timing

Together, these findings imply that contralateral force-related feedback evokes ipsilateral presynaptic inhibition. For this to be possible, contralateral force must occur immediately before the observed DRP. Indeed, in all experiments, contralateral force onset just preceded DRP onset. The strong temporal coupling suggests that contralateral stance onset determines when sensory inflow is maximally inhibited during ipsilateral flexion. In contrast, ipsilateral force exhibited significantly weaker coupling and exerted little influence on the timing of ipsilateral presynaptic inhibition. Motor output also exhibited weak coupling, further confirming that afferent input, not motor output, is largely responsible for the majority of presynaptic inhibition during non-fictive locomotion. To some extent, the rhythmic alternation of locomotion inherently couples left to right and flexion to extension, such that a temporal relationship with stance on one-side will be reflected in motor output and force on the other side. However, variability in this phasing from step-to-step showed that presynaptic inhibition timing was best predicted by contralateral ground contact not motor output or ipsilateral events.

In sum, contralateral stance-phase force influences not only the extent but also the timing of presynaptic inhibition and, therefore, the timing of sensory inflow during ipsilateral swing.

3.4.3 Contralaterally-derived presynaptic inhibition may help preserve ipsilateral swing

Absence of the L2 DRP retarded production of ipsilateral swing, while the presence of extremely large L2 DRPs seemed to disinhibit flexion during quiescence and enhance ventral root activity. While not conclusive, these results imply that presynaptic inhibition of sensory inflow during swing may ensure successful flexion by blocking potentially counterproductive afferent inputs (Fig. 3.14). Once the contralateral limb is loaded, the ipsilateral limb can safely follow through with swing; flexing the limb without sufficient contralateral loading would result in a fall unless an aerial phase was intended. Thus, it would be reasonable for contralateral limb loading to signal ipsilateral swing carry-through by inhibiting afferent feedback that would otherwise impede flexor muscle activation (Duysens and Pearson 1980a; Pang and Yang 2000).

Alternatively, the connection between DRP and kinematic or ventral root flexion may reflect central coupling rather than an effect of presynaptic inhibition. For example, *in vitro* locomotion and *in vivo* fictive locomotion can both exhibit deletions, in which a muscle group or groups fails to burst for period of time (Lafreniere-Roula and McCrea 2005). If central circuits produced an ipsilateral flexor deletion with a contralateral extensor deletion, the contralateral force-sensitive DRP and ipsilateral flexion would both be missing. Because the DRP is eliminated by contralateral plate removal or dorsal root rhizotomy, the DRP itself is not centrally-evoked, but the force that generates the DRP and the apparently related ipsilateral flexion could be centrally coupled. In addition, the GABAergic interneurons generating the presynaptic inhibition may have additional actions on central circuits, motoneurons, or premotor interneurons, as GABAergic

interneurons with presynaptic axo-axonic synapses often have axo-dendritic synapses on motoneurons and premotor interneurons (Hughes et al. 2005; Pierce and Mendell 1983). Thus, flexion could be affected through direct actions on the spinal locomotor circuitry or motoneurons by the same interneurons producing presynaptic inhibition. Although presynaptic inhibition appears to contribute to swing-phase flexion, more studies are needed to confirm this hypothesis.

It should also be noted that the relationship between contralateral force and ipsilateral flexion may differ depending on the mechanics of the task. For example, during pedaling, contralateral force may actually reduce flexor activity, while the absence of contralateral movement and force increases net flexor activity (Ting et al. 1998; Ting et al. 2000). Because the limbs are coupled via a crank during pedaling, contralateral limb extension creates flexor torque on the ipsilateral limb such that less flexion muscle activity is required during the recovery phase. Thus, the neural control strategy for pedaling may be wired to reduce unnecessary flexion in the presence of sufficient contralateral extension force and mechanically-generated recovery phase torque. In contrast, during locomotion when crank coupling is not present, sufficient contralateral limb loading may actually signal flexion because the body is now supported by the other limb, making swing and forward progression possible and safe. Such task-specific changes in interlimb coupling may reflect changes in presynaptic inhibition patterns and/or changes in central coupling.

3.4.4 Proposed circuitry

The few studies mapping contralateral pathways at rest suggest that Ibs *produce* contralateral presynaptic inhibition, while Ias and II do not (Devanandan et al. 1965). As

discussed, my results are consistent with Ib afferents in contralateral toe flexors generating the observed presynaptic inhibition.

However, the *receiving* afferents are more difficult to discern. In order for contralaterally-evoked presynaptic inhibition to preserve swing-phase flexion, the presynaptic inhibition would need to inhibit afferent activity that would otherwise impede flexion. For example, inhibition of flexor Ib afferents could facilitate swing by removing negative force feedback (disinhibiting) onto flexor motoneurons during peak muscle contraction. Previous work in the cat suggests that Ib inhibition of flexor motoneurons may be replaced by disynaptic excitation during locomotion (Quevedo et al. 2000). Presynaptic inhibition during the swing phase could serve to inhibit the inhibitory pathways typically available at rest (Brizzi et al. 2002) while postsynaptic mechanisms increased excitability of interneurons in the excitatory pathways (Burke 1999; Quevedo et al. 2000), resulting in a change in the balance of inhibitory and excitatory pathways onto flexors. Alternatively, inhibition of extensor Ia afferents could facilitate swing by preventing excitatory feedback onto extensor motoneurons in response to extensor stretch. According to a limited number of previous studies, Ib afferents receive crossed presynaptic inhibition from contralateral Ib afferents (Devanandan et al. 1965), but whether Ia afferents *receive* contralateral presynaptic inhibition from any afferents is up for debate (Jankowska et al. 1966). In the pentobarbital anesthetized cats, Devanandan did not find any evidence of crossed inhibition of Ia afferents, but pentobarbital can depress polysynaptic transmission and, thus, mask pathways that may mediate slightly weaker crossed inhibition of Ia afferents (Eccles 1946; Mehta and Ticku 1999; Ziskind-Conhaim 1990). In the anaesthetized cat, only higher threshold afferents, including flexor

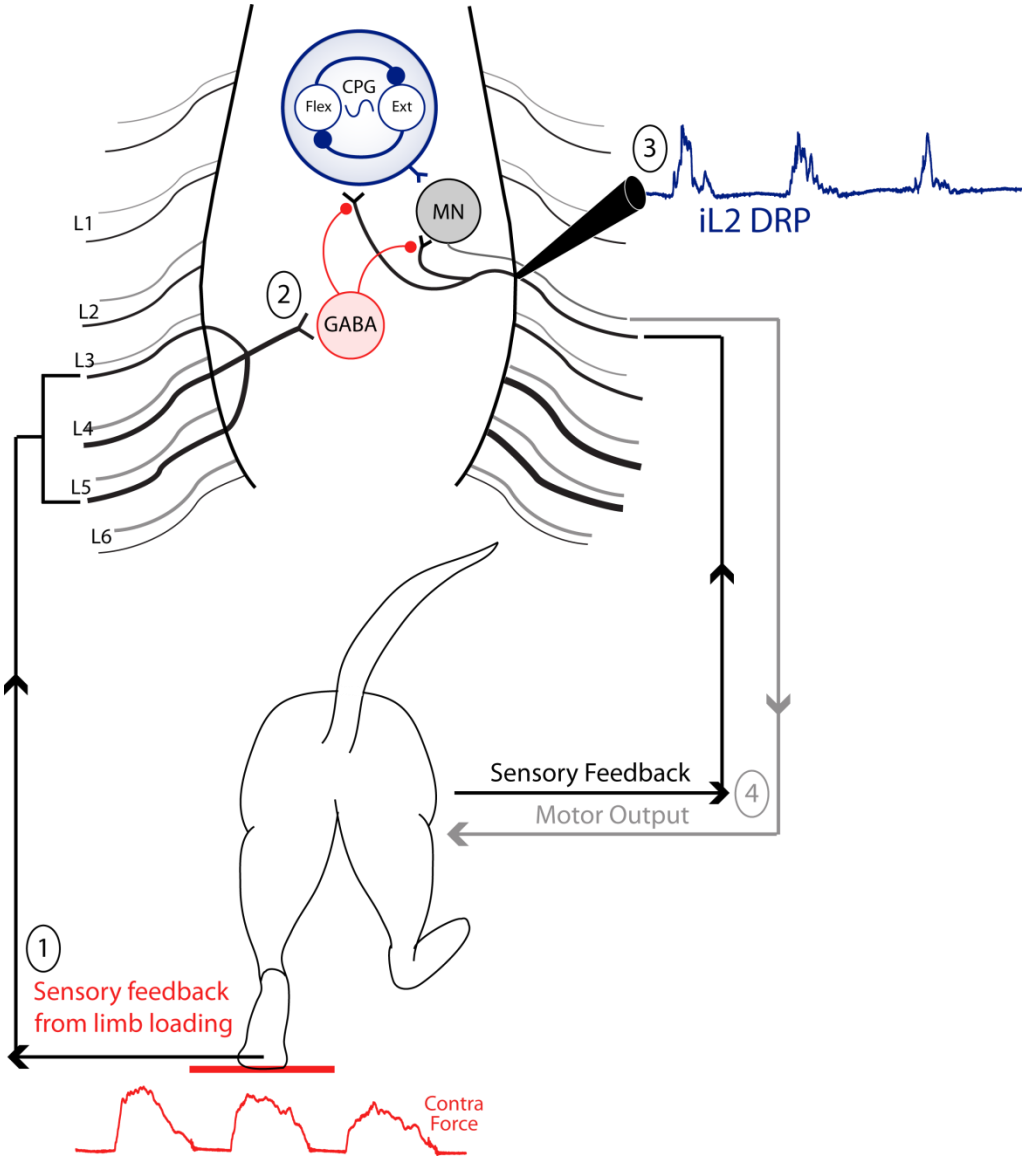

Figure 3.14: Proposed Circuitry

Proposed circuitry underlying contralateral presynaptic inhibition evoked by contralateral limb loading. Sensory events and dorsal roots are shown in black. Motor effects and ventral roots are in gray. A simplified representation of the central pattern generator (CPG) is also shown. The sequence of events are numbered 1-4. 1: Contralateral limb loading and toe contact activate Ib afferents that then enter contralateral dorsal roots L3-L5. The magnitude of the activation scales with force. 2: These afferents then activate a crossing, GABAergic pathway for producing crossed presynaptic inhibition. Since the majority of identified commissural interneurons receiving Ib input are glutamatergic, not GABAergic (Bannatyne et al. 2009), the pathway may likely include glutamatergic commissural interneurons that subsequently activate a GABAergic interneuron. 3: Sensory input from the ipsilateral limb is then presynaptically inhibited. This inhibition is recorded as a DRP at the iL2 (as well as iL5) dorsal root. 4: By blocking sensory inputs and/or closing sensory pathways, presynaptic inhibition may impact ipsilateral motor output during the swing/flexion phase.

reflex afferents (typically group III not II), could produce presynaptic inhibition of contralateral Ia afferents. However, cycling studies have shown the contralateral passive and active limb movement depress the H-reflex (Brooke et al. 1997; Collins et al. 1993; McIlroy et al. 1992), suggesting that afferents from the contralateral limb can modulate Ia transmission. While pre- and post-synaptic actions cannot be distinguished in these cases, presynaptic inhibition has been proposed as the responsible mechanism (Collins et al. 1993; McIlroy et al. 1992). In summary, Ib afferents very likely receive crossed presynaptic inhibition from contralateral Ib afferents, but whether Ia afferents receive similar inhibition remains unclear.

Based on my findings combined with previously identified pathways, Figure 3.14 illustrates the proposed underlying circuitry for generating the patterns of contralateral presynaptic inhibition described in this study. In this proposed pathway, force-sensitive Ib afferents from toe flexors would sense contralateral force magnitude at toe contact and activate a commissural pathway for GABAergic presynaptic inhibition. Given that most commissural interneurons receiving group I input in laminae VI--VIII are glutamatergic, this pathway may well involve an interposed glutamatergic interneuron in addition to a GABAergic interneuron (Bannatyne et al. 2009; Jankowska et al. 2009). Subsequent inhibition of Ib afferents from hip and ankle flexors may then preserve ipsilateral swing by removing negative force feedback during peak muscle contraction. This explanation agrees with recent findings by Faist and colleagues showing that loading may be essential for inhibition of Ib pathways in healthy humans (Faist et al. 2006). Inhibition of Ia afferents from hip and ankle extensors may also contribute by reducing extensor resistance. It should be noted that previously unidentified pathways may exist or become

disinhibited during non-fictive locomotion (Jankowska 1992; Jankowska et al. 1966), but the proposed circuitry provides the most parsimonious explanation.

3.4.5 Functional implications

The primary finding of this study is that the contralateral limb, particularly limb loading, contributes significantly to ipsilateral sensory regulation and thereby couples the sensory state of the two limbs. Interlimb coordination is vital for successful bipedal or quadrupedal locomotion (Ting et al. 1998). For example, when one leg is lifted off the ground or is unexpectedly perturbed, the other limb(s) must respond to stabilize the animal and/or continue forward progression. My results show that interlimb coupling is not only achieved through central pattern generating circuits, supraspinal commands, and crossed reflex pathways, but also through force-sensitive presynaptic inhibition. Through this presynaptic inhibition, contralateral force informs the ipsilateral limb of contralateral sensorimotor state. It then shapes ipsilateral sensory sensitivity, potentially reducing unneeded inputs and focusing attention on important inputs needed to direct limb placement or adjust swing if perturbed (e.g. (Bouyer and Rossignol 2003a; Forssberg 1979; Quevedo et al. 2005; Rossignol et al. 2006; Van Wezel et al. 1997)).

3.4.5.1 Task-dependent reflex modulation

Presynaptic inhibition also provides a mechanism for modulating reflex gain to match task and environmental demands depending on ground reaction force profiles. Studies in fictive locomotion show that central circuits, such as the spinal locomotor circuitry, regulate reflex transmission via presynaptic inhibition in both a phase- and task-dependent manner. For example, the effectiveness of muscle afferent-evoked presynaptic inhibition of the monosynaptic reflex varies with the phase of locomotion (Gossard and

Rossignol 1990; Ménard et al. 2003) and the patterns of centrally-evoked presynaptic inhibition change between fictive locomotion or fictive scratching (Cote and Gossard 2003). In this way, central circuits can differentially regulate their sensory inputs depending on the task and the locomotor phase. The results presented here suggest that contralateral-afferent-evoked presynaptic inhibition provides another layer for phase and task-dependent modulation of sensory regulation. During typical walking, this form of presynaptic inhibition is likely maximum during contralateral stance and ipsilateral swing. As the task changes, the force profiles will change, leading to changes in both the magnitude and timing of this presynaptic inhibition. Similarly, changes in interlimb phasing between gaits or changes in stance-swing interlimb timing will also change the timing of contralateral-afferent-evoked presynaptic inhibition.

In addition to phase- and task-dependent modulation, contralateral-afferent-evoked presynaptic inhibition also allows for further fine tuning of sensory inflow on a step-to-step basis. If ground stability, ground contact, limb orientation, or any other perturbation causes changes in limb loading, contralateral-afferent-evoked presynaptic inhibition will change, allowing the spinal cord to adjust ipsilateral sensory feedback as needed. Altering reflex gains in response to these peripheral cues allows animals or humans to shape the sensitivity of their motor program to various peripheral signals and perturbations (Prochazka 1989).

3.4.5.2 Relationship to H-reflex studies

H- reflex studies during human locomotion further confirm that reflex gain is modulated across the step cycle. In particular, studies on the soleus H-reflex suggest that the monosynaptic reflex gain is highest during ipsilateral stance and lowest during swing

(e.g. (McIlroy et al. 1992; Stein 1995)). Many of these studies hypothesized that H-reflex modulation likely occurred presynaptically, but were unable to test their hypothesis directly due to the limitations of H-reflex measurements. This study shows that locomotor-related presynaptic inhibition of L2 and L5 afferents reaches maximum during ipsilateral swing, meaning that reflex gain would be highest during stance and most presynaptically suppressed during swing. Thus, the temporal pattern of presynaptic inhibition matches the observed reflex gain modulation, confirming that presynaptic inhibition could be responsible for H-reflex modulation across the step cycle. However, given the mixed reports on crossed presynaptic inhibition of Ia afferents, more studies are needed to determine whether presynaptic inhibition actually contributes to contralateral modulation of H-reflexes. Further, H-reflexes modulation must be interpreted with caution as they do not always accurately represent modulation of the physiological stretch reflex. As shown by Sinkjaer and colleagues, modulation of the electrically-activated H-reflex can differ significantly from modulation of the physiologically-activated stretch reflex during human walking (Anderson and Sinkjaer 1999).

Stein and colleagues also observed that H-reflex gains are lower during running than walking (Capaday and Stein 1987; Edamura et al. 1991). They were unable to account for these changes based on locomotor speed or background EMG activity (i.e. motor output), leaving the source undetermined. However, force area (impulse) and force peak are both higher in running compared to walking (Munro et al. 1987; Nilsson and Thorstensson 1989). Based on my results, such higher peak forces would lead to increased swing-phase presynaptic inhibition and reduced reflex gain. Reducing reflex gain during running relative to walking could prevent saturation of motoneuron pools to

maintain input sensitivity, as suggested by Stein (Stein 1995). Without reflex gain reduction, the higher stretch and contraction velocity and the increased synchrony from shortened stance times could lead to motoneuron saturation. Again though, the probability of contralateral Ia inhibition remains unclear.

3.4.5.3 Potential role in speed

As mentioned above, increases in locomotor speed are typically accompanied by increases in peak limb forces. According to my results, as limb force and locomotor speed increase, swing phase presynaptic inhibition increases (Figs. 3.6 and 3.8). As a result, the swing phase becomes more and more feedforward, with less attention to sensory feedback, as locomotor speed or strength rise. Previous modeling and intact animal studies have suggested that intrinsic mechanical stability increases with speed, making neural feedback-derived stability less important (Kubow 1999; Ting et al. 1994). Interjoint coordination is also reduced at higher speeds (Yen and Chang 2010). Reducing sensory feedback with presynaptic inhibition at higher forces and speeds, would allow the intrinsic mechanical stability of the musculoskeletal system to dominate while also preventing unwanted perturbations while the limb is off the ground.

In addition, rises in presynaptic inhibition with speed could prevent irrelevant information from perturbing or destabilizing locomotion. The faster an animal walks, the less relevant an afferent event becomes once it reaches the spinal cord because the conduction delay is now longer relative to the gait cycle. At extremely high speeds, the lag between peripheral event and central action could actually make sensory feedback de-stabilizing. It is important to note that the SCHP never reaches extreme speeds, but rather steps in place (net forward speed 0m/s) at a fairly low rate (0.1 - 0.4 Hz). But, the

relationships between neural activity and behavior offer us insight into the circuitry behind intact adult behaviors and help us understand how the circuit might function under different mechanical conditions.

3.4.6 Limitations

The most obvious limitation of neonatal *in vitro* preparations is the compounding factor of development. Due to developmental changes, mechanisms observed in neonates can differ from those in adulthood. However, the agreement between my results and the patterns of reflex modulation observed in adult animals, as well as in humans, suggest that the same presynaptic mechanism likely persists into adulthood. My results also reflect similar patterns to those reported by Yakhnitsa et al in the adult rat (Yakhnitsa et al. 1988). In both cases, this study provides insight into the mechanism underlying their observations. Previous researchers have also questioned the behavioral relevance of neonatal models since neonates at this age exhibit different walking patterns (Smith and Feldman 1987), but early work on the SCHP demonstrated that, when given appropriate sensory feedback, the neonatal spinal cord can produce adult-like locomotor patterns. I also showed that sensory feedback could alter and pattern locomotion, even at this early developmental stage (Hayes et al. 2009a).

On the other hand, the wide range of patterns exhibited during *in vitro* locomotion allows us to explore a broader variety of locomotor behaviors, such as the waxing and waning pattern and deletions, that provide us with insight into underlying mechanisms. The support of the spinal cord in the *in vitro* SCHP also enables us to perform unique mechanical perturbations, such as the single limb plate removal, that would not be feasible in the intact animal requiring consistent body weight support.

Finally, some sensory inputs, such non-paw cutaneous inputs, are absence in the SCHP. These inputs may contribute to presynaptic inhibition or may modulate PAD pathways during locomotion (Eguibar et al. 1997b; Enríquez et al. 1996; Rudomin 2009) and, thus, should be addressed in future studies.

3.4.7 Conclusions

My results show that the contralateral limb, particularly limb loading, strongly influences both the magnitude and timing of ipsilateral presynaptic inhibition and, thus, the extent and timing of sensory access to spinal circuits. As contralateral limb loading increases for a given step or a given task, ipsilateral presynaptic inhibition increases, such that sensory inputs are not allowed through the inhibited afferent pathways and into the spinal cord during the swing phase. The timing of contralateral afferent activation also determines when sensory feedback is allowed in and when it is presynaptically inhibited. In this way, contralateral-afferent-evoked presynaptic inhibition neuromechanically couples the sensorimotor states of the limbs. While further studies are needed to fully understand the implications of these findings, contralateral presynaptic inhibition may play a role in swing-phase flexor activation, preserving swing in the presence of sufficient contralateral limb support and allowing inhibition of swing in its absence. Additionally, by responding to the limb loading condition, contralateral presynaptic inhibition can also modulate reflex sensitivity and interlimb coupling based on locomotor speed, task, and step-to-step environmental perturbations.

CHAPTER 4

CONCLUSIONS

During locomotion, the spinal cord must integrate sensory feedback with central commands to generate the appropriate motor output. Sensory feedback informs the nervous system about the state of the limbs and the environment, enabling the spinal cord to adapt motor output for unexpected perturbations and adjust muscle timing and magnitude on a step-by-step basis. In this way, sensory feedback "regulates" spinal motor output, but the spinal cord must also "regulate" sensory feedback. Each task requires a different sensorimotor strategy, emphasizing specific sensory cues and directing those cues through selected pathways to create appropriate muscle, joint, and interlimb coordination patterns. Presynaptic inhibition allows the spinal cord to select which sensory inputs to focus on and which to ignore, preventing motoneuron saturation and counterproductive reflex actions. Presynaptic inhibition also routes sensory feedback to the appropriate postsynaptic targets, such as reflex pathways, central pattern generating circuits, or ascending systems (Jankowska 1992; Rudomin 2009). Understanding how the spinal cord both uses and regulates sensory feedback is vital for designing locomotor rehabilitation strategies for patients with sensorimotor impairments.

4.1 Summary and discussion of key findings

The primary goal of this work was to investigate sensory regulation in the spinal cord during locomotion, addressing how sensory feedback regulates spinal motor output and, in turn, how the spinal cord regulates sensory feedback via presynaptic inhibition. **Aim 1** was to develop a model that combined the advantages of *in vitro* and *in vivo*

preparations that would expand our ability to study spinal sensorimotor circuitry. Classic *in vitro* preparations, such as the isolated spinal cord, offer many advantages, including pharmacological and neural access and the stability for intracellular or technically challenging recordings. However, they lack sensory feedback which strongly influences not only motor output but also the function of the circuitry being studied. They also lack behavioral observability, preventing us from understanding how the mechanics influence spinal function and vice versa. While *in vivo* models offer intact sensory feedback with behavioral observability in a functional environment, direct neural measurements that require cord stability are difficult during unrestrained movement. For example, H-reflex modulation can be measured but presynaptic inhibition cannot. Acute neural and pharmacological manipulations are also more difficult in the intact animal, although possible in models like the decerebrate cat. Here, I developed the *in vitro* spinal cord-hindlimb preparation (SCHP) in the neonatal rat, combining exquisite neural accessibility and manipulability with intact sensory modulation and behavioral observability.

Using the SCHP in **Aim 2**, I carried out the first biomechanical characterization of hindlimb locomotion generated *in vitro,* providing a behavioral context for the many neural mechanisms elucidated during neurochemically-induced locomotion in previous *in vitro* spinal cord models. First, I showed that neurochemically-induced (specifically NMDA and 5HT) locomotion is flexible rather than stereotyped. Even when activated by the same neurochemicals, the neonatal spinal cord produces different kinematics and muscle activation patterns depending on the mechanosensory environment. During ventral-up airstepping, the SCHP produced a pattern that closely resembled *in vivo* airstepping, with prolonged-extensor phase plateaus, in-phase flexion and extension in all

three joints, and flexor-dominated muscle duty cycles. During dorsal-up treadmill stepping, the SCHP exhibited kinematic and muscle activation patterns similar to "typical" (i.e. overground or treadmill) intact rat locomotion, including knee flexion during stance and extensor-dominated muscle duty cycles. Importantly, the differences were not purely mechanical changes, but rather sensory feedback actually altered the muscle activation patterns outputted by the spinal cord. For example, ground contact and the corresponding sensory feedback were required to produce the muscle phasing and extensor-dominated muscle duty cycles typical of intact rat locomotion. As shown by the mechanical perturbations, sensory feedback from unilateral swing assistance and bilateral passive stepping-like movements also reinforced, strengthened, or even initiated locomotion in the SCHP. Together these findings from Aim 2 highlight the role of sensory feedback in sculpting and regulating spinal motor output to fit the task and respond to the mechanical environment. The findings also confirm the efficacy of the SCHP for studying spinal function during sensory-influenced, behaviorally-relevant locomotion.

Precisely because sensory feedback can so strongly influence spinal motor output, such as muscle phasing, muscle duty cycles, and activation strength, sensory feedback must be tightly regulated. A primary mechanism for selectively regulating sensory inflow to the spinal cord is presynaptic inhibition. Prior to the SCHP, our knowledge of presynaptic inhibition during behavior was limited because it was nearly impossible to monitor PAD or DRPs due to spinal cord instability during unrestrained movement. Studies of peripheral nerve stimulation during fictive locomotion, as well as inferences from H-reflex studies, suggested that central circuits and multimodal afferents interacted

to create task-specific patterns of presynaptic inhibition, but the patterns created by natural afferent patterns interacting with the spinal locomotor circuitry remained elusive. Many questions remained unanswered: How do hindlimb mechanics and ground interaction influence presynaptic inhibition patterns? What biomechanical variables and types of sensory feedback contribute to presynaptic inhibition? Is presynaptic inhibition coupled between limbs, such that one limb's movement influences the other limb's sensory regulation? What is the balance between centrally-generated and afferent-generated presynaptic inhibition during non-fictive locomotion?

One of the greatest advantages of the SCHP is the ability to mechanically stabilize the spinal cord while retaining sensory feedback and intact limb movement. In **Aims 3 and 4**, I harnessed these advantages to study the role and patterns of presynaptic inhibition during non-fictive locomotion. Specifically, I investigated how ipsilateral and contralateral hindlimb mechanics modulate presynaptic inhibition. I hypothesized that contralateral limb movement and loading would influence presynaptic inhibition and, thus, sensory regulation on the ipsilateral limb. Indeed, my results demonstrated that during non-fictive locomotion, the contralateral limb, particularly limb loading, plays a pivotal role in regulating ipsilateral sensory inflow at the presynaptic terminal. Contralateral stance-phase force positively modulates both the magnitude and timing of ipsilateral swing-phase presynaptic inhibition and, thus, the extent and timing of sensory inflow to spinal circuits; as contralateral limb loading during stance increases, ipsilateral swing-phase presynaptic inhibition increases and less sensory information enters through the inhibited afferents to act on spinal circuits. In contrast, neither ipsilateral joint movement nor loading appears to influence ipsilateral presynaptic inhibition. Ipsilateral

sensory feedback certainly modulates ipsilateral sensorimotor state through traditional reflex pathways and can even alter limb mechanics (Nichols et al. 1999; Nichols and Houk 1973), but it does not appear to play as strong a role as contralateral feedback in presynaptic sensory regulation.

According to my results, contralaterally-derived presynaptic inhibition may contribute to swing-phase flexion generation on the ipsilateral limb. Although this finding deserves further investigation, presynaptic inhibition may inhibit signals that would otherwise retard flexion generation by inhibiting flexor motoneurons or inappropriately activating extensor motoneurons during swing (see Fig. 3.14 and discussion below). This form of interlimb coupling may prevent falling. If the contralateral limb is sufficiently loaded such that continuing swing is safe, presynaptic inhibition preserves flexion. Without this presynaptic inhibition, flexion is susceptible to disturbance (see Fig. 3.9). Although the spinal locomotor circuitry and other sensory inputs can still produce some flexion in this case, this flexion activity may sometimes be insufficient without the contributions of presynaptic inhibition.

Such interlimb coupling between the contralateral and ipsilateral limbs is appropriate for many rhythmic tasks and consistent with previous observations that moving or loading the contralateral limb can alter ipsilateral reflex gains (Brooke et al. 1995b; Collins et al. 1993; Faist et al. 2006; McIlroy et al. 1992) and muscle activation patterns (Alibiglou et al. 2009; Ting et al. 1998; Ting et al. 2000). Importantly, the coupling may be task-specific such that the directionality of these effects differs depending on the task. During cycling, contralateral extensor force reduces flexor activity, while the absence of contralateral movement and force increases net flexor

activity (Ting et al. 1998; Ting et al. 2000). In contrast, my findings suggest that presynaptic inhibition evoked by contralateral limb loading may help preserve flexion during stepping. This difference likely reflects the use of different sensorimotor control strategies for cycling versus stepping. During cycling, contralateral limb extension creates flexor torque on the ipsilateral limb such that less flexion muscle activity is required during the recovery phase. Although the studies decoupled the limb by powering the contralateral crank when the contralateral limb was inactive, the neural control strategy for pedaling may still be wired to reduce unnecessary flexion in the presence of sufficient contralateral extension force and mechanically-generated recovery-phase torque. During locomotion when crank coupling is not present, sufficient contralateral limb loading may actually signal flexion because the body is now supported by the other limb, making swing and forward progression possible and safe. Alternatively, the discrepancies could reflect differences in bipedal (humans) and quadrupedal (rats) sensorimotor strategies or developmental changes in the behavioral consequences of presynaptic inhibition. Thus, further studies are needed to fully understand the implications of contralateral loading on ipsilateral flexor generation during locomotion.

Figure 3.14 shows the proposed circuitry underlying contralateral presynaptic inhibition generation and its resulting ipsilateral motor effects. Based on the properties of the DRPs, as well as their elimination with contralateral dorsal root rhizotomy, the force-sensitive contralateral presynaptic inhibition is generated by afferent activity from the toes entering the lumbar dorsal roots rather than by central circuits. Although pathways can become disinhibited or inhibited during locomotion, studies at rest typically show us what pathways exist and might be utilized during behavior. Early studies in the

anesthetized cat suggested that Ib afferents produced presynaptic inhibition on contralateral Ib afferents, while Ia and group II afferents did not produce any crossed actions, implicating Ib afferents in the observed contralateral presynaptic inhibition patterns. In addition, toe contact was required for the observed DRP patterns, implicating afferents at the toe. During locomotion in the cat, Ib afferents in extrinsic toe flexors, such as FDL and likely FHL, fire during stance with peak activation occurring at stance onset (Prochazka and Gorassini 1998; Prochazka et al. 1976), such that Ib activation could readily initiate contralateral presynaptic inhibition upon toe contact and respond to limb loading. Given this, I propose that Ib afferents from toe flexors initiate the contralateral presynaptic inhibition that preserves ipsilateral flexion during non-fictive locomotion. The exact afferents receiving the inhibition is unclear, with Ib afferents being the most likely but Ia afferents being possible as well (Brooke et al. 1997; Devanandan et al. 1965; Jankowska et al. 1966). In either case, contralateral presynaptic inhibition acts during swing-phase flexion in response to sufficient contralateral limb loading.

Interestingly, the likely involvement of Ib afferents in presynaptic interlimb control may reflect a broader pattern of afferent organization. While Ia afferents play a prominent role in muscle and single joint stiffness, Ib afferents are thought to coordinate whole limb muscle activation and interjoint coordination (Jankowska 1992; Nichols et al. 1999). Ia afferents largely serve to coordinate at the local level, while Ib afferents regulate more wide spread interactions. In fact, activation of Ib afferents affects almost every muscle in the hindlimb and interneurons in Ib pathways receive highly convergent input from Ia, Ib, II, and cutaneous afferents as well as from descending systems (Jankowska 1992). Given their role in multi-joint coordination on the ipsilateral limb, it is

not surprising that Ib pathways might also coordinate actions between limbs. Descending systems have been shown to select (inhibit and disinhibit) specific populations of Ib interneurons to facilitate single limb muscle coordination for a given task (Fournier et al. 1983). Descending systems may similarly adjust these pathways to facilitate appropriate interlimb sensory regulation.

4.2 Function of force-sensitive contralateral presynaptic inhibition

Every task requires a different set of sensorimotor strategies. Descending systems can reconfigure neural circuits and reflex gains in preparation for a task, but force-sensitive contralateral presynaptic inhibition may also help adjust sensorimotor strategies by responding to task-specific loading conditions. For example, peak ground reaction forces are higher in running than walking and tend to increase with speed (Munro et al. 1987; Nilsson and Thorstensson 1989). In walking, running, or cycling, contralateral loading is out-of-phase with ipsilateral loading, but, during hopping, contralateral and ipsilateral forces are in-phase. According to the results in Chapter 3, such changes in the magnitude and timing of contralateral force significantly alter sensory regulation by changing the magnitude and timing of presynaptic inhibition, leading to changes in reflex gain, sensory inflow, and possibly postsynaptic target. As such, force-sensitive contralateral presynaptic inhibition can modify sensorimotor integration and shape the sensitivity of motor output to select sensory cues in a task-dependent manner. By blocking specific inputs, presynaptic inhibition can heighten focus on the most relevant cues, such as limb placement cues, cutaneous cues during swing, or perturbations demanding bilateral responses (e.g. (Bouyer and Rossignol 2003a; Forssberg 1979; Quevedo et al. 2005; Rossignol et al. 2006; Van Wezel et al. 1997)).

Contralateral presynaptic inhibition may also regulate sensory feedback on a step-to-step basis. In combination with central interlimb coupling and crossed reflex actions, contralateral presynaptic inhibition may help coordinate the limbs to ensure coordinated, bilateral responses to perturbations. Because it grades with limb loading conditions, contralateral presynaptic inhibition will change with ground stability, ground contact, limb orientation, or any other perturbations that induce changes in limb loading, allowing the spinal cord to adjust ipsilateral sensory feedback in response to peripheral cues even when the ipsilateral limb is off the ground. If one limb senses a change in ground stability or falls in a hole, the other limb needs to adjust its strategy. In this way, contralateral presynaptic inhibition, in concert with central interlimb coupling and crossed reflex actions, coordinates the limbs to ensure the appropriate bilateral responses to perturbation and multi-limb interactions required for successful locomotion.

4.3 Neuromechanical interactions

During movement, the passive mechanical properties of the musculoskeletal system interact with central output and neural reflexes to produce movement. Limb mechanical properties, including muscle stiffness, segmental inertias, and joint stiffness, all filter the effect of motor commands from the spinal cord. The same muscle activation can result in different endpoint forces depending on the posture of the limb and moment arms of the muscles. Contralateral limb posture can even reverse reflex responses at the spinal level (Grillner and Rossignol 1978a) and alter the reflexive response to perturbations (Hiebert et al. 1994). In turn, sensory feedback affects limb mechanics. Ia monosynaptic reflexes linearize muscle stiffness and work with passive muscle properties to determine the muscle's response to stretch or joint movement (Houk 1979; Nichols and

Houk 1973). With their more distributed and stronger non-parent muscle actions, Ib afferents help regulate whole limb stiffness and interjoint coordination (Jankowska 1992; Nichols 2002).

This interplay is exemplified by the studies in Chapter 2. Even when activated by the same neurochemical drive, the motor behavior produced by the spinal cord was significantly altered by the mechanical environment and the corresponding feedback (Hayes et al. 2009a). Without ground interaction, the SCHP exhibited an airstepping-like behavior with all joints acting in-phase. By simply reversing orientation and providing ground contact, the knee flexed during stance out-of-phase with the hip and ankle. The relative muscle phasing and duty cycles are also significantly altered, demonstrating how mechanical interactions of the limbs and their sensory feedback alter neural function.

Contralateral force-sensitive presynaptic inhibition provides another layer of neuromechanical interaction. Not only does sensory feedback affect mechanics and mechanics impact motor output, but limb mechanics also dynamically regulate the efficacy and pathway of sensory feedback. Specifically, contralateral limb loading activates presynaptic inhibition that regulates ipsilateral sensory inflow. On the contralateral side, the loading experienced by receptors in the contralateral limb is influenced by mechanics and neural activity including limb posture, muscle and joint stiffness, motor commands, and receptor responsiveness. The presynaptic inhibition produced on the ipsilateral side could potentially influence these factors on the ipsilateral side because the sensory feedback received or blocked can influence muscle stiffness, motor output, and limb posture. Clearly, the web of neuromechanical interactions is highly complex with numerous sites for regulation and modulation. While seemingly

cumbersome, this complexity allows the nervous system great flexibility to produce a wide range of behaviors and employ a wide range of sensorimotor strategies. Using this complexity, the nervous system can sculpt motor output (Chapter 2) and sensory feedback (Chapter 3) to match the environment, the task, limb mechanics, or even step-to-step perturbations.

4.4 Role of limb loading in regulating motor output and sensory feedback

Both studies demonstrated an essential role of limb loading, particularly ground contact, in sensorimotor regulation. Even with no change in descending input or intentional task selection, removing ground contact limb loading and changing limb orientation had profound effects on joint coordination and muscle activation patterns. The changes in sensory feedback associated with ground contact and limb loading, such as muscle stretch and tension, were sufficient to significantly alter joint coordination, the phasing between flexors and extensors, and their relative duty cycles in the SCHP. Thus, the sensory signals that respond to limb loading seem vital for regulating task-specific spatiotemporal features of muscle activation. Our findings affirm previous work in the cat showing that ground contact loading, with the resulting ankle extensor loading and Ib activity, are vital for ankle extensor activation (Donelan and Pearson 2004). Additionally, in humans, inhibition of Ib reflexes (Faist et al. 2006) and muscle activation patterns and joint kinematics in reduced gravity (Ferris et al. 2001) all depend on phasic limb loading (for earlier review see (Dietz and Duysens 2000)).

Further, Chapter 3 showed that contralateral limb endpoint force at toe contact strongly influences the extent and timing of swing-phase presynaptic inhibition on the ipsilateral limb. Thus, limb loading plays a vital role in regulating sensory inflow,

particularly during swing. As discussed before, contralateral presynaptic inhibition may preserve flexion without unwanted perturbations, heighten attention on relevant inputs, and allow feedback from one limb to regulate feedback on the other. Interestingly, this load-related generation of contralateral presynaptic inhibition may explain some of the changes between dorsal-up and ventral-up SCHP behavior seen in Chapter 2. When ground contact and associated limb loading were absent in the ventral- up condition, contralaterally-generated swing-phase presynaptic inhibition was presumably reduced as seen in the plate removal experiments. In this condition, the hip and ankle exhibited prolonged extensor-phase plateaus before initiating swing onset that closely resembled the hip and ankle extensor pauses seen without DRPs in Figure 3.9, suggesting that the presynaptic inhibition may lead to extensor-phase plateaus as uninhibited sensory feedback interferes with swing production. These plateaus were not present in the dorsal-up condition in which ground contact and presumably stronger contralateral presynaptic inhibition were both present. Alternatively, the plateaus may simply result from extension activity without ground resistance, causing the limb to reach peak extension before central circuits initiate flexion activity. Although causality is not proven, presynaptic inhibition provides one possible mechanism for this behavior.

4.5 Implications for sensorimotor rehabilitation

After spinal cord injury and other neural insults, such as stroke and Parkinson's disease, the circuitry within the spinal cord responsible for producing the rhythmic patterns underlying locomotion often remains intact, but descending control from the brain is severed or impaired. After injury, sensory feedback is one of the few natural inputs available for accessing and controlling this residual spinal circuitry. Thus,

understanding how sensory feedback functions during locomotion and how it can be used to facilitate locomotion is vital for designing effective locomotor rehabilitation strategies. Studies in the SCHP reported in Chapter 2 show that, even without descending inputs, sensory feedback can help establish task-appropriate motor patterns. Stepping-like assistance can reinforce weak locomotion and even initiate locomotion in the presence of subthreshold neurochemical drive. As suggested by human (Domingo et al. 2007; Gottschall and Kram 2005; Harkema et al. 1997; Lam et al. 2008) and rat studies (de Leon et al. 2002), assisting and/or resisting swing and providing stance-phase limb loading may be important during locomotor training with spinal cord injury patients. In the future, the SCHP will greatly enhance and expand our ability to study sensory interactions with spinal circuits with increased acuity and manipulability. For example, the SCHP allows us to apply drugs in known concentrations to test the role of neuromodulators in behavior and even identify the location of their actions using split bath techniques. Intracellular interconnectivity studies can be used to dissect the locomotor and sensorimotor integration circuitry. The SCHP also offers a tractable platform for testing neural interfaces, spinal cord stimulators, and other therapeutic agents.

Additionally, sensory regulation is often dysfunctional after spinal cord injury and other neural injuries or diseases, such as stroke, peripheral nerve injury, or Parkinson's disease (Calancie et al. 1993; Enríquez et al. 1996; Garcia et al. 2006; Milanov 1992; Morita et al. 2000; Yang et al. 1991). Due to the loss or damage of descending systems, presynaptic inhibition is typically reduced and results in spasticity (Calancie et al. 1993; Faist et al. 1999; Morita et al. 2000; Stein 1995; Yang et al. 1991). Spasticity can

interfere with locomotor training by resisting robotic or manual limb movements. Additionally, the lack of presynaptic sensory modulation makes appropriate use of sensory feedback for locomotion and task learning difficult. Drugs, like the $GABA_B$ agonist baclofen, are often used to reduce spasticity and increase tonic inhibition (Taricco et al. 2006), but pharmacology cannot restore phasic, task-specific modulation. On the other hand, peripheral inputs can be readily manipulated to restore sensory regulation. The results from Chapter 3 suggest that contralateral limb loading is an important variable for establishing appropriate sensory regulation during locomotion. Much research has focused on how ipsilateral peripheral inputs and manipulations can restore regulation, particularly H-reflex regulation (Fung and Barbeau 1994; Knikou 2010), but the present results suggest that contralateral limb loading may be an even more powerful input. Contralateral manipulations may be particularly useful in hemiparesis seen in stroke and certain spinal cord injuries because the unimpaired limb could be used as a regulatory gateway to the paretic limb. Contralateral manipulations during body-weight supported treadmill training, such as phasic loading at the foot or electrical stimulation during contralateral stance and ipsilateral swing, may help restore ipsilateral presynaptic inhibition.

4.6 Future directions

By combining behavioral observability and intact sensory feedback with all the neural accessibility and manipulability of *in vitro* preparations, the SCHP opens the door for an array of studies on spinal sensorimotor circuitry. As shown in Appendix A, intracellular recordings of specific neuronal populations can be performed during locomotion to investigate the neuronal basis of rhythmogenesis during locomotion.

Because sensory feedback so strongly affects motor output, the components of this network may change depending on sensory conditions. Such questions could not be addressed without a preparation like the SCHP. Intracellular recordings on dorsal horn neurons, in combinations with monitors of presynaptic inhibition, can be used to study sensory integration and variations in sensory responses across the locomotor cycle. Neuro-modulators and transmitters can also be applied in the absence of the blood brain barrier to understand their role in patterning behavior, which can be quantified by electromyography and kinematic or kinetic analyses of limb movement. Overall, the SCHP truly expands our ability to investigate the spinal circuitry and neural mechanisms responsible for locomotion.

Future studies regarding presynaptic inhibition will focus on confirming the identity of the giving and receiving afferents involved in force-sensitive presynaptic inhibition. Intra-axonal recordings of afferents combined with contralateral toe loading manipulations will be used to test the hypothesis that toe Ib afferent induce force-scalable presynaptic inhibition of Ib afferents during non-fictive locomotion. The role of supraspinal systems in modulating presynaptic inhibition should also be considered. As with classic *in vitro* spinal cord preparations, the brain stem can be left intact and nuclei stimulated to map the modulator role of descending brain stem systems. Different descenging monoaminergic systems have been shown to modulate both reflex and PAD-generating pathways (Bras et al. 1989; Bras et al. 1990). The resulting differences in presynaptic inhibition, as well as locomotor pattern, could be explored in the SCHP.

The impact of contralateral force-sensitive presynaptic inhibition on motor output also deserves further investigation. While ventral root recordings and kinematics used

here provided some insight, more specific measures of swing-phase flexion activity, such as EMG recordings from flexor muscles or intracellular recordings from flexor motoneurons, will allow us to better identify the effects of presynaptic inhibition. In addition, the impact of contralateral presynaptic inhibition on specific sensory pathways should be investigated by simultaneously measuring reflex gains and monitoring presynaptic inhibition across a range of contralateral force conditions. Reflex gains could readily be monitored in the SCHP by stimulating the dorsal roots or peripheral nerves at various thresholds and measuring the effect in the ventral roots, muscles, or even intracellularly in motoneurons. Changes in reflex pathways could then be related to changes in presynaptic inhibition, including the changes that naturally occur from step-to-step as well as changes induced by experimentally altering limb loading or toe contact.

In conclusion, both the current and future work carried out in the SCHP enhance our understanding of spinal control of movement, particularly the role of sensory regulation in creating robust and task-appropriate locomotor activity. I hope that the knowledge gained advances our ability to more effectively treat neural injuries and diseases that impair spinal sensorimotor function.

APPENDIX A

INTRACELLULAR RECORDINGS FROM DORSAL HORN INTERNEURONS DURING UNRESTRAINED HINDLIMB LOCOMOTION

A.1 Introduction

Intracellular recordings from spinal cord neurons during locomotion are important for understanding the organization of the spinal circuitry responsible for locomotion. Unlike extracellular recordings, intracellular recordings allow us to quantify subthreshold inhibitory and excitatory inputs, such as locomotor drive potentials (Jordan 1983; Kiehn 2006), and carefully detail the input-output properties of each neuron. As such, intracellular recordings are vital for identifying the essential neuronal elements for locomotor rhythmogenesis, sensory integration, and coordination.

As discussed in Chapter 2, intracellular recordings during non-fictive mammalian locomotion have not been technically possible due to the movement of the spinal cord associated limb movement. Many have performed intracellular recordings in the isolated spinal cord without limbs attached or with neuromuscular blockage or deafferentation (e.g. (Kiehn et al. 2000; Tresch and Kiehn 1999), for review see (Kiehn and Butt 2003)). Although these studies provide insight into the neuronal contributions to rhythmogensis, without movement-related sensory feedback, numerous inputs to these neurons are inactive. Because sensory inputs have profound effects on motor output, they undoubtedly influence the functioning including those comprising spinal locomotor circuitry. To best understand the functional relevance of spinal interneuron synaptic and cellular properties during locomotion, intracellular recordings should be performed

during sensory modulated, behaviorally relevant locomotion.

Wheatley and Stein made progress towards this goal by developing the mudpuppy spinal cord-forelimb preparation (Wheatley and Stein 1992). The preparation consisted of the cervical spinal cord, brachial plexus, and right forelimb maintained *in vitro* and combined simultaneous sharp intracellular and electromyographic muscle activity recordings. Using this preparation, Stein and colleagues identified groups of interneurons that received locomotor drive potentials and whose activity correlated with flexor or extensor muscle group activity, providing insight into which neurons may be involved in rhythmogenesis or relay rhythmic input to motoneurons (Cheng et al. 2002; Wheatley et al. 1994b; Wheatley and Stein 1992). However, no such model exists for mammals or for hindlimb locomotion. Further, the mudpuppy preparation has been abandoned because intracellular recordings were simply too difficult due to the thick extracellular consistency and heavy myelination (R.B. Stein personal communication, 2008). Finally, impalement by traditional sharp electrodes, as used in the mudpuppy, have been shown to induce current leaks that alter the passive properties of the membrane, while whole-cell patch recordings more accurately report the neuronal properties, such as resting potential and input resistances (Staley et al. 1992). As demonstrated here, the dorsal-up SCHP developed in Chapter 2 provides a mammalian, hindlimb *in vitro* preparation for whole-cell patch clamp intracellular recordings during unrestrained hindlimb locomotion.

Using the dorsal-up SCHP developed in Chapter 2, I performed the first whole-cell patch recordings from mammalian dorsal horn interneurons during unrestrained locomotion in the SCHP, confirming the suitability of the SCHP for stable intracellular recordings from small neurons. The primary purpose of these recordings was to show that

interneurons can be characterized by their membrane and input properties and held stable for extended periods of neurochemically-induced locomotion. Here, I identified dorsal horn interneurons that are nearly quiescent at rest, but receive increased sub- or supra-threshold synaptic inputs during locomotion. One dorsal horn interneuron exhibited rhythmic drive potentials and fired repetitively during locomotion at a rate proportional to locomotor strength. Portions of these results have been presented previously in abstract form (Hayes et al. 2009b; Hayes and Hochman 2009).

A.2 Methods

The neonatal rat SCHP used here is described in Chapter 2 (Hayes et al. 2009a). Briefly, the spinal cord and hindlimbs were isolated from neonatal rats postnatal day 2-5. Ventral and dorsal roots from ~T12-S2 were left intact, but all other roots were cut and paraspinal musculature removed. Following dissection, the SCHP was transferred to a perfusion and recording chamber. The cord was placed dorsal up on a Sylgard step and thoroughly stabilized with insect pins through the remaining ribs and paraspinal musculature, as well as the cut roots rostral to the segments of interest. The cord and limbs were perfused with oxygenated artificial cerebrospinal fluid (aCSF) circulated at 20-30 mL/min. Hindlimbs hung pendant and were free to locomote on a low fricition teflon surface. Addition of 2-4 µM N-methyl D-aspartate (NMDA) and 40-60µM serotonin (5HT) to the aCSF perfusion system then activated hindlimb locomotion.

Whole-cell "blind" patch clamp recordings (e.g.(Hochman and Schmidt 1998; Machacek and Hochman 2006)) from dorsal horn interneurons were performed during unrestrained hindlimb locomotion. Two ventral horn interneurons were also recorded. Neuron location was estimated based on site of entry and depth of penetration. Patch

electrodes were pulled from glass capillary tubes (1.5mm OD, WPI) in a two-stage puller (Narishige PP83) and filled with cesium fluoride. Recordings targeted segments from caudal thoracic (T11) through the lumbar enlargement (L6) which are known to receive hindlimb afferent input and related to spinal locomotor output. Recordings were collected through an Axopatch 1D amplifier (Axon Instruments), sampled at 5kHz (Digidata 1322A, 16-bit DAQ; Axon Instruments), and recorded for off-line analysis (Clampex; Axon Instruments). Upon impalement, the resting membrane potential was determined in current clamp without junction potential compensation. In current clamp, depolarizing and hyperpolarizing current was injected to characterize the voltage response of the cell including its firing properties. In voltage clamp, current response to a series of voltage steps was monitored. Steady state and peak current flow were computed for each step change in holding voltage to characterize the IV (current-voltage) relationship of the cell. During locomotion, interneuron activity was recording using current clamp to view spiking and membrane potential oscillations. Simultaneous recordings were made from lumbar dorsal and ventral roots to monitor afferent input and motor output as described in Chapter 3. For most cells, dorsal roots were also stimulated to characterize the low (50µA/50µsec) and high threshold (500µA/500µsec) afferent inputs to the cells. Responses to toe and/or tail pinches were also performed to test the cells response to natural noxious stimuli that activate high threshold inputs.

Additional off-line analyses were performed using custom programs in Matlab. Step cycles were defined from ventral root L2/L3 burst onset to burst onset. For both the ventral and dorsal roots, bursts onset and offset was detected using a threshold detector (Gozal 2010). Interneuronal activity was quantified by spike density (number of spikes

per 5% bin, 20 bins per step cycle) and spike frequency (1/interspike interval, Hz).

A.3 Results and Discussion

Stable intracellular recordings were made from a total of nine cells (n = 9) in four SCHPs. Seven neurons were located in the dorsal horn and two slightly ventral to the central canal. All neurons were quiescent at rest with some spontaneous synaptic inputs. During locomotion, two neurons, both in the dorsal horn, showed no observable change in activity, but all other neurons showed an increase in synaptic input or began spiking in response to locomotion (n = 7). Four neurons did not initiate spiking during locomotion, but exhibited an increase in synaptic activity, either predominantly excitatory (n = 3) or inhibitory (n = 1). Three neurons began spiking with hindlimb movement (n = 2 dorsal horn, n = 1 ventral horn).

Electrical stimulation to assess synaptic inputs was not performed on all neurons, particularly those recorded early in these studies. When inputs were identified via electrical stimulation, neurons that spiked during locomotion received excitatory input from low threshold afferents and were synaptically inhibited by high threshold stimuli (n = 2/3, 3rd not tested). In comparison, neurons not recruited during locomotion tended to be excited by high threshold input (n = 3/4, 4th not tested). High threshold afferent input is likely associated with noxious stimuli and, thus, is less likely during locomotion. Rather, these neurons may be associated with nocioceptive signaling pathways.

Two of the three neurons recruited into spiking during locomotion were not rhythmically modulated in relation to dorsal or ventral activity. However, one dorsal horn interneuron located in the T12 segment exhibited rhythmic spiking that increased with ipsilateral L3 dorsal root activity and reached maximum during ipsilateral flexion,

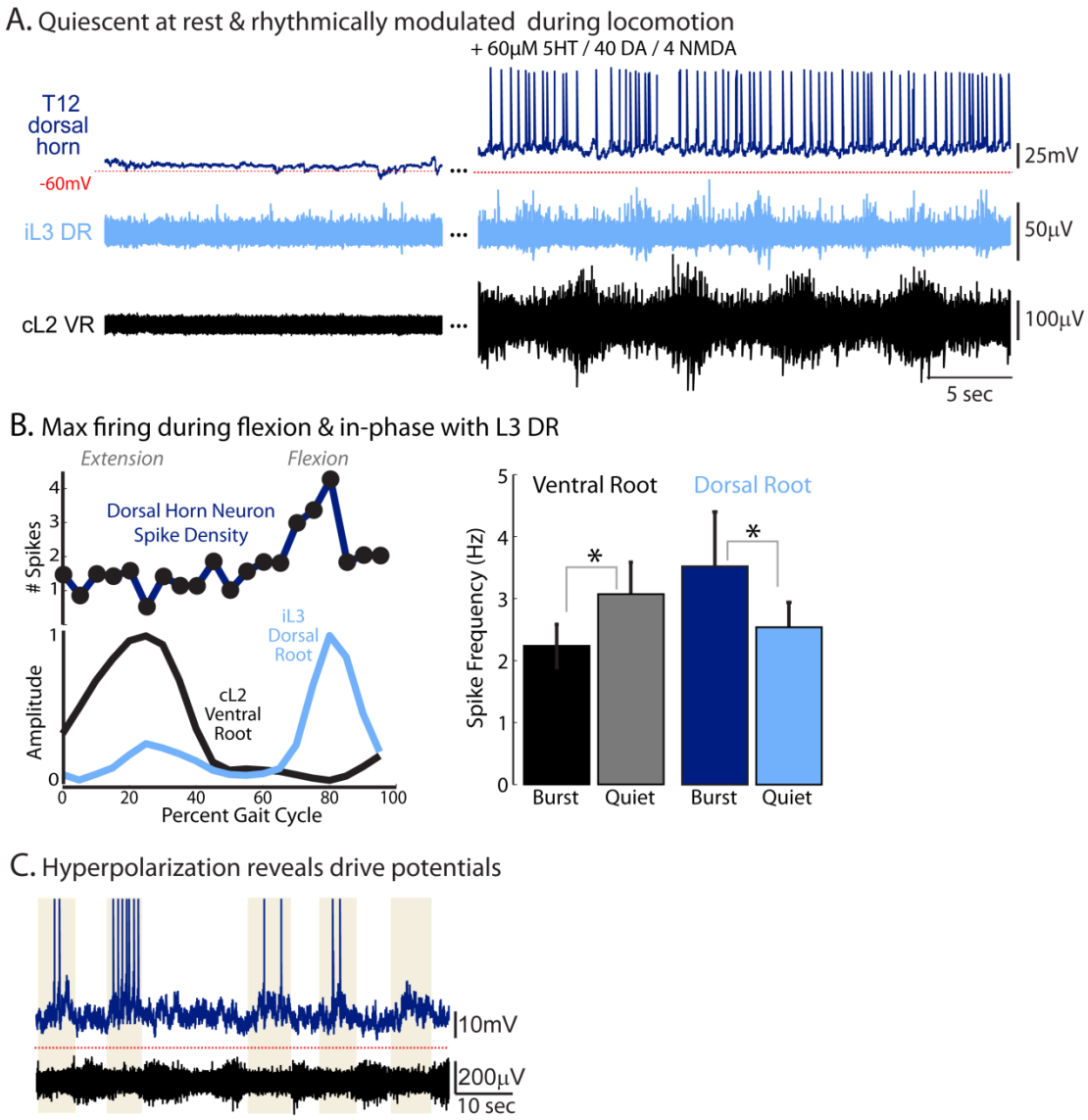

Figure A.1: Activity of rhythmically active dorsal horn interneuron during hindlimb locomotion

A: Whole-cell patch clamp recordings from the T13 dorsal horn interneuron (dark blue) are shown relative to extracellular recordings of ipsilateral L3 dorsal root (iL3 DR, light blue) and contralateral L2 ventral root activity (cL2 VR, black). Resting membrane potential was -60mV. The interneuron was quiescent as rest, but showed rhythmic spiking during neurochemically-induced locomotion. B: (Right) Locomotor cycles were time normalized. Spike density (# spikes/bin) and rectified integrated ventral root and dorsal root activity were computed for each 5% bin and averaged across 47 cycles. Spike density was highest during the flexion phase, out-of-phase with cL2 VR (contralateral flexion) and in-phase with iL3 DR. (Left) Rhythmic modulation was confirmed by showing that the mean spike frequency was significantly lower during the cL2 VR burst than during quiescence and significantly higher during the iL3 DR burst than during quiescence. C: Slight hyperpolarizing the membrane potential reduced spiking to reveal rhythmic membrane oscillations similar to previously described drive potentials. Highlighted regions emphasize these oscillations.

as shown in Figure A.1a and b. All subsequent results and figures describe this interneuron.

During locomotion, spike frequency for this interneuron was significantly higher during L3 dorsal root bursting and significantly lower during contralateral L2 ventral root activity (i.e. out-of-phase with contralateral flexion, in-phase with ipsilateral flexion) ($p<0.05$, Fig. A.1b). Slightly hyperpolarizing the membrane with current injection revealed rhythmic depolarizing drive potentials (Fig. A.1C) similar to those previously observed in motoneurons and interneurons (Hochman and Schmidt 1998; Kiehn et al. 1996). All subsequent results and figures describe the activity in this interneuron. These rhythmic potentials have been implicated in the shaping and generation of rhythmic motor output (Hochman and Schmidt 1998; Kiehn 2006; Kiehn et al. 1996; Kiehn et al. 2000). In the dorsal horn, rhythmic drive potentials likely reflect excitatory and inhibitory afferent inputs from cyclic limb movements and may well contribute to locomotor drive.

This interneuron received strong, excitatory low-threshold afferent input, but was inhibited by high threshold inputs (Fig A.2a and b). Toe pinch during locomotion evoked inhibition followed by rebound firing (Fig A.2c), consistent with inhibition from high threshold stimulation. As stated above, activity in low-threshold afferents likely evoked the observed spiking. The rhythmic modulation and phasing of the spiking (Fig. A.1) suggests that the low-threshold inputs are preferentially activated during flexion.

Interestingly, the response to dorsal column stimulation was state-dependent (Fig A.2D). At rest, dorsal column stimulation excited the interneuron; once locomotion was activated by NMDA, serotonin, and dopamine, dorsal column stimulation at the same strength inhibited the neuron. Dorsal column stimulation may antidromically activate

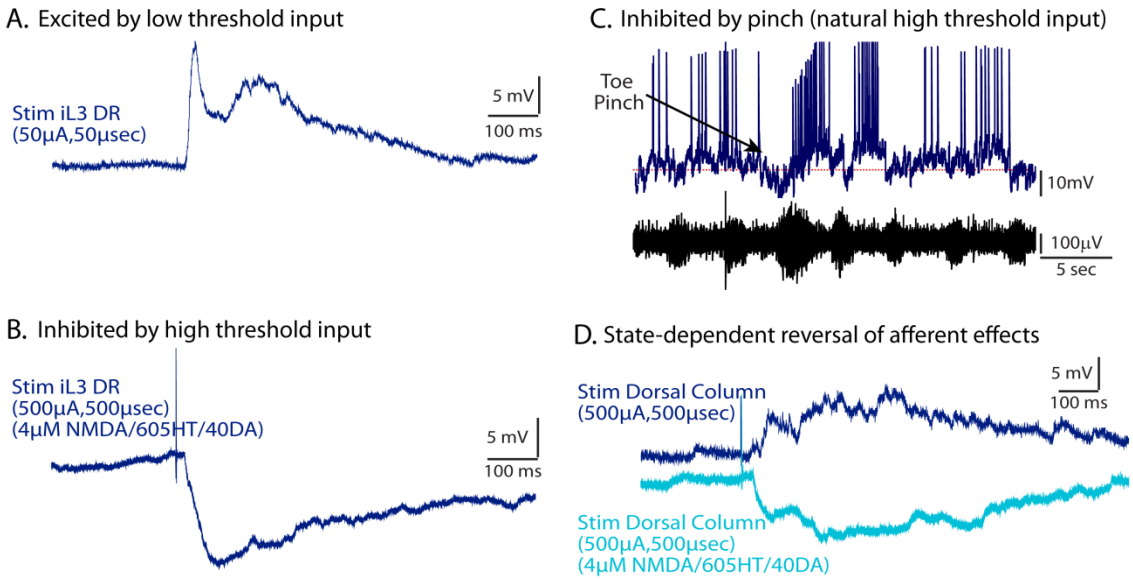

Figure A.2: Low and high threshold afferent input characterization

A: Stimulation of the ipsilateral L3 dorsal root (iL3 DR) at 50µA for 50µsec evoked an EPSP, showing that the interneuron received excitatory input from low threshold afferents. B: Stimulation of the same root at 500µA for 500µsec evoked an IPSP, showing that the interneuron received inhibitory input from high threshold afferents strong enough to overwhelm the excitatory from low threshold afferents. C: Interneuron activity (dark blue) is shown relative to the contralateral L2 ventral root (black). During locomotion induced by 4µM NMDA, 60µM 5HT, and 40µM DA, toe pinch produced inhibition followed by rebound excitation, confirming that high threshold afferents produce inhibition when activated naturally as well as electrically. D: Response to stimulation of the dorsal column rostral to the interneuron was state-dependent. Dorsal column stimulation produced an EPSP at rest, but an IPSP during neurochemically-induced locomotion. An antidromic spike was not elicited in either case. Thus, the neuron is not directly activated, but rather acted on synaptically by neurons travelling in the dorsal column, such as afferents or postsynaptic dorsal column neurons. The synaptic effect is reversed by locomotion and/or the applied neurochemicals

primary afferents or postsynaptic dorsal column afferents (Angaut-Petit 1975a; b; Giesler et al. 1984), with intraspinal collaterals branches capable of directly or indirectly producing synaptic actions on this interneuron. For example, the state-dependent reversal may reflect presynaptic inhibition at excitatory synapses and disinhibition or reduced threshold for neurons with inhibitory input onto the interneuron of interest. In either case, the state-dependency of inputs highlights the need for studying neuronal activity during locomotion as the interconnections and properties can change depending on the state and task. The SCHP allows for task-relevant study of interneurons during non-fictive hindlimb locomotion.

A.4 Conclusions

Although these findings are preliminary, whole-cell patch intracellular recordings during locomotion are an important step in the study of spinal locomotor circuitry and sensory processing. These findings confirm that stable intracellular recordings can be carried in the SCHP at rest and maintained through unrestrained hindlimb locomotion. The cell remained healthy for extensive characterization, including afferent stimulation, mechanical perturbations, and descending tract stimulation. Even perturbations that evoked aggressive limb movement, such high threshold dorsal root stimulation or pinch, did not disturb spinal cord and patch electrode stability. Further, dorsal and ventral horn recordings through the caudal thoracic and lumber region were successful. In the future, the SCHP will continue to advance the understanding of spinal locomotor circuitry through intracellular investigations of identified interneuronal populations.

APPENDIX B

FORCE PLATFORM CALIBRATION

B.1 Calibration method

This Appendix briefly illustrates the calibration of the 2D single limb force platforms used in Chapter 3. Each platform was calibrated separately by applying *n* known weights in configuration 1 and then in configuration 2 (Fig B.1). The masses ranged from 0 to 5 grams were used, applying loads of 0 to 49mN. The weights were then applied in reverse order to ensure no changes in transduction over time. For each weight, voltage from sensor 1 and sensor 2 were recorded in Clampex (Digidata 1322A 16-Bit DAQ, Axon Instruments). As described in Chapter 3, the influence matrix [I] was then calculated according to:

$$[V_{2xn}] = [I_{2x2}] \,.\, [L_{2xn}] \text{ such that } [I_{2x2}] = [V_{2xn}].\, [L_{2xn}]^{-1} \quad \text{(Eqn. 1)}$$

where [V] is the voltage data in response to the known applied loads in μV, [L] is the known loads in mN, [I] is the influence matrix describing the relationship, and n is the number of known weights. After calibration, vertical and fore-aft forces from locomotor trials could then be computed according to:

$$[F_{2xn}] = [I_{2x2}]^{-1}.\, [V_{2xn}] \text{ where } [I_{2x2}]^{-1} = \{[V_{2xn}].\, [F_{2xn}]^{-1}\}^{-1} \quad \text{(Eqn. 2)}$$

where [F] is the force matrix that includes both vertical and fore-aft forces computed from the conversion matrix $[I]^{-1}$ (Chang et al. 1997).

To test transducer linearity, the measured voltage for each weight application was plotted against the known load. Accuracy of the calibration was then tested by comparing the computed load calculated by Equation 2 against the known applied load.

B.2 Calibration results

All transducer showed strong linearity between measured voltage and applied load. Table B.1 shows the R^2 value for each condition. Figure B.1 shows the relationship data with line fit for platforms 1 and 2 in configuration 1.

As shown in Figure B.2, the computed force was nearly equal to the applied force for each calibration with a slope of near 1, confirming the accuracy of our calibration. The ratio was The R^2 exceeded 0.99, showing consistency across forces.

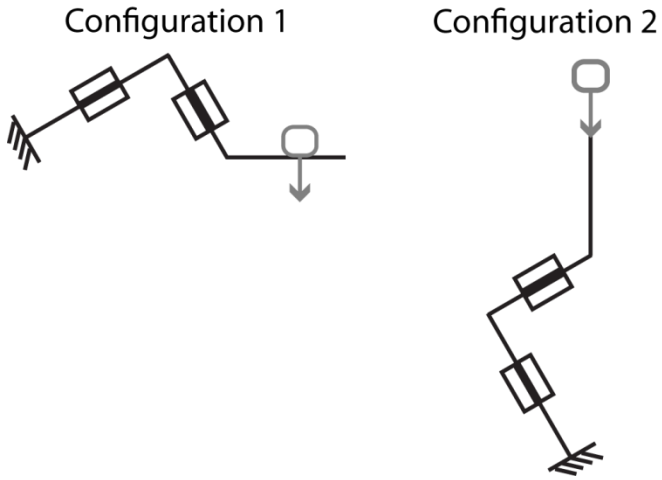

Figure B.1: Calibration orientations
Known weights were applied as shown in configuration 1 and configuration 2 for each force platform.

Table B.1: R2 values for force transducer calibrations

	Sensor 1 Configuration 1	Sensor 2 Configuration 1	Sensor 1 Configuration 2	Sensor 2 Configuration 2
Platform 1	0.9955	0.9795	0.9814	0.9795
Platform 2	0.9974	0.9855	0.9913	0.9839

R^2 values for voltage deflection versus applied force are shown for sensor 1 and sensor 2 of each force platform and for each calibration configuration.

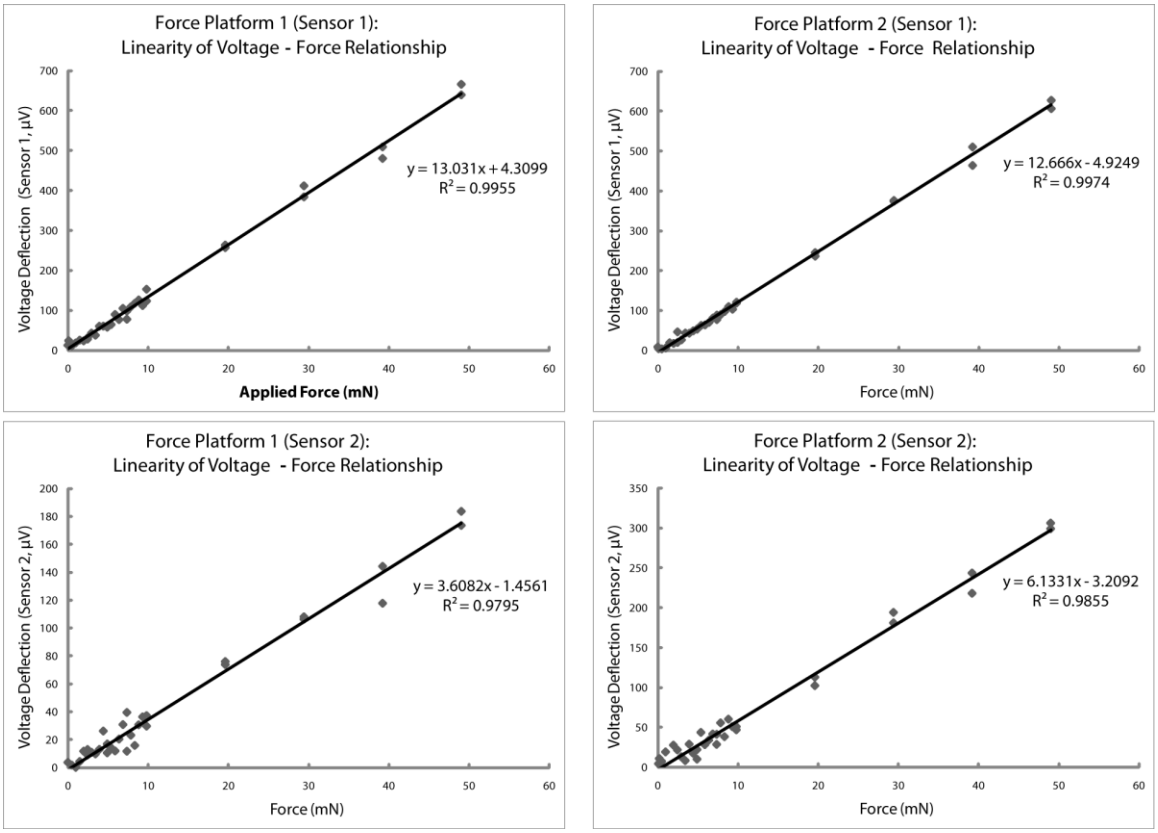

Figure B.2: Linearity of transducers

The graphs on the left show the relationship between the recorded voltage deflection (µV) and the applied force (mN) for sensor 1 (top) and sensor (bottom) of platform 1. The graphs on the right show the same relationships for platform 2.

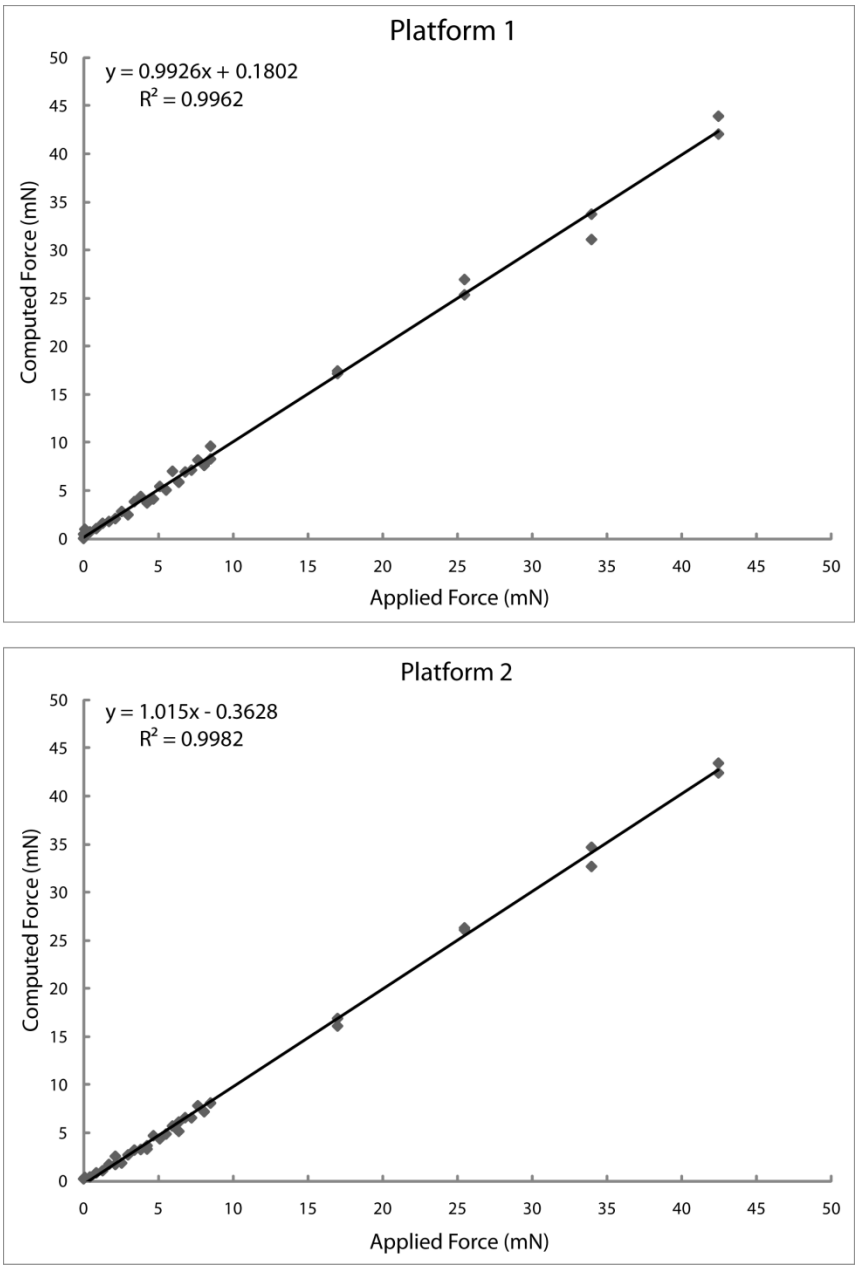

Figure B.3: Computed force versus applied force

Computed force is plotted against applied force for platform 1 (top) and platform 2 (bottom) to show the accuracy of the calibration. For both platforms, the computed force was nearly equal to the applied force such with a slope near 1 and high R^2 values.

REFERENCES

Alibiglou L, Lopez-Ortiz C, Walter CB, and Brown DA. Bilateral limb phase relationship and its potential to alter muscle activity phasing during locomotion. *J Neurophysiol* 102: 2856-2865, 2009.

Anderson JB, and Sinkjaer T. The stretch reflex and H-reflex of the human soleus muscle during walking. *Motor Control* 3: 151-157, 1999.

Andersson O, and Grillner S. Peripheral control of the cat's step cycle: II. Entrainment of the central pattern generators for locomotion by sinusoidal hip movements during fictive locomotion. *Acta Physiologica Scandinavica* 118: 229-239, 1983.

Angaut-Petit D. The dorsal column system: I. Existence of long ascending postsynaptic fibres in the cat's fasciculus gracilis. *Experimental Brain Research* 22: 457-470, 1975a.

Angaut-Petit D. The dorsal column system: II. Functional properties and bulbar relay of the postsynaptic fibres of the cat's fasciculus gracilis. *Experimental Brain Research* 22: 471-493, 1975b.

Atsuta Y, Garcia-Rill E, and Skinner RD. Characteristics of electrically induced locomotion in rat in vitro brain stem-spinal cord preparation. *J Neurophysiol* 64: 727-735, 1990.

Atsuta Y, Garcia-Rill E, and Skinner RD. Electrically induced locomotion in the in vitro brainstem-spinal cord preparation. *Dev Brain Res* 42: 309-312, 1988.

Bagust J, and Kerkut GA. An in vitro preparation of the spinal cord of the mouse. In: *Electrophysiology of isolated mammalian CNS preparations*, edited by Kerkut GA, and Wheal HV. New York: Academic Press, 1981, p. 337-365.

Baldissera F, Hultborn H, and Illert M. Integration in spinal neuronal systems. In: *Handbook of Physiology The Nervous System Motor Control* edited by Brookes VB. Bethesda, MD: America Physiological Society, 1981, p. 509-595.

Bannatyne BA, Edgley SA, Hammar I, Jankowska E, and Maxwell DJ. Differential Projections of Excitatory and Inhibitory Dorsal Horn Interneurons Relaying Information from Group II Muscle Afferents in the Cat Spinal Cord. *J Neurosci* 26: 2871-2880, 2006.

Bannatyne BA, Liu TT, Hammar I, Stecina K, Jankowska E, and Maxwell DJ. Excitatory and inhibitory intermediate zone interneurons in pathways from feline group I and II afferents: differences in axonal projections and input. *J Physiol* 587: 379-399, 2009.

Bardoni R, Torsney C, Tong C-K, Prandini M, and MacDermott AB. Presynaptic NMDA Receptors Modulate Glutamate Release from Primary Sensory Neurons in Rat Spinal Cord Dorsal Horn. *J Neurosci* 24: 2774-2781, 2004.

Berens P. CircStat: A Matlab toolbox for circular statistics. *Journal of Statistical Software* 31: 1-21, 2009.

Biewener AA, and Full R. Force platform and kinematic analysis. In: *Biomechanics - Structures and Systems*, edited by Biewener AA. New York: Oxford University Press, 1992, p. 45-75.

Birznieks I, Jenmalm P, Goodwin AW, and Johansson RS. Encoding of Direction of Fingertip Forces by Human Tactile Afferents. *J Neurosci* 21: 8222-8237, 2001.

Bonasera SJ, and Nichols TR. Mechanical actions of heterogenic reflexes linking long toe flexors with ankle and knee extensors of the cat hindlimb. *J Neurophysiol* 71: 1096-1110, 1994.

Bouyer LJG, and Rossignol S. Contribution of cutaneous inputs from the hindpaw to the control of locomotion. I. Intact cats. *Journal of Neurophysiology* 90: 3625-3639, 2003a.

Bouyer LJG, and Rossignol S. Contribution of cutaneous inputs from the hindpaw to the control of locomotion. II. Spinal cats. *Journal of Neurophysiology* 90: 3640-3653, 2003b.

Brant HE, and Chang Y-H. Global limb control and local interjoint locomotor compensation strategies after peripheral nerve injury in the rat. Program No. Neuroscience 2006 Atlanta, Georgia: Society for Neuroscience, 2006. Online.

Brant HE, Hochman S, and Chang Y-H. A comparison of motor outcomes between in vitro and in vivo rat locomotion. Program No. Neuroscience 2006 Atlanta, Georgia: Society for Neuroscience, 2006. Online.

Bras H, Cavallari P, Jankowska E, and McCrea D. Comparison of effects of monoamines on transmission in spinal pathways from group I and II muscle afferents in the cat. *Experimental Brain Research* 76: 27-37, 1989.

Bras H, Jankowska E, Noga B, and Skoog B. Comparison of Effects of Various Types of NA and 5-HT Agonists on Transmission from Group II Muscle Afferents in the Cat. *European Journal of Neuroscience* 2: 1029-1039, 1990.

Brizzi L, Ting LH, and Zytnicki D. Positive Proprioceptive Feedback Elicited By Isometric Contractions of Ankle Flexors on Pretibial Motoneurons in Cats. *J Neurophysiol* 88: 2207-2214, 2002.

Brooke JD, Cheng J, Collins DF, McIlroy WE, Misiaszek JE, and Staines WR. SENSORI-SENSORY AFFERENT CONDITIONING WITH LEG MOVEMENT: GAIN CONTROL IN SPINAL REFLEX AND ASCENDING PATHS. *Progress in Neurobiology* 51: 393-421, 1997.

Brooke JD, Cheng J, Misiaszek JE, and Lafferty KB. Amplitude modulation of the soleus H-reflex in the human during active and passive stepping movements. *J Neurophysiol* 73: 102-111, 1995a.

Brooke JD, McIlroy WE, Collins DF, and Misiaszek JE. Mechanisms within the human spinal cord suppress fast reflexes to control the movement of the legs. *Brain Research* 679: 255-260, 1995b.

Burke RE. The use of state-dependent modulation of spinal reflexes as a tool to investigate the organization of spinal interneurons. *Experimental Brain Research* 128: 263-277, 1999.

Calancie B, Broton JG, John Klose K, Traad M, Difini J, and Ram Ayyar D. Evidence that alterations in presynaptic inhibition contribute to segmental hypo- and hyperexcitability after spinal cord injury in man. *Electroencephalography and Clinical Neurophysiology/Evoked Potentials Section* 89: 177-186, 1993.

Capaday C, and Stein RB. Difference in the amplitude of the human soleus H reflex during walking and running. *The Journal of Physiology* 392: 513-522, 1987.

Capaday C, and Stein RB. The effects of postsynaptic inhibition on the monosynaptic reflex of the cat at different levels of motoneuron pool activity. *Experimental Brain Research* 77: 577-584, 1989.

Cattaert D. Studying the nervous system under physiological conditions. Focus on "Contribution of force feedback to ankle extensor activity in decerebrate walking cats". *J Neurophysiol* 92: 1967-1968, 2004.

Chang Y-H, Bertram JEA, and Ruina A. A dynamic force and moment analysis system for brachiation. *Journal of Experimental Biology* 200: 3013-3302, 1997.

Cheng J, Jovanovic K, Aoyagi Y, Bennett DJ, Han Y, and Stein RB. Differential distribution of interneurons in the neural networks that control walking in the mudpuppy (Necturus maculatus) spinal cord. *Experimental Brain Research* 145: 190-198, 2002.

Collins DF, McIlroy WE, and Brooke JD. Contralateral inhibition of soleus H-reflexes with different velocities of passive movement of the opposite leg. *Brain Research* 603: 96-101, 1993.

Conway BA, Hultborn H, and Kiehn O. Proprioceptive input resets central locomotor rhythm in the spinal cat. *Experimental Brain Research* 68: 643-656, 1987.

Cote M-P, and Gossard J-P. Task-Dependent Presynaptic Inhibition. *J Neurosci* 23: 1886-1893, 2003.

Cunningham CB, Schilling N, Anders C, and Carrier DR. The influence of foot posture on the cost of transport in humans. *J Exp Biol* 213: 790-797, 2010.

de Leon RD, Kubasak MD, Phelps PE, Timoszyk WK, Reinkensmeyer DJ, Roy RR, and Edgerton VR. Using robotics to teach the spinal cord to walk. *Brain Research Reviews* 40: 267-273, 2002.

Devanandan MS, Holmqvist B, and Yokota T. Presynaptic depolarization of group I muscle afferents by contralateral afferent volleys. *Acta Physiologica Scandinavica* 63: 46-54, 1965.

Dietz V, and Duysens J. Significance of load receptor input during locomotion: a review. *Gait & Posture* 11: 102-110, 2000.

Domingo A, Sawicki GS, and Ferris DP. Kinematics and muscle activity of individuals with incomplete spinal cord injury during treadmill stepping with and without manual assistance. *J Neuroeng Rehabil* 4: 32, 2007.

Donelan JM, and Pearson KG. Contribution of force feedback to ankle extensor activity in decerebrate walking cats. *J Neurophysiol* 92: 2093-2104, 2004.

Dubuc R, Cabelguen JM, and Rossignol S. Rhythmic fluctuations of dorsal root potentials and antidromic discharges of primary afferents during fictive locomotion in the cat. *J Neurophysiol* 60: 2014-2036, 1988.

Duenas SH, and Rudomin P. Excitability changes of ankle extensor group Ia and Ib fibers during fictive locomotion in the cat. *Exp Brain Res* 70: 15-25, 1988.

Duysens J, and Pearson KG. Inhibition of flexor burst generation by loading ankle extensor muscles in walking cats. *Brain Research* 187: 321-332, 1980a.

Duysens J, and Pearson KG. Inhibition of flexor burst generation by loading of ankle extensor muscles in walking cats. *Brain Research* 187: 321-332, 1980b.

Eccles JC. Presynaptic Inhibition in the Spinal Cord. *Prog Brain Res* 12: 65-91, 1964.

Eccles JC. Synaptic potentials of motoneurons. *J Neurophysiol* 7: 87-120, 1946.

Eccles JC, Eccles RM, Iggo A, and Lundberg A. Electrophysiological investigations on Renshaw cells. *J Physiol (Lond)* 159: 461-478, 1961a.

Eccles JC, Eccles RM, and Lundberg A. The convergence of monosynaptic excitatory afferents onto many different species of alpha motoneurons. *J Physiol* 137: 22-50, 1957.

Eccles JC, Eccles RM, and Magni F. Central inhibitory action attributable to presynaptic depolarization produced by muscle afferent volleys. *J Physiol* 159: 147-166, 1961b.

Eccles JC, Kostyuk PG, and Schmidt RF. Central pathways responsible for depolarization of primary afferent fibres. *J Physiol* 161: 237-257, 1962a.

Eccles JC, Kostyuk PG, and Schmidt RF. Presynaptic inhibition of the central actions of flexor reflex afferents. *J Physiol* 161: 258-281, 1962b.

Eccles JC, and Lundberg A. Integrative pattern of Ia synaptic actions on motoneurons of hip and knee muscles. *J Physiol* 144: 271-298, 1958.

Eccles JC, Schmidt RF, and Willis WD. Depolarization of the central terminals of cutaneous afferent terminals. *J Neurophysiol* 26: 646-661, 1963.

Eccles JC, Schmidt RF, and Willis WD. Presynaptic inhibition of the spinal monosynaptic reflex pathway. *J Physiol* 161: 282-297, 1962c.

Eccles RM, Holmqvist B, and Voorhoeve PE. Presynaptic Depolarization of Cutaneous Afferents by Volleys in Contralateral Muscle Afferents. *Acta Physiologica Scandinavica* 62: 474-484, 1964.

Edamura M, Yang J, and Stein R. Factors that determine the magnitude and time course of human H- reflexes in locomotion. *J Neurosci* 11: 420-427, 1991.

Eguibar JR, Quevedo J, Jimenez I, and Rudomin P. Selective cortical control of information flow through different intraspinal collaterals of the same muscle afferent fiber *Brain Research* 643: 328-333, 1994.

Eguibar JR, Quevedo J, and Rudomin P. Selective cortical and segmental control of primary afferent depolarization of single muscle afferents in the cat spinal cord. *Experimental Brain Research* 113: 411-430, 1997a.

Eguibar JR, Quevedo J, and Rudomin P. Selective cortical and segmental control of primary afferent depolarization of single muscle afferents in the cat spinal cord. *Experimental Brain Research* 113: 411-430, 1997b.

Engberg I, and Lundberg A. An electromyographic analysis of stepping in the cat. *Experientia (Basel)* 18: 174-176, 1962.

Enríquez M, Jiménez I, and Rudomin P. Segmental and supraspinal control of synaptic effectiveness of functionally identified muscle afferents in the cat. *Experimental Brain Research* 107: 391-404, 1996.

Faist M, Ertel M, Berger W, and Dietz V. Impaired modulation of quadriceps tendon jerk reflexes during spastic gait: differences between spinal and cerebral lesions. *Brain* 122: 567-579, 1999.

Faist M, Hoefer C, Hodapp M, Dietz V, Berger W, and Duysens J. In humans Ib facilitation depends on locomotion while suppression of Ib inhibition requires loading. *Brain Research* 1076: 87-92, 2006.

Ferris DP, Aagaard P, Simonsen EB, Farley CT, and Dyhre-Poulsen P. Soleus H-reflex gain in humans walking and running under simulated reduced gravity. *The Journal of Physiology* 530: 167-180, 2001.

Forssberg H. Stumbling corrective reaction: a phase-dependent compensatory reaction during locomotion. *J Neurophysiol* 42: 936-953, 1979.

Forssberg H, and Grillner S. The locomotion of the acute spinal cat injected with clonidine i.v. *Brain Res* 50: 184-186, 1973.

Fournier E, Karz R, and Pierrot-Deseilligny E. Descending control of reflex pathways in the production of voluntary isolated movements in man. *Brain Research* 288: 375-377, 1983.

Frank K, and Fourtes MGF. Presynaptic and postsynaptic inhibition of monosynaptic reflexes. *Fed Proc* 16: 39-40, 1957.

Fung J, and Barbeau H. Effects of conditioning cutaneomuscular stimulation on the soleus H-reflex in normal and spastic paretic subjects during walking and standing. *J Neurophysiol* 72: 2090-2104, 1994.

Garcia C, Chavez D, Jimenez I, and Rudomin P. Changes in primary afferent depolarization during the unmasking of sural responses following acute section of cutaneous nerves in the anesthetized cat. Program No. 146.10. Neuroscience 2006 Atlanta, GA: Society for Neuroscience, 2006. Online.

Garraway SM, and Hochman S. Serontonin increases the incidence of primary afferent-evoked long-term depression in rat deep dorsal horn neurons. *J Neurophysiol* 85: 1864-1872, 2001.

Giesler GJ, Nahin RL, and Madsen AM. Postsynaptic dorsal column pathway of the rat. I. Anatomical studies. *Journal of Neurophysiology* 51: 260-275, 1984.

Gillis GB, and Biewener AA. Hindlimb muscle function in relation to speed and gait: *In vivo* patterns of strain and activation in a hip and knee extensor of the rat (Rattus Norvegicus) *J Exp Biol* 204: 2717-2731, 2001.

Gorassini MA, Prochazka A, Hiebert GW, and Gauthier MJ. Corrective responses to losss of ground support during walking I. Intact cats. *J Neurophysiol* 71: 603-610, 1994.

Gossard JP. Control of transmission in muscle group Ia afferents during fictive locomotion. *J Neurophysiol* 76: 4104-4112, 1996.

Gossard JP, Cabelguen JM, and Rossignol S. Intra-axonal recordings of cutaneous primary afferents during fictive locomotion in the cat. *J Neurophysiol* 62: 1177-1188, 1989.

Gossard JP, Cabelguen JM, and Rossignol S. An intracellular study of muscle primary afferents during fictive locomotion in the cat. *J Neurophysiol* 65: 914-926, 1991.

Gossard JP, and Rossignol S. Phase-dependent modulation of dorsal root potentials evoked by peripheral nerve stimulation during fictive locomotion in the cat. *Brain Research* 537: 1-13, 1990.

Gottschall JS, and Kram R. Energy cost and muscular activity required for leg swing during walking. *J Appl Physiol* 99: 23-30, 2005.

Gozal EA. Trace Amines as Novel Modulators of Spinal Motor Function. In: *Department of Biomedical Engineering*. Atlanta, GA: Georgia Institute of Technology and Emory University, 2010.

Greene EC. *Anatomy of the Rat*. New York, NY: Hafner Publishing Company, 1963.

Grigg P, and Greenspan BJ. Response of primate joint afferent neurons to mechanical stimulation of knee joint. *J Neurophysiol* 40: 1-8, 1977.

Grillner P, and Rossignol S. Contralateral reflex reversal controlled by limb position in the acute spinal cat injected with clonidine i.v. *Brain Research* 144: 411-414, 1978a.

Grillner S, and Matsushima T. Neural mechanisms of intersegmental coordination in lamprey: local excitability changes modify the phase coupling along the spinal cord. *J Neurophysiol* 67: 373-388, 1992.

Grillner S, and Rossignol S. On the initiation of the swing phase of locomotion in chronic spinal cats. *Brain Res* 146: 269-277, 1978b.

Grillner S, and Rossignol S. On the initiation of the swing phase of locomotion in chronic spinal cats. *Brain Res* 146: 269-277, 1978c.

Hagbarth KE, and Kerr DIB. Central influences on spinal afferent conduction. *J Neurophysiol* 17: 295-307, 1954.

Harkema SJ, Hurley SL, Patel UK, Requejo PS, Dobkin BH, and Edgerton VR. Human Lumbosacral Spinal Cord Interprets Loading During Stepping. *J Neurophysiol* 77: 797-811, 1997.

Harrison PJ, and Zytnicki D. Crossed actions of group I muscle afferents in the cat. *J Physiol* 356: 263-273, 1984.

Hayes HB, Chang Y-H, and Hochman S. An in vitro spinal cord-hindlimb preparation for studying behaviorally relevant rat locomotor function. *J Neurophysiol* 101: 1114-1122, 2009a.

Hayes HB, Chang Y-H, and Hochman S. Modulation of sensory input and interneuronal activity during non-fictive locomotion in the in vitro spinal cord-hindlimb rat preparation. Program No. 564.10. Neuroscience 2009b Chicago, Illinois: Society for Neuroscience, 2009b. Online.

Hayes HB, and Hochman S. Sensory processing by spinal neurons during non-fictive locomotor behavior. Cellular and Network Functions in the Spinal Cord Madison, Wisconsin, June 2009.

Heckman CJ, and Binder MD. Computer simulations of the effects of different synaptic input systems on motor unit recruitment. *J Neurophysiol* 70: 1827-1840, 1993.

Heglund NC. A simple design for a force-plate to measure ground reaction forces. *J Exp Biol* 93: 333-338, 1981.

Hiebert GW, Gorassini MA, Jiang W, Prochazka A, and Pearson KG. Corrective responses to loss of ground support during walking. II. Comparison of intact and chronic spinal cats. *J Neurophysiol* 71: 611-622, 1994.

Hiebert GW, and Pearson KG. Contribution of sensory feedback to the generation of extensor activity during walking in the decerebrate cat. *J Neurophysiol* 81: 758-770, 1999.

Hiebert GW, Whelan PJ, Prochazka A, and Pearson KG. Contributions of hindlimb flexor muscle afferents to the timing of phase transitions in the cat step cycle. *J*

Neurophysiol 75: 1126-1137, 1996.

Hochman S, and Schmidt BJ. Whole cell recordings of lumbar motoneurons during locomotor-like activity in the in vitro neonatal rat spinal cord. *J Neurophysiol* 79: 743-752, 1998.

Hochman S, Shreckengost J, Kimura H, and Quevedo J. Presynaptic inhibition of primary afferent by depolarization: observations supporting nontraditional mechanisms. *Ann N Y Acad Sci* 1198: 140-152, 2010.

Holmqvist B. Crossed spinal reflex actions evoked by volleys in somatic afferents. *Acta Physiologica Scandinavica Suppl* 52: 1-66, 1961.

Honeycutt CF, and Nichols TR. Disruption of cutaneous feedback alters magnitude but not direction of muscle responses to postural perturbations in the decerebrate cat. *Experimental Brain Research* 203: 765-771, 2010.

Houk JC. Regulation of stiffness by skeletomotor reflexes. *Ann Rev Physiol* 41: 99-114, 1979.

Howland J, Lettvin JT, McCulloch WS, Pitts W, and Wall PD. Reflex inhibition by dorsal root interaction. *J Neurophysiol* 18: 1-17, 1955.

Hughes DI, Mackie M, Nagy GG, Riddell JS, Maxwell DJ, SzabÃ³ G, ErdÃ©lyi F, Veress G, SzÅ±cs P, Antal M, and Todd AJ. P boutons in lamina IX of the rodent spinal cord express high levels of glutamic acid decarboxylase-65 and originate from cells in deep medial dorsal horn. *Proceedings of the National Academy of Sciences of the United States of America* 102: 9038-9043, 2005.

Hultborn H. State-dependent modulation of sensory feedback. *J Physiol* 533: 5-13, 2001.

Hultborn H, Meunier S, Pierrot-Deseilligny E, and Shindo M. Changes in presynaptic inhibition of Ia fibres at the onset of voluntary contraction in man. *J Physiol* 389: 757-772, 1987.

Iizuka M, Kiehn O, and Kudo N. Development in neonatal rats of the sensory resetting of the locomotor rhtyhm induced by NMDA and 5-HT. *Exp Brain Res* 114: 193-204, 1997.

Iles JF. Evidence for cutaneous and corticospinal modulation of presynaptic inhibition of Ia afferents from the human lower limb. *J Physiol* 491: 197-207, 1996.

Jankowska E. Interneuronal relay in spinal pathways from proprioceptors. *Progress in Neurobiology* 38: 335-378, 1992.

Jankowska E, Bannatyne BA, Stecina K, Hammar I, Cabaj A, and Maxwell DJ. Commissural interneurons with input from group I and II muscle afferents in feline lumbar segments: neurotransmitters, projections and target cells. *The Journal of Physiology* 587: 401-418, 2009.

Jankowska E, Lund S, and Lundberg A. The effect of DOPA on the spinal cord 4. Depolarization evoked in the contralateral terminals of contralateral Ia afferent terminals by volleys in the flexor reflex afferents. *Acta Physiologica Scandinavica* 68: 337-341, 1966.

Jankowska E, Riddell JS, and McCrea DA. Primary afferent depolarization of myelinated fibers in the joint and interosseus nerves of the cat. *J Physiol* 466: 115-131, 1993.

Johansson RS, R. R, C. H, and L. B. Somatosensory control of precision grip during unpredictable pulling loads. I. Changes in load force amplitude. *Exp Brain Res* 89: 181-191, 1992.

Jordan LM. Factors determining motoneuron rhythmicity during fictive locomotion. *Soc Exp Biol Symp* 37: 423-444, 1983.

Juvin L, Simmers J, and Morin D. Locomotor rhythmogenesis in the isolated rat spinal cord: a phase-coupled set of symmetrical flexion-extension oscillators. *J Physiol* 583: 115-128, 2007.

Kiehn O. Locomotor circuits in the mammalian spinal cord. *Annual Review of Neuroscience* 29: 279-306, 2006.

Kiehn O, and Butt SJB. Physiological, anatomical, and genetic identification of CPG neurons in the developing mammalian spinal cord. *Progress in Neurobiology* 70: 347-361, 2003.

Kiehn O, Iizuka M, and Kudo N. Resetting from low threshold afferents of N-methyl-

D-aspartate-induced locomotor rhythm in the isolated spinal cord-hindlimb preparation from newborn rats. *Neurosci Lett* 148: 43-46, 1992.

Kiehn O, Johnson BR, and Raastad M. Plateau properties in mammalian spinal interneurons during transmitter-induced locomotor activity. *Neuroscience* 75: 263-273, 1996.

Kiehn O, and Kjaerulf O. Spatiotemporal characteristics of 5-HT and dopamine-induced rhythmic hindlimb activity in the in vitro neonatal rat. *J Neurophysiol* 75: 1472-1482, 1996.

Kiehn O, Kjaerulf O, Tresch MC, and Harris-Warrick RM. Contributions of intrinsic motor neuron properties to the production of rhythmic motor output in the mammalian spinal cord. *Brain Res Bull* 53: 649-659, 2000.

Kjaerulff O, and Kiehn O. Distribution of networks generating and coordinating locmotor activity in the neonatal rat spinal cord in vitro: A lesion study. *J Neurosci* 16: 5777-5794, 1996.

Knikou M. Plantar cutaneous afferents normalize the reflex modulation patterns during stepping in chronic human spinal cord injury. *J Neurophysiol* 103: 1304-1314, 2010.

Kremer E, and Lev-Tov A. GABA-receptor-independent dorsal root afferents depolarization in the neonatal rat spinal cord. *J Neurophysiol* 79: 2581-2592, 1998.

Kriellaars DJ, Brownstone RM, Noga BR, and Jordan LM. Mechanical entrainment of fictive locomotion in the decerebrate cat. *J Neurophysiol* 71: 2074-2086, 1994.

Kubow TM. The role of the mechanical system in control: a hypothesis of self-stabilization in hexapedal runners. *Phil Trans Royal Soc (London) Serial B* 354: 849-862, 1999.

Kudo N, and Yamada T. N-Methyl-D,L-aspartate-induced locomotor activity in a spinal cord-hindlimb muscles preparation of the newborn rat studied in vitro. *Neurosci Lett* 75: 43-48, 1987.

Lafreniere-Roula M, and McCrea DA. Deletions of Rhythmic Motoneuron Activity During Fictive Locomotion and Scratch Provide Clues to the Organization of the Mammalian Central Pattern Generator. *J Neurophysiol* 94: 1120-1132, 2005.

Lam T, and Pearson KG. Proprioceptive Modulation of Hip Flexor Activity During the Swing Phase of Locomotion in Decerebrate Cats. *J Neurophysiol* 86: 1321-1332, 2001.

Lam T, Wirz M, Lunenburger L, and Dietz V. Swing phase resistance enhances flexor muscle activity during treadmill locomotion in incomplete spinal cord injury. *Neurorehabil Neural Repair* 22: 438-446, 2008.

Lee CJ, Bardoni R, Tong C-K, Engelman HS, Joseph DJ, Magherini PC, and MacDermott AB. Functional Expression of AMPA Receptors on Central Terminals of Rat Dorsal Root Ganglion Neurons and Presynaptic Inhibition of Glutamate Release. 35: 135-146, 2002.

Lev-Tov A, and Pinco M. In vitro studies of prolonged synaptic depression in the neonatal rat spinal cord. *J Physiol* 447: 149-169, 1992.

Loeb GE, and Duysens J. Activity patterns in individual hindlimb primary and secondary muscle spindle afferents during normal movements in unrestrained cats. *J Neurophysiol* 42: 420-440, 1979.

Lopez-Garcia JA, and King AE. Pre- and Post-synaptic Actions of 5-Hydroxytryptamine in the Rat Lumbar Dorsal Horn In Vitro: Implications for Somatosensory Transmission. *European Journal of Neuroscience* 8: 2188-2197, 1996.

Machacek DW, and Hochman S. Noradrenaline Unmasks Novel Self-Reinforcing Motor Circuits within the Mammalian Spinal Cord. *J Neurosci* 26: 5920-5928, 2006.

Mazzaro N, Grey MJ, and Sinkjaer T. Contribution of afferent feedback to the soleus muscle activity during human locomotion *J Neurophysiol* 93: 167-177, 2005.

McCrea DA, Shefchyk SJ, Stephens MJ, and Pearson KG. Disynaptic group I excitation of synergist ankle extensor motoneurones during fictive locomotion in the cat. *Journal of Physiology (London)* 487: 527-539, 1995.

McIlroy WE, Collins DF, and Brooke JD. Movement features and H-reflex modulation. II. Passive rotation, movement velocity and single leg movement. *Brain Research* 582: 85-93, 1992.

Mehta AK, and Ticku MK. An update on GABAA receptors. *Brain Research Reviews* 29: 196-217, 1999.

Menard A, Leblond H, and Gossard J-P. The Modulation of Presynaptic Inhibition in Single Muscle Primary Afferents during Fictive Locomotion in the Cat. *J Neurosci* 19: 391-400, 1999.

Ménard A, Leblond H, and Gossard J-P. Modulation of monosynaptic transmission by presynaptic inhibition during fictive locomotion in the cat. *Brain Research* 964: 67-82, 2003.

Menard A, Leblond H, and Gossard JP. Sensory integration in presynaptic inhibitory pathways during fictive locomotion in the cat. *J Neurophysiol* 88: 163-171, 2002.

Milanov I. A comparative study of methods for estimation of presynaptic inhibition. *Journal of Neurology* 239: 287-292, 1992.

Misiaszek JE, Barclay JK, and Brooke JD. Mechanisms within the spinal cord are involved in the movement-induced attenuation of an H reflex in the dog. *J Neurophysiol* 76: 3589-3592, 1996.

Morita H, Shindo M, Ikeda S, and Yanagisawa N. Decrease in presynaptic inhibition on heteronymous monosynaptic Ia terminals in patients with Parkinson's disease. *Mov Disord* 15: 830-834, 2000.

Mott FW, and Sherrington CS. Experiments upon the influence of sensory nerves upon movement and nutrition of the limbs. *Proc R Soc London* 57: 481-488, 1895.

Munro CF, Miller DI, and Fuglevand AJ. Ground reaction forces in running: A reexamination. *Journal of Biomechanics* 20: 147-155, 1987.

Musienko PE, Bogacheva IN, and Gerasimenko YP. Significance of peripheral feedback in the generation of stepping movements during epidural stimulation of the spinal cord. *Neurosci Behav Physiol* 37: 181-190, 2007.

Nichols TR. The Contributions of Muscles and Reflexes to the Regulation of Joint and Limb Mechanics. *Clinical Orthopaedics and Related Research* 403: S43-S50, 2002.

Nichols TR, Cope TC, and Abelew TA. Rapid spinal mechanisms of motor coordination. *Excercise and sport sciences reviews* 27: 255-284, 1999.

Nichols TR, and Houk JC. Reflex compensation for variations in the mechanical properties of a muscle. *Science* 181: 182-184, 1973.

Nicolopoulos-Stournaras S, and Iles JF. Motor neuron columns in the lumbar spinal cord of the rat. *The Journal of Comparative Neurology* 217: 75-85, 1983.

Nilsson J, and Thorstensson A. Ground reaction forces at different speeds of human walking and running. *Acta Physiologica Scandinavica* 136: 217-227, 1989.

O'Donovan MJ, Pinter MJ, Dum RP, and Burke RE. Actions of the FDL and FHL muscles in intact cats: functional dissociation between anatomical synergists. *J Neurophysiol* 47: 1126-1143, 1982.

Pang MYC, and Yang JF. The initiation of the swing phase in human infant stepping: importance of hip position and leg loading. *The Journal of Physiology* 528: 389-404, 2000.

Pearson KG. Proprioceptive regulation of locomotion. *Current Opinion in Neurobiology* 5: 786-791, 1995.

Pearson KG, and Collins DF. Reversal of the influence of group Ib afferents from plantaris on activity in medial gastrocnemius muscle during locomotor activity. *J Neurophysiol* 70: 1009-1017, 1993.

Pearson KG, Misiaszek JE, and Fouad K. Enhancement and resetting of locomotor activity by muscle afferents. *Ann N Y Acad Sci* 860: 203-215, 1998.

Peng YB, Wu J, Willis WD, and Kenshalo DR. GABA(A) and 5-HT(3) receptors are involved in dorsal root reflexes: possible role in periaqueductal gray descending inhibition. *J Neurophysiol* 86: 49-58, 2001.

Perreault MC, Angel MJ, Guertin P, and McCrea DA. Effects of stimulation of hindlimb flexor group II afferents during fictive locomotion in the cat. *The Journal of Physiology* 487: 211-220, 1995.

Pierce JP, and Mendell L. Quantitative ultrastructure of Ia boutons in the ventral horn: scaling and positional relationships. *Journal of Neuroscience* 13: 4748-4763, 1983.

Prochazka A. Sensorimotor gain control: a basic strategy of motor systems? *Prog Neurobiol* 33: 281-307, 1989.

Prochazka A, and Gorassini MA. Ensemble firing of muscle afferents recorded during normal locomotion in cats. *J Physiol* 507: 293-304, 1998.

Prochazka A, Trend P, Hulliger M, and Vincent S. Ensemble proprioceptive activity in the cat step cycle: towards a representative look-up chart. *Progress in Brain Research* 80: 61-74, 1989.

Prochazka A, Westerman RA, and Ziccone SP. Discharges of single hinblimb afferents in the freely moving cat. *J Neurophysiol* 39: 1090-1104, 1976.

Quevedo J, Fedirchuk B, Gosgnach S, and McCrea DA. Group I disynaptic excitation of cat hindlimb flexor and bifunctional motoneurones during fictive locomotion. *The Journal of Physiology* 525: 549-564, 2000.

Quevedo J, Stecina K, and McCrea DA. Intracellular Analysis of Reflex Pathways Underlying the Stumbling Corrective Reaction During Fictive Locomotion in the Cat. *J Neurophysiol* 94: 2053-2062, 2005.

Ross KT, and Nichols TR. Heterogenic Feedback Between Hindlimb Extensors in the Spontaneously Locomoting Premammillary Cat. *J Neurophysiol* 101: 184-197, 2009.

Rossignol S, Dubuc R, and Gossard JP. Dynamic sensorimotor interactions in locomotion. *Physiol Rev* 86: 89-154, 2006.

Rudomin P. In search of lost presynaptic inhibition. *Experimental Brain Research* 196: 139-151, 2009.

Rudomin P, Jimenez I, Solodkin M, and Duenas S. Sites of action of segmental and descending control of transmission on pathways mediating PAD of Ia- and Ib-afferent fibers in cat spinal cord. *J Neurophysiol* 50: 743-769, 1983.

Rudomin P, Romo R, and Mendell L. *Presynaptic Inhibition and Neural Control*. New York: Oxford University Press, 1998.

Rudomin P, and Schmidt RF. Presynaptic inhibition in the vertebrate spinal cord

revisited. *Experimental Brain Research* 129: 1-37, 1999.

Rudomin P, Solodkin M, and Jimenez I. Synaptic potentials of primary afferent fibers and motoneurons evoked by single intermediate nucleus interneurons in the cat spinal cord. *J Neurophysiol* 57: 1288-1313, 1987.

Russo RE, Delgado-Lezama R, and Houndgaard J. Dorsal root potential produced by a TTX-insensitive micro-circuitry in the turtle spinal cord. *Journal of Physiology* 528: 115-122, 2000.

Seki K, Perlmutter SI, and Fetz EE. Sensory input to primate spinal cord is presynaptically inhibited during voluntary movement. *Nature Neuroscience* 6: 1309-1316, 2003.

Shreckengost J, Calvo J, Quevedo J, and Hochman S. Bicuculline-Sensitive Primary Afferent Depolarization Remains after Greatly Restricting Synaptic Transmission in the Mammalian Spinal Cord. *J Neurosci* 30: 5283-5288, 2010.

Sinkjaer T, Andersen JB, Ladouceur M, Christensen LOD, and Nielson JB. Major role for sensory feedback in soleus EMG activity in the stance phase of man. *J Physiol* 523: 817-827, 2000.

Smith JC, and Feldman JL. In vitro brainstem-spinal cord preparations for study of motor systems for mammalian respiration and locomotion. *J Neurosci Methods* 21: 321-333, 1987.

Smith JC, Feldman JL, and Schmidt BJ. Neural mechanisms generating locomotion studied in mammalian brain stem-spinal cord in vitro. *FASEB J* 2: 2283-2288, 1988.

Solodkin M, Jimenez I, and Rudomin P. Identification of common interneurons mediating pre- and postsynaptic inhibition in the cat spinal cord. *Science* 224: 1453-1456, 1984.

Staley KJ, Otis TS, and Mody I. Membrane properties of dentate gyrus granule cells: comparison of sharp microelectrodes and whole-cell recordings. *J Neurophysiol* 67: 1346-1358, 1992.

Stecina K, Quevedo J, and McCrea DA. Parallel reflex pathways from flexor muscle afferents evoking resetting and flexion enhancement during fictive locomotion and

scratch in the cat. *The Journal of Physiology* 569: 275-290, 2005.

Stehouwer DJ, McCrea AE, and Hartesveldt CV. L-DOPA-induced air-stepping in preweanling rats. II. Kinematic analyses. *Dev Brain Res* 82: 143-151, 1994.

Stein RB. Presynaptic inhibition in humans. *Progress in Neurobiology* 47: 533-544, 1995.

Stein RB, Misiaszek JE, and Pearson KG. Functional role of muscle reflexes for force generation in the decerebrate walking cat. *J Physiol* 525: 781-791, 2000.

Takahashi T. The minimal inhibitory synaptic currents evoked in neonatal rat motoneurones. *The Journal of Physiology* 450: 593-611, 1992.

Taricco M, Pagliacci MC, Telaro E, and Adone R. Pharmacological interventions for spasticity following spinal cord injury: results of a Cochrane systematic review. *Europa Medicophysica* 42: 5-15, 2006.

Thota AK, Watson SC, Knapp E, Thompson B, and Jung R. Neuromechanical control of locomotion in the rat. *Journal of Neurotrauma* 22: 442-465, 2005.

Ting L, Blickhan R, and Full R. Dynamic and static stability in hexapedal runners. *J Exp Biol* 197: 251-269, 1994.

Ting LH, Christine RC, Brown DA, Kautz SA, and Zajac FE. Sensorimotor state of the contralateral leg affects ipsilateral muscle coordination of pedaling. *J Neurophysiol* 80: 1341-1351, 1998.

Ting LH, Kautz SA, Brown DA, and Zajac FE. Contralateral movement and extensor force generation alter flexion phase muscle coordination in pedaling. *J Neurophysiol* 83: 3351-3365, 2000.

Ting LH, and Macpherson JM. Ratio of shear to load ground reaction force may underlie the directional tuning of the automatic postural response to rotation and translation. *J Neurophysiol* 92: 808-823, 2004.

Tresch MC, and Kiehn O. Coding of locomotor phase in populations of neurons in rostral and caudal segments of the neonatal rat lumbar spinal cord. *Journal of*

Neurophysiology 82: 3563-3574, 1999.

Van Wezel BMH, Ottenhoff FAM, and Duysens J. Dynamic Control of Location-Specific Information in Tactile Cutaneous Reflexes from the Foot during Human Walking. *J Neurosci* 17: 3804-3814, 1997.

Wallraff HG. Goal-oriented and compass-oriented movements of displaced homing pigeons after confinement in differentially shielded aviaries. *Behavioral Ecology and Sociobiology* 5: 201-255, 1979.

Wheatley M, Jovanovic K, Stein RB, and Lawson V. The activity of interneurons during locomotion in the in vitro necturus spinal cord *J Neurophysiol* 71: 2025-2032, 1994a.

Wheatley M, Jovanovic K, Stein RB, and Lawson V. The activity of interneurons during locomotion in the in vitro necturus spinal cord. *J Neurophysiol* 71: 2025-2032, 1994b.

Wheatley M, and Stein RB. An in vitro preparation of the mudpuppy for simulataneous intracellular and electromyographic recording during locomotion. *J Neurosci Methods* 42: 129-137, 1992.

Whelan PJ, Hiebert GW, and Pearson KG. Plasticity of the extensor group I pathway controlling the stance to swing transition in the cat. *Journal of Neurophysiology* 74: 2782-2787, 1995a.

Whelan PJ, Hiebert GW, and Pearson KG. Stimulation of the group I extensor afferents prolongs the stance phase in walking cats. *Exp Brain Res* 103: 20-30, 1995b.

Yakhnitsa IA, Pilyavskii AI, and Bulgakova NV. Phase-dependent changes in dorsal root potential during actual locomotion in rats. *Translated from Neirofiziologiya* 20: 333-340, 1988.

Yakovenko S, McCrea DA, Stecina K, and Prochazka A. Control of Locomotor Cycle Durations. *J Neurophysiol* 94: 1057-1065, 2005.

Yang JF, Fung J, Edamura M, Blunt R, Stein RB, and Barbeau H. H-reflex modulation during walking in spastic paretic subjects. *Can J Neurol Sci* 18: 443-452, 1991.

Yen JT, and Chang Y-H. Rate-dependent control strategies stabilize limb forces during human locomotion. *Journal of The Royal Society Interface* 7: 801-810, 2010.

Zar JH. *Biostatistical Analysis*. Englewood Cliffs, NJ: Prentice-Hall, 1974.

Ziskind-Conhaim L. NMDA receptors mediate poly- and monosynaptic potentials in motoneurons of rat embryos. *J Neurosci* 10: 125-135, 1990.

Zytnicki D, and Jami L. Presynaptic inhibition can act as a filter of input from tendon organs during muscle contraction. In: *Presynaptic inhibition and neural control* edited by Rudomin P, Romo R, and Mendell L. Oxford: Oxford University Press, 1998, p. 303-314.

VITA

Heather Brant Hayes

Heather Brant Hayes (nee: Heather Elizabeth Brant) was born in Jacksonville, Florida, where she attended Episcopal High School and graduated as the Salutatorian for the Class of 2000. In 2004, she received a Bachelor of Engineering in Biomedical Engineering at Vanderbilt University in Nashville, Tennessee in 2004. She graduated summa cum laude with a 4.0 grade point average as the Valedictorian of the School of Engineering. She also received the Founder's Medal for first honors in the School of Engineering. In Fall 2004, Heather began her graduate work at the Georgia Institute of Technology, pursuing a doctorate in Bioengineering in the Wallace H. Coulter Department of Biomedical Engineering. Her research focuses on neuroengineering and spinal cord sensorimotor circuitry. She hopes that her work will inform and improve rehabilitation for persons with spinal cord injuries and other motor disorders. When she is not working on her research, Heather is involved in her church, where she volunteers with Shepherd Friends at The Shepherd Center. She values spending time with her husband, family, and friends, as well as spending time outdoors hiking, snow skiing, or just being active.